

**Functional Analysis of *Aspergillus oryzae* through the
Development of Molecular Breeding Techniques and
its Applications in the Food Industry**

Takehiko Todokoro

2024

CONTENTS

Abbreviations	2
General introduction	4
Chapter I Development of molecular breeding techniques for <i>Aspergillus oryzae</i> and its application in sake production	
Section 1. Identification of a novel pyrithiamine resistance marker gene <i>thiI</i> for genome co-editing in <i>Aspergillus oryzae</i>	8
Section 2. Development of high-efficiency targeted knock-in method using CRISPR/Cas9 in <i>Aspergillus oryzae</i>	24
Section 3. Identification of the gene responsible for the production of the precursor of the off-flavor compound 4-vinylguaiaicol in sake.....	40
Chapter II Development of production technology for the iron chelator deferriferrichrysin from <i>Aspergillus oryzae</i> and evaluation of its functional properties in food applications	
Section 1. Production of deferriferrichrysin and evaluation as a novel food-grade antioxidant.....	56
Section 2. Inhibition of lipid oxidation and hexanal production in cooked meats by deferriferrichrysin.....	76
Conclusions	89
References	91
Acknowledgements	109
List of publications	110

ABBREVIATIONS

4-VG	4-vinylguaiacol
ANOVA	analysis of variance
CMC	sodium carboxymethylcellulose
CRISPR	clustered regularly interspaced short palindromic repeats
CRISPR-Cas9	CRISPR-associated protein 9
Dfcy	deferriferrichrysin
DO	dissolved oxygen concentration
DSB	double-strand break
EDTA	ethylenediaminetetraacetic acid
Fcy	ferrichrysin
GPY	glucose-peptone-yeast
GRAS	generally regarded as safe
HS-GC-MS	headspace gas chromatography-mass spectrometry
HA	homology arm
HPLC	high-performance liquid chromatography
HR	homologous recombination
MDA	malondialdehyde
MFA	methyl ferulate
MMEJ	microhomology-mediated end-joining

NHEJ	non-homologous end-joining
O/W	oil in water
PAM	protospacer adjacent motif
PCR	polymerase chain reaction
PDA	potato dextrose agar
PEG	polyethylene glycol
PT	pyrithiamine
PV	peroxide value
sgRNA	single-guide RNA
SSA	single-strand annealing
SLH	hydrolysate of sake lees
TALENs	transcription activator-like effector nucleases
TBARS	thiobarbituric acid reactive substances
UTR	untranslated region
UV	ultraviolet
YE	yeast extract

GENERAL INTRODUCTION

The fungus *Aspergillus oryzae* has long been used in the production of traditional Japanese food products such as sake, shochu, miso, and shoyu. Furthermore, *A. oryzae* is currently utilized as a source of cosmetic materials and a host for the production of heterologous proteins. This industrially important fungus *A. oryzae* is still in need of the development of molecular breeding methods and functional elucidation. Furthermore, it is highly meaningful to develop functional materials that can contribute to solving issues such as food loss, utilizing *A. oryzae* which has a long history of food use.

In Chapter I, the author focused on the development of the novel molecular breeding technique of *A. oryzae*. Genetic engineering using *A. oryzae* has been extensively studied for its fundamental and practical importance. In *A. oryzae*, targeted genetic engineering by classical transformation is laborious owing to the low frequency of homologous recombination (HR). The host strain needs to be modified to improve the HR efficiency by disturbing the non-homologous end-joining (NHEJ) repair pathway via the disruption of *ligD* or *ku70* (1,2). Recently, genome editing technologies such as clustered regularly interspaced short palindromic repeat (CRISPR)/CRISPR-associated protein 9 (Cas9)(3) have been successfully applied in the genetic engineering of *A. oryzae* (4,5). Although genome editing may need to be performed repeatedly to yield multiple mutants, only a few marker genes have been identified from the internal genes of *A. oryzae*, primarily because of its high resistance to different types of antibiotics (6). Among known marker genes in *A. oryzae*, *thiA* is preferred because its corresponding agent pyrithiamine (PT; an analog of thiamine) functions at a low concentration in the medium. However, PT resistance conferred by the *thiA* gene is affected only when a mutation occurs in the limited region of 5' untranslated region (UTR) (7), preventing the application of *thiA* in

genome editing. There was a need for the development of alternative marker gene that can be used for genome editing. Therefore, in Section 1, the author first developed molecular breeding methods for *A. oryzae* through the identification of a novel PT resistance marker gene *thil* that can be used in the CRISPR/Cas9 genome editing system.

The genome editing technologies have enabled the acquisition of targeted knock-out mutants without the preparation of a host strain, as mentioned above. On the other hand, acquiring targeted knock-in mutants was still laborious since it was based on HR, wherein long length homology (usually > 500 bp) of the template is essential (1,8). Recently, two alternative DNA double-strand break (DSB) repair pathways, namely microhomology-mediated end-joining (MMEJ) and single-strand annealing (SSA), have been employed as targeted knock-in methods in combination with genome editing technologies in mammalian cells (9). Compared with HR, MMEJ/SSA requires a shorter homology length of the template, thereby making template preparation easier. However, the application of MMEJ/SSA in *A. oryzae* has not been sufficiently studied. Therefore, in Section 2, the author developed more convenient and efficient targeted knock-in method based on MMEJ/SSA.

In the following Section 3, by using the developed genome editing technology, the author worked on the elucidation of the unknown mechanism related to the sake brewing, one of the most important industrial applications of *A. oryzae*. 4-Vinylguaiacol (4-VG) is an undesired off-flavor for sake (10). In sake, 4-VG is formed from its precursor ferulic acid (4-hydroxy-3-methoxycinnamic acid) via enzymatic conversion by *Saccharomyces cerevisiae* or other contaminant microorganisms such as *Bacillus* spp. (11) and *Lactobacillus* spp. (12). In *S. cerevisiae*, phenylacrylic acid decarboxylase (PAD1) and ferulic acid decarboxylase (FDC1) are required for 4-VG formation, and loss of function of either of the two proteins diminishes 4-VG production (13). Although *S. cerevisiae*

strains used for sake brewing have lost their ability to produce 4-VG because of the loss of function of *FDC1* (14), 4-VG formation due to contamination by wild yeast and bacteria remains a problem, as it reduces sake quality (15). In sake brewing, ferulic acid, the precursor of 4-VG, is thought to be released from feruloyl polysaccharide by feruloyl esterase produced by *Aspergillus oryzae* or *S. cerevisiae*. However, the mechanism of the release of ferulic acid in sake brewing is still unknown and needs to be elucidated to overcome the problem. The author investigated the functions of candidate genes by utilizing the genome editing and identified the gene responsible for the 4-VG production in sake brewing.

In Chapter II, the author focused on the iron chelator deferriferrichrysin (Dfcy) produced by *A. oryzae*. *A. oryzae* has a long history of use in food production, but the utilization of its products other than enzymes as food ingredients has not been sufficiently explored. Dfcy is a cyclic hexapeptide siderophore produced by *A. oryzae* and related species. Dfcy binds ferric ion with high affinity and specificity. Dfcy is a desirable candidate for a food-grade iron-chelator because of its safety for consumption, as it has long been ingested along with sake. In recent years, the development of new food additives and preservatives to prevent food deterioration and extend shelf life has been of great interest in the food industry. In particular, lipid oxidation is a major issue that leads to the deterioration of many food products, causing food loss, reduction in nutritional quality, and even health risks. Metal chelators such as ethylenediaminetetraacetic acid (EDTA) are used to prevent lipid oxidation in foods because metals, especially iron, are the main catalyst of lipid oxidation (16). Recently, increasing demand for natural products has led to the exploration of natural alternatives of EDTA such as organic acids and herbal extracts. These compounds, however, have not shown satisfactory results, likely because of their lower binding constant to iron and lower stability compared to EDTA (16).

Therefore, investigating Dfcy as a novel natural chelator material that can inhibit lipid oxidation is a valuable challenge. In the first Section 1, the author developed the production technology of Dfcy and evaluated its functional properties in food applications. The author first acquired high Dfcy-producing strains and optimized the production conditions, achieving a significant improvement in the production levels. The author also revealed for the first time that Dfcy inhibits lipid oxidation in an oil-in-water (O/W) model system.

Furthermore, lipid oxidation is responsible for the quality deterioration of meat by producing primary and secondary oxidation products, thereby reducing the nutritional quality of meat (17). It also imparts an unpleasant off-odor to the heat-processed meat, thus affecting consumers' acceptability of meat. Additionally, lipid oxidation products such as malondialdehyde (MDA) and 4-hydroxy-nonenal pose health hazards to humans (18). Although the potential of Dfcy to inhibit lipid oxidation in O/W model was discovered, its antioxidant efficiency in real food products has not yet been elucidated. In the Section 2, the author investigated the potential of Dfcy as antioxidant of meat products. Dfcy suppressed the lipid oxidation and generation of unpleasant odors during meat processing, demonstrating its high functional value in the food industry.

Chapter I

Development of molecular breeding techniques for *Aspergillus oryzae* and its application in sake production

Section 1

Identification of a novel pyrithiamine resistance marker gene *thiI* for genome co-editing in *Aspergillus oryzae*

Transformation of *A. oryzae* is a common procedure because of its fundamental and practical importance. Recently, as a novel transformation technology, genome editing systems have been successfully applied in the genetic engineering of *A. oryzae* (4,5). The CRISPR/Cas9 system is a powerful tool used for genome editing because of its high specificity for the target gene and its flexibility toward choice of target gene (3). The CRISPR/Cas9 system requires two components: the Cas9 endonuclease and a single-guide RNA (sgRNA) for the site-specific cleavage of the target DNA sequence. The selection of the target is flexible because the only requirement is the presence of a protospacer adjacent motif (PAM), 5'-NGG-3' DNA motif, immediately after the target sequence. The CRISPR/Cas9 system was discovered in prokaryotes, and today, it is being applied to various eukaryotes, including fungi such as *Trichoderma reesei* (19), *Schizosaccharomyces pombe* (20), and *A. oryzae* (5).

There are two major methods for application of the CRISPR/Cas9 system to fungal cells. The first method involves direct introduction of Cas9/sgRNA ribonucleoprotein (21), whereas the second method involves transformation with a plasmid expressing Cas9 mRNA and sgRNA (5). Direct ribonucleoprotein introduction has several advantages, including ease of procedure and fast completion, since laborious plasmid construction is

bypassed. However, the efficiency of genome editing is not sufficiently high when transformants are selected without a positive selection marker, and thus, selection of transformants is a problem for the direct ribonucleoprotein introduction method (22). Recently, several groups have reported a new method for efficient transformation called genome co-editing, which uses two Cas9 nucleases, each harboring a different sgRNA; one recognizes the target gene and the other recognizes a selectable marker gene (6,7). Although transformation may need to be performed repeatedly to yield multiple mutants, only a few positive selection marker genes have been identified from the internal genes of *A. oryzae*, primarily because of its high resistance to different types of antibiotics (6). Among known selectable marker genes in *A. oryzae*, including, *sC* (24), *niaD* (25), *pyrG* (26), and *thiA*, *thiA* is preferred because its corresponding agent pyriithiamine (PT; an analog of thiamine) functions at a low concentration in the medium (0.1 mg/L). However, PT resistance conferred by the *thiA* gene is affected only when a mutation occurs in the limited region of 5' UTR (7). Consequently, the opportunities for target design are limited, preventing the application of *thiA* in genome editing.

In this study, the author identified a novel PT resistance marker gene *thiI*, that can be used in genome co-editing. *thiI* possessed distinct advantages compared to the conventional marker genes. Loss of *thiI* function does not cause auxotrophy, which is useful when investigating phenotypic changes caused by target gene disruption. Furthermore, PT functions as low as 0.1 mg/L and background colonies are comparatively rare. Overall, *thiI* marker is a promising tool for industrially important fungus *A. oryzae*.

Materials and methods

Fungal strains and media

A. oryzae strain RIB40 was used as a host strain for transformation. For collection of

spores, RIB40 was inoculated onto potato dextrose agar (PDA; Nihon Pharmaceutical Co., Ltd., Tokyo, Japan) supplemented with 3% NaCl and incubated at 30°C for 7 days. For generation of PT-resistant mutants, a 0.1% Tween 80 solution containing 1×10^7 spores of RIB40 was irradiated with ultraviolet (UV) light. To compare PT resistance phenotypes, a *thiA* de-repressed mutant of RIB40 was used (27). The basal medium used for transformation and phenotype screening was Czapek–Dox minimal medium prepared with the following compounds: 1 g/L K₂HPO₄, 0.5 g/L MgSO₄·7H₂O, 0.5 g/L KCl, 30 g/L sucrose, 0.01 g/L FeSO₄·7H₂O, and 5 g/L NaNO₃ (28). The initial pH was adjusted to 5.0 using 0.1 M HCl. For selection of PT-resistant strains, PT was added to the basal medium at a concentration of 0.1 mg/L. For protoplast formation, glucose-peptone-yeast (GPY) medium was prepared with 20 g/L glucose, 10 g/L polypeptone (Nihon Pharmaceutical Co., Ltd., Tokyo, Japan), and 5 g/L yeast extract (YE; Becton, Dickinson and Company, NJ, USA). Spore color was confirmed using PDA supplemented with 3% NaCl. Siderophore production was confirmed using PDA supplemented with 500 mg/L FeSO₄·7H₂O (100 mg/L as Fe).

Preparation of sgRNA and Cas9

For genome editing, recombinant Cas9 nuclease of *Streptococcus pyogenes* harboring two nuclear localization signals (one on the C-terminus and another on the N-terminus) was used (EnGen Cas9 NLS; New England Biolabs Inc., MA, USA). sgRNA was prepared using an *in vitro* synthesis kit (EnGen sgRNA Synthesis Kit, *S. pyogenes*; New England Biolabs Inc., MA, USA). For sgRNA synthesis, a target sequence unique for each target gene was searched using CRISPRdirect (<https://crispr.dbcls.jp/>) (29). The genome editing efficiency was estimated using CHOPCHOP (<http://chopchop.cbu.uib.no/>) (30). The oligonucleotide templates for *in vitro* synthesis of

sgRNA were prepared as shown in Table 1-1. sgRNA was synthesized according to the manufacturer's protocol; synthesis was followed by purification using RNA Clean & Concentrator kit (Zymo Research, CA, USA). The Cas9 protein (5 µg; 20 mM) and sgRNA (40 mM) were mixed and then incubated for 10 min at 15°C before performing polyethylene glycol (PEG) transformation as described below.

Table 1-1. Oligonucleotide sequences used in the study.

Oligonucleotide name	Sequence (5'-3')	Description
RNA _{syn} _AO09010200 0476	TTCTAATACGACTCACTATA GGCGAAGACGAGACGCGAG GGTTTTAGAGCTAGA	synthesis of sgRNA specific to AO090102000476 target sequence: GCGAAGACGAGACGCGAGGG
RNA _{syn} _wA	TTCTAATACGACTCACTATA GCCAGAATGCGGAGACAGG GGTTTTAGAGCTAGA	synthesis of sgRNA specific to <i>wA</i> target sequence: CCAGAATGCGGAGACAGGGG
RNA _{syn} _sreA	TTCTAATACGACTCACTATA GAAACCCGTGAAATCAACA GGTTTTAGAGCTAGA	synthesis of sgRNA specific to <i>sreA</i> target sequence: AAACCCGTGAAATCAACAGG
AO090102000476 P32 38943	GAAATGCGAGATGCGGTTCC	Primer for amplification and sequencing of AO090102000476
AO090102000476_N32 39781	CGGTAAGTCCAGCGACTCAG	Primer for amplification and sequencing of AO090102000476
AO090102000476 5U TR_N3241141	TTACTGGCCCTGCGATACTG	Primer for amplification and sequencing of AO090102000476
AO090102000476_3U TR_P3236608	AACGAGAGGCCAAAGAAGCC T	Primer for amplification and sequencing of AO090102000476
AothiA_P2326896	ATTATGGAGTGCAGTGGG G	Primer for amplification and sequencing of <i>thiA</i>
AothiA_N2328412	GGACGGGTGATCAAGTCCTC	Primer for amplification and sequencing of <i>thiA</i>
AowA_P3040056	TCCGCCAAAGCAAATGTTGG	Primer for amplification and sequencing of <i>wA</i>
AowA_P3041517	ACCACTGTGGCATCTCTTCG	Primer for amplification and sequencing of <i>wA</i>
AowA_N3042748	GTGAGGTACCCACCTTCACA C	Primer for amplification and sequencing of <i>wA</i>
AowA_N3044459	AGCTTCATCAGTCTTTAAGC CA	Primer for amplification and sequencing of <i>wA</i>
AosreA_N3158805	CCTTCCCTGGGTTGTCGTC C	Primer for amplification and sequencing of <i>sreA</i>
AosreA_N3157933	TCGGTAAAGAATGGCACCCC	Primer for amplification and sequencing of <i>sreA</i>
AosreA_P3156824	GTCAGAAAGCAACTGCTGC G	Primer for amplification and sequencing of <i>sreA</i>
AosreA_P3155607	AGGAGGGTCTTGAGCTTTGC	Primer for amplification and sequencing of <i>sreA</i>

Genome editing by CRISPR/Cas9

Genome editing was accomplished by protoplast-PEG transformation as previously described (31), with the following modifications. In total, 1×10^6 spores were scraped from a PDA plate and were inoculated into 100 mL GPY medium in Erlenmeyer flasks. After incubation for 16 h at 30°C with shaking at 120 rpm, the culture was collected on a glass filter 11G1, washed twice with 0.8 M NaCl, and resuspended in an enzyme mixture containing 2 g/L of Yatalase (Takara Bio, Shiga, Japan) and 1 g/L of lysing enzyme (Sigma-Aldrich, Tokyo, Japan). The suspension was gently shaken in the incubator at 30°C for 3 h. The formation of protoplasts was confirmed by observing the cells under a microscope. Protoplasts were filtered through a glass filter, centrifuged at $3,000 \times g$ for 1 min, and resuspended in a solution containing 10 mM CaCl₂ and 10 mM Tris-HCl at pH 7.5 to a final volume of 50 μ L to yield a protoplast density of $1 \times 10^5/\mu$ L. Cas9 nuclease (5 μ g) was mixed with sgRNA (at twice the molar concentration of Cas9) in the buffer supplied by the manufacturer and incubated at 15°C for 10 min. The Cas9–sgRNA solution was then added to the protoplast preparation. Next, 50 μ L of solution containing 60% (w/v) PEG 4000 (Nacalai Tesque, Kyoto, Japan), 50 mM CaCl₂, and 10 mM Tris-HCl at pH 7.5 was added. The preparation was then gently mixed and incubated for 60 min at 15°C. The preparation was mixed with Czapek-dox medium containing 0.1 mg/L PT, 0.8 M NaCl, and 0.5% agar, and this was overlaid onto the same medium containing 1% agar. After incubation for 4 to 5 days at 30°C, colonies growing well were identified as PT-resistant mutants and picked for further analysis. To confirm spore color, PT-resistant colonies were sub-cultured on PDA supplemented with 3% NaCl, followed by incubation at 30°C for 5 days. To confirm siderophore production, PT-resistant colonies were sub-cultured on PDA supplemented with 500 mg/L FeSO₄·7H₂O (100 mg/L as Fe), followed by incubation at 30°C for 3 days.

Bioinformatics analysis

For validation of mutations induced by genome editing, genomic DNA was extracted from each mutant and amplified using polymerase chain reaction (PCR). Sequencing was performed using a 3730xl DNA Analyzer (Thermo Fisher Scientific, MA, USA). Primers used in this study are shown in Table 1-1. Whole genome sequencing was performed using Hiseq X platform (Illumina, CA, USA), and the obtained data were analyzed using the Geneious software (Biomatters Ltd., Auckland, New Zealand). Conserved domain searches were performed on the NCBI website (<http://www.ncbi.nlm.nih.gov/Structure/cdd/wrpsb.cgi>). Homologous amino acid sequences were searched using BlastP (protein–protein BLAST) on the NCBI website (<http://blast.ncbi.nlm.nih.gov/Blast.cgi>) against the databases of *A. oryzae* RIB40, *Aspergillus nidulans* FGSC A4, and *Aspergillus niger* CBS 513.88, using *S. pombe* Thi9 (NP_593353.1) as the query sequence. Sequences with E values lower than 1×10^{-30} were used for multiple sequence alignment, and a phylogenetic tree was constructed by the neighbor-joining method using Clustal Omega (18,19). Expected Thi9 orthologs (XP_001822643.1, XP_001400106.2, XP_868888.1) were re-aligned with Thi9 using Clustal Omega.

Results

Isolation of novel PT-resistant mutant and search for candidate gene mutation

A. oryzae strain RIB40 spores were mutagenized by UV light irradiation to generate PT-resistant mutants. The survival rate of the spores was 0.6%. PT-resistant mutants were selected on a Czapek–Dox agar plate containing 0.1 mg/L PT. Ten surviving colonies were identified on the plate, and these were transferred onto a new plate with the same medium composition to confirm that the phenotype was stable. After confirmation of a

stable PT resistance phenotype, genomic DNA was extracted from individual strains and the DNA sequence around *thiA*, the only gene conferring PT resistance previously identified in *A. oryzae* (7), was analyzed. Nine out of 10 selected mutants harbored mutations in the 5' UTR of *thiA* as shown in This observation is consistent with the known mechanism of PT resistance, i.e., de-repression of *thiA*-dependent thiamine synthesis, although the mutation patterns were more variable than those reported previously. The single PT-resistant clone (PTR1), which had not acquired a mutation in the 5' UTR of *thiA*, was further analyzed by whole genome sequencing to identify the mutation conferring PT resistance. The genome of PTR1 was analyzed by mapping the sequencing reads to the reference genome of RIB40, allowing about 3500 mutations to be identified.

These mutations comprised 442 substitution mutations, 11 frame shift mutations, and 18 insertion-deletions, in the deduced amino acid sequences. The genes affected were analyzed with a BLAST homology search and a conserved domain search of their deduced amino acid sequence to evaluate their function. The author's attention was directed to AO090102000476, whose amino acid sequence possessed a conserved amino acid permease (GABA permease) domain, because the sequence had similarity to thiamine transporter Thi9 of *S. pombe* (34). To investigate whether AO090102000476 is

WT	-115	TGAGATTATACGGCTAAAACCTTGATCTGGATAATACCAGCGAAAAGGATCATGCC	-61
Mutant1	-115	T A AGATTATACGGCTAAAACCTTGATCTGGATAATACCAGCGAAAAGGATCATGCC	-61
Mutant2	-115	TGAG G TTATACGGCTAAAACCTTGATCTGGATAATACCAGCGAAAAGGATCATGCC	-61
Mutant3	-115	TGAGATTATAC A GGCTAAAACCTTGATCTGGATAATACCAGCGAAAAGGATCATGCC	-61
Mutant4	-115	TGAGATTATAC A GCTAAAACCTTGATCTGGATAATACCAGCGAAAAGGATCATGCC	-61
Mutant5	-115	TGAGATTATAC AA CTAAAACCTTGATCTGGATAATACCAGCGAAAAGGATCATGCC	-61
Mutant6	-115	TGAGATTATACGGCTAAAACCTTGATCT A GATAATACCAGCGAAAAGGATCATGCC	-61
Mutant7	-115	TGAGATTATACGGCTAAAACCTTGATCTGGAT-ATACCAGCGAAAAGGATCATGCC	-61
Mutant8	-115	TGAGATTATACGGCTAAAACCTTGATCTGGATAATACCAGCGAAA A GATCATGCC	-61
		<div style="display: flex; justify-content: space-around; width: 100%;"> Region B Region A </div>	
WT	-230	GTGGGCCGGTG	-220
Mutant9	-230	GTGG CC GGTG	-220

Fig. 1-1. Sequences of *thiA* 5'UTR of pyrithiamine-resistant mutants generated by UV irradiation. Formerly reported motifs comprising riboswitch-like domain are indicated (regions A and B).

a homolog of Thi9, the genome sequence of *A. oryzae* RIB40 was subjected to BlastP analysis using Thi9 as a query sequence. Concomitantly, two representative Aspergilli, *A. nidulans* FGSC A4 and *A. niger* CBS 513.88, were subjected to BlastP analysis using Thi9 as a query sequence. Fig. 1-2 shows the phylogenetic tree constructed from the alignment results. The amino acid sequence of AO090102000476 (XP_001822643.1) showed 51.4% amino acid identity with Thi9, and it had the highest similarity to Thi9 within the genome of *A. oryzae* RIB40. The sequence with second-highest amino acid identity (XP_001825876.1) within the genome of *A. oryzae* RIB40 showed only 27.6% identity.

To investigate the phylogenetic distribution of these hypothetical Thi9 orthologs, amino acid sequences showing high similarity were re-aligned using CLUSTAL Omega. As shown in Fig. 1-2, proteins XP_001822643.1 (*A. oryzae*), XP_868888.1 (*A. nidulans*), and XP_001400106.2 (*A. niger*), presented the closest relationship to Thi9. As shown in Fig. 1-3, PTR1 was associated with a nonhomologous amino acid change (R368H)

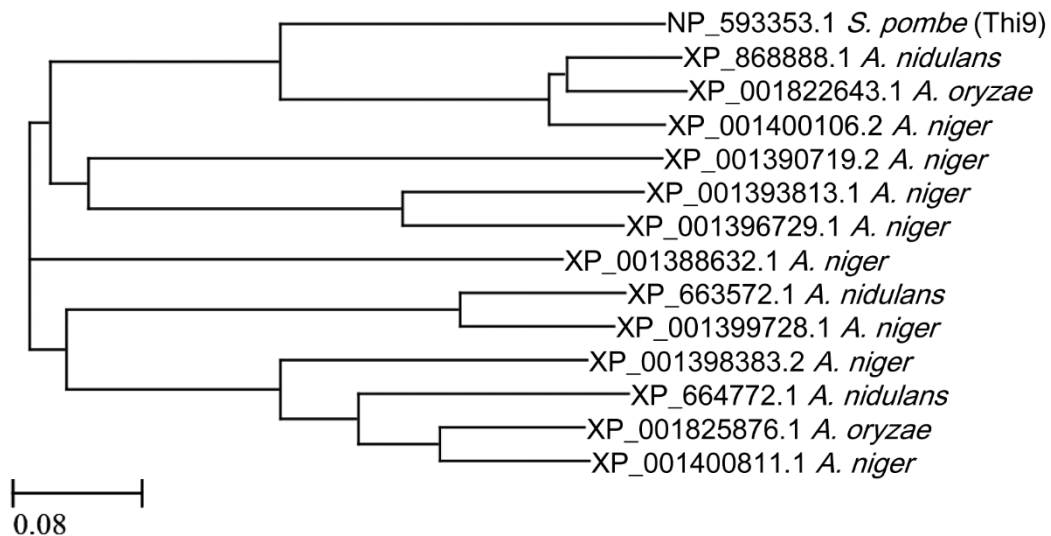


Fig. 1-2. Phylogenetic tree generated using Clustal Omega with the neighbor-joining method. The scale bar represents 0.08 substitutions per amino acid position.

within a highly conserved region (marked with an asterisk) of XP_001822643.1 (the protein encoded by AO090102000476). The author hypothesized that AO090102000476, hereafter referred to as *thi1*, encodes the only thiamine transporter in *A. oryzae* and mutation in this gene accounted for the PT resistance of PTR1.

```

XP_001822643.1 (A. oryzae) 1 ---MFAAQDQADLVDNDLHEINBEVRSQTES-----DDP
XP_001400106.2 (A. niger) 1 -MASEPHQHSQLVDFEPTVEGGEEVRSQTES-----RDP
XP_868888.1 (A. nidulans) 1 ---MSPSHQHPSQLLEQIPVG---EETRSQTES-----DDP
Thi9 (S. pombe) 1 MPSSQISLSDPELQDTSSSSSRKAEPLIYAGPIDPARRPDVFQEGFEDVSVTDDDN
XP_001822643.1 (A. oryzae) 34 AALLTMGYKPVLRHTYTFENFATTFEALYFVGGVVRTFSTGIAAGNLAYWTSYLVTH
XP_001400106.2 (A. niger) 36 RALLTMGYKPVLRHTYTFLENSTTFEALYFVGGVVRTSTGIAAGNLAYWTSYLVTH
XP_868888.1 (A. nidulans) 30 AALLTMGYKPVLRHTYTFENFATTFEALYFVGGVVRTFSTGIAAGNLAYWTSYLVTH
Thi9 (S. pombe) 61 NEILLTMGYKPVLRHTYTFEFSFPAFASLDVNSVVRTPESWGISFGPPAYWAMLVTH
XP_001822643.1 (A. oryzae) 94 VFTYITAAVIAEVCASPSAGSIYLWAEAGGPRFGRLLGFVAVWSTTAWTTFCASNTQ
XP_001400106.2 (A. niger) 96 VFTYITAAVIAEVCASPSAGSIYLWAEAGGPRFGRLLGFVAVWSTTAWTTFCASNTQ
XP_868888.1 (A. nidulans) 90 VFTYITAAVIAEVCASPSAGSIYLWAEAGGPRFGRLLGFVAVWSTTAWTTFCASNTQ
Thi9 (S. pombe) 21 FCQITLADCLADCSALHAGSIFLWAAASGPRFGRFSEVAVWSTTAWTTFCASNTQ
XP_001822643.1 (A. oryzae) 154 SAVNYMSELTVFVDFPDTSSVKFRAVQWICTEILLALAA LNFMPF YFRVWFVSS
XP_001400106.2 (A. niger) 156 SAVNYMSELTVFVDFPDTSSVKFRAVQWICTEILLALAA LNFMPF YFRVWFVSS
XP_868888.1 (A. nidulans) 150 SAVNYMSELTVFVDFPDTSSVKFRAVQWICTEILLALAA LNFMPF YFRVWFVSS
Thi9 (S. pombe) 181 STANLFAEITFNPEFNDSVKFRAVQWIAE LLVFTILLNPPYKRFKASM
XP_001822643.1 (A. oryzae) 214 FVYLDRLNFWLPIGANFWGFRABEAFMSTYNGTC-----
XP_001400106.2 (A. niger) 216 FVYLDFFLNFWLPIGANFWGFRABEAFMSTYNGTC-----
XP_868888.1 (A. nidulans) 210 FVYLDFFLNFWLPIGANFWGFRABEAFMSTYNGTC-----
Thi9 (S. pombe) 241 FVYLDVFNFWLPIGATKRWVTEITDQGYIKEVDANGNPIASLSKI
XP_001822643.1 (A. oryzae) 253 APAGWNWCLSYLATAGILIGFDASGHVAEETKHAS TAARGIFWSTVVSIGGLATIILE
XP_001400106.2 (A. niger) 255 APAGWNWCLSYLATAGILIGFDASGHVAEETKHAS TAARGIFWSTVVSIGGLATIILE
XP_868888.1 (A. nidulans) 249 APAGWNWCLSYLATAGILIGFDASGHVAEETKHAS TAARGIFWSTVVSIGGLATIILE
Thi9 (S. pombe) 301 VPKGNWCLSYLATAGILIGFDASGHVAEETKHAS TAARGIFWSTVVSIGGLATIILE
XP_001822643.1 (A. oryzae) 313 LFCAPPDITLFSFGS---PQPFVPLYAVVLGRGGHFMNVICIVALWLNATAIVAASR
XP_001400106.2 (A. niger) 315 LFCAPPDITLFSFGS---PQPFVPLYAVVLGGHFMNVICIVALWLNATAIVAASR
XP_868888.1 (A. nidulans) 309 LFCAN-----PATAIVAASR
Thi9 (S. pombe) 361 LFCEDLDITLFTALYNDNSPQPFVNFYSYLGRGGHVMNVITLLETLVNLSLVAASR
XP_001822643.1 (A. oryzae) 369 LVFAVARDGVLFPSSWVSKVHN--GPRNAVIVVMVVALICTLLPSDVAFVTSLSAAGV
XP_001400106.2 (A. niger) 371 LVFAVARDGVLFPSSWVSKVHN--GPRNAVIVVMVVALICTLLPSDVAFVTSLSAAGV
XP_868888.1 (A. nidulans) 324 LVFAVARDGVLFPSSWVSKVHN--GPRNAVIVVMVVALICTLLPSDVAFVTSLSAAGV
Thi9 (S. pombe) 421 LVFAVARDGVLFPSSWVSKVSKTQENAVVVALICTLLPSDVAFVTSLSAAGV
XP_001822643.1 (A. oryzae) 428 PSAAYGLICLARLCTPKRFPKPNWSLGRSKPQFIGVFNWGWVAVLFSPIYAFVPTG
XP_001400106.2 (A. niger) 430 PSAAYGLICLARLCTPKRFPKPNWSLGRSKPQFIGVFNWGWVAVLFSPIYAFVPTG
XP_868888.1 (A. nidulans) 383 PSAAYGLICLARLCTRNHPKPNWSLGRSKPQFIGVFNWGWVAVLFSPIYAFVPTG
Thi9 (S. pombe) 481 PSAAYGLVAFQRLFTKRDLPKGRNSLGRSKPCLVFNVALAVVNVSPYTPVPTG
XP_001822643.1 (A. oryzae) 488 ANLNYAPIIMAGVTIFALISYFMPPEAWLEDRISHFIDSKGAQATVEVERFSGDQG
XP_001400106.2 (A. niger) 490 ANLNYAPIIMAGVTIFALISYFMPPEAWLEDRISHFIDSKGAGVSVVEVWCSGNHR
XP_868888.1 (A. nidulans) 443 ANLNYAPIIMAGVTIFALISYFMPPEAWLEDRISHFIDSKGAVTETEVSTSR---
Thi9 (S. pombe) 541 PSFNVAWIMGVLFPACTIVTFRSRANRYRYESDSEHSASVIRKV-----
XP_001822643.1 (A. oryzae) 548 TSTPRL-----
XP_001400106.2 (A. niger) 550 QPEATSSSGREEN-----
XP_868888.1 (A. nidulans) -----
Thi9 (S. pombe) -----

```

Fig. 1-3. Comparison of amino acid sequences of Thi9 and the closest orthologs; *Aspergillus oryzae* XP_001822643.1, *Aspergillus nidulans* XP_001400106.2, and *Aspergillus niger* XP_868888.1. The location of the amino acid substitution found in mutant PTR1 is marked with an asterisk (R368H).

Investigation of the effect of loss of function of *thiI* using genome editing

Next, the author conducted genome editing using a CRISPR/Cas9 system targeting *thiI* to acquire a loss-of-function mutant to test the author's hypothesis. The target sequence was selected using web-based tools, and the sgRNA was prepared using an *in vitro* RNA synthesis kit. The recombinant protein introduction method was adopted because of its advantages (speed and ease of use). Introduction of the Cas9-RNA complex targeting *thiI* successfully generated 50–100 PT-resistant mutants in one procedure. PCR amplification and sequencing revealed several mutations around the *thiI* target sequence. Examples of the mutation variations are shown in Fig. 1-4.

The phenotype of *thiI* mutant was subsequently investigated. No significant difference was observed between the *thiI* mutant and the RIB40 wild type strain when grown on standard Czapek–Dox minimal agar and PDA (Fig. 1-5). Moreover, PT resistance phenotype of these mutants was compared with that of the *thiA*-de-repression mutant (*thiA*^{DR}), and no difference in growth rate was observed. Phenotypic analysis was also performed on thiamine-rich medium (1–10 mg/L thiamine was added to Czapek–Dox-based medium). The *thiI* mutant showed no growth defect compared to *thiA*^{DR} or WT (Fig. 1-6). Therefore, the phenotype of *thiI* mutant (positively selectable with no auxotrophy) was favorable for the use of *thiI* as a gene marker.

WT	CACGCCGTCGCGGGCTACGGCGAAGACGAGACGCGAGGCGGCTACGATTGCG
Mutant1	CACGCCGTCGCGGGCTACGGCGAAGACGAGACG--AGGCGGCTACGATTGCG
Mutant2	CACGCCGTCGCGGGCTACGGCGAAGACGAGACGCG-----CTACGATTGCG
Mutant3	CACGCCGTCGCGGGCTACGGCGAAGACGAG-----GCGGCTACGATTGCG
Mutant4	CACGCCGTCGCGGGCTACG-----ATTGCG
Mutant5	CACGCCGTCGCGGGCTACG----- (1800bp insertion) ----ATTGCG

Fig. 1-4. Sequences of *thiI* mutants generated by genome editing. Shaded sequence and boxed sequence indicate target sequence and protospacer adjacent motif (PAM), respectively.

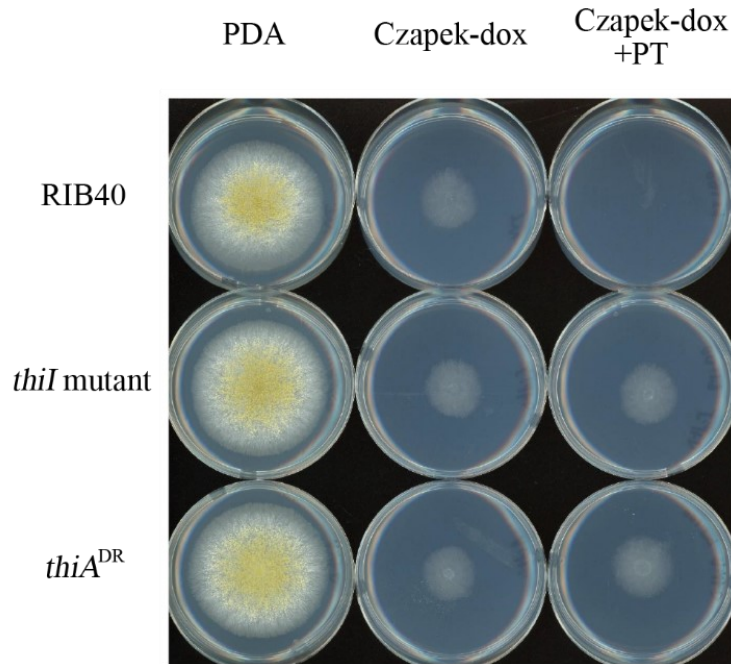


Fig. 1-5. Growth of *thiI* mutant. Wild type RIB40, RIB40 *thiI* mutant (*thiI* mutant), and RIB40 *thiA* de-repressed strain (*thiA*^{DR}) were grown on Czapek–Dox agar (with or without 0.1 mg/L pyrithiamine) and on potato dextrose agar (PDA) at 30°C for 5 days.

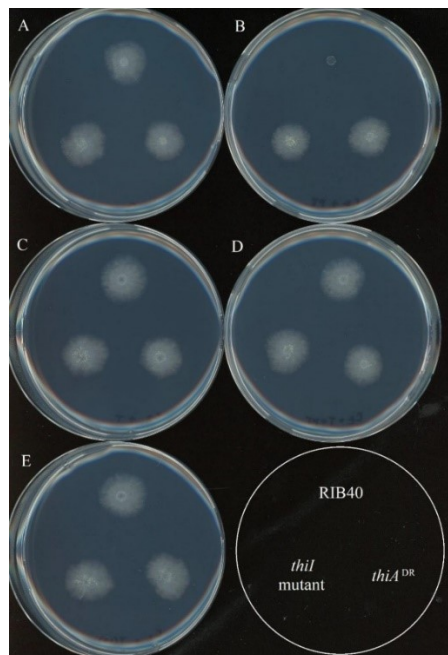


Fig. 1-6. Growth of *thiI* mutant. Wild type RIB40, RIB40 *thiI* mutant (*thiI* mutant), and RIB40 *thiA* de-repressed strain (*thiA*^{DR}) were grown on Czapek–Dox agar (A), Czapek–Dox agar with 0.1 mg/L pyrithiamine (B), Czapek–Dox agar with 1.0 mg/L thiamine (C), Czapek–Dox agar with 1.0 mg/L thiamine and 0.1 mg/L pyrithiamine (D), or Czapek–Dox agar with 10 mg/L thiamine (E) at 30°C for 5 days.

Use of *thiI* as a gene marker for genome co-editing

wA and *sreA* were employed as target genes because loss-of-function mutations in these genes could be easily observed by phenotypic appearance. The *wA* gene is a polyketide synthase involved in spore coloration (35), whereas *sreA* is a negative regulator of siderophore production (36). Loss-of-function mutations in these genes can be observed by whitened spore occurrence (5) or red-colored siderophore production (37). For genome co-editing, Cas9 proteins and sgRNA directed toward *thiI* or target gene (*wA* or *sreA*) were prepared separately, mixed in a 1:1 ratio, and then introduced into protoplasts using the PEG transformation method. Colonies were then transferred to the alternative medium (PDA supplemented with NaCl or FeSO₄·7H₂O) to count the number of loss-of-function mutants. Whitened spores or colored colonies that appeared on the plates are shown in Fig. 1-7. The loss-of-function mutants were counted to estimate the frequency of loss-of-function of the target genes. The frequency was estimated to be 5.5% and 8.2% for *wA* and *sreA*, respectively, from an average of three independent experiments (Table 1-2). Mutations around the target site were verified as shown in Fig. 1-8.

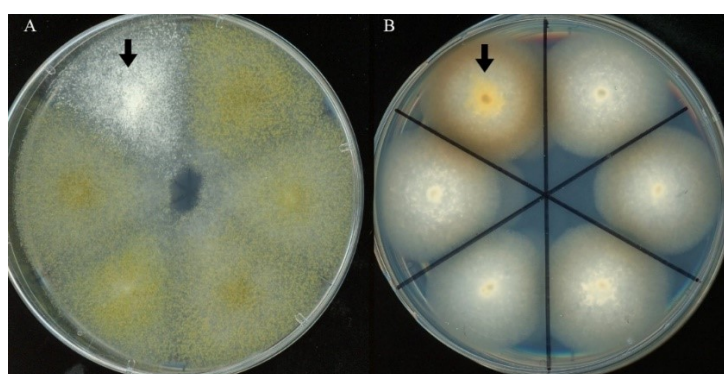


Fig. 1-7. Appearance of colonies obtained by genome co-editing of *thiI* and *wA* (A) and of *thiI* and *sreA* (B). Mutants that exhibited whitened spores or siderophore production are indicated by arrows. Pictures were taken from the upper side (A) and the bottom side (B), respectively.

A

```

WT      CTTCACCAGAATGCGGAGACAG-----GGGAGGCTCACCGT
Mutant1 CTTCACCAGAATGCGGAGACAGG---(1bp insertion)-GGGAGGCTCACCGT
Mutant2 CTTCACCAGAATGCGGAGACAG--(169bp insertion)-GGGAGGCTCACCGT
Mutant3 -----(400bp insertion)-GGGAGGCTCACCGT

```

B

```

WT      GAGCCGAAACCCGTGAAATCAAC-----AGGCGGCGGCGCGGA
Mutant1 GAGCCGAAACCCGTGAAATCAACC--(1bp insertion)-AGGCGGCGGCGCGGA
Mutant2 GAGCCGAAACCCGTGAAATCAAC--(65bp insertion)-AGGCGGCGGCGCGGA
Mutant3 GAGCCGAAACCCGTGAAATCAAC-(550bp insertion)-AGGCGGCGGCGCGGA
Mutant4 -----(42bp deletion)-----
Mutant5 -----(390bp deletion)-AGGCGGCGGCGCGGA

```

Fig. 1-8. Sequences of *wA* (A) and *sreA* (B) mutants generated by genome co-editing. Shaded sequence and boxed sequence indicate target sequence and protospacer adjacent motif (PAM), respectively.

Table 1-2. Number of mutants obtained by genome co-editing.

Target gene	Number of colonies		Target gene mutation frequency
	Pyrithiamine resistance	Target gene mutation	
<i>wA</i>	75	5	6.7%
	48	2	4.2%
	54	3	5.6%
<i>sreA</i>	42	3	7.1%
	36	2	5.6%
	51	6	11.8%

Discussion

In this study, the author identified a novel PT resistance marker gene *thiI*, and showed that this marker gene has application as a selectable marker in genome co-editing. Despite the long-term use of *A. oryzae* in basic studies and industrial applications, only a limited number of marker genes are known. Furthermore, only a few internal genes have practical application as markers for positive selection, including, *sC*, *niaD*, *pyrG*, and *thiA*. Despite their extensive use as positive selection markers, these four genes have their own disadvantages. The genes *sC* and *niaD* encode sulfate adenylyltransferase and nitrate reductase, respectively, and mutants harboring *sC* or *niaD* markers show impaired sulfate or nitrate utilization. The *pyrG* gene encodes an orotidine-5'-phosphate decarboxylase, and the use of the *pyrG* marker results in the loss of pyrimidine base biosynthesis. The *thiA* gene encodes a thiamine synthase, and PT resistance is acquired by a mutation in the 5' UTR of the gene, which acts as a riboswitch in thiamine synthesis regulation. Within the 5' UTR, mutation or deletion in a 13-bp sequence termed as region

A causes de-repression of thiamine synthesis, resulting in PT resistance. However, deletion of its immediately adjacent region of 23 bp, named as region B, causes just disruption of thiamine synthesis without acquiring PT resistance (7). Furthermore, in this study, the author identified several more variants of PT-resistant mutants, indicating a rather complicated mechanism that needs further elucidation. At present, application of *thiA* as a marker gene for genome editing is difficult when considering two limitations: first, shortness of the sequence for target site design, and second, mutation point and length cannot be precisely controlled in CRISPR/Cas9 genome editing. Thus, use of these markers had problems, i.e., causing auxotrophy or difficulty in application for genome editing. In contrast, use of *thiI* for genome co-editing has a distinct advantage compared to the use of the aforementioned conventional marker genes. *thiI* is preferred as a marker for genome editing because loss of *thiI* function does not cause auxotrophy. This is useful when investigating phenotypic changes caused by the effect of target gene loss-of-function, as comparison can be made using standard synthetic Czapek–Dox medium. Further study of *thiI* mutants on biological specimens such as plant leaves or steamed rice is also expected because mutants generated by other marker genes are auxotrophs and might have difficulty in growing on biological specimens on which supplementation of specific nutrients is difficult.

Although the author generated PT-resistant mutants by genome editing of *thiI*, there remains a possibility that PT resistance was the result of the gain of alternative function by the remaining part of the ThiI protein. The author also generated another mutant in which the whole *thiI* coding sequence was replaced by the gene expression cassette of interest with classical HR. The mutant showed the same growth phenotype (PT resistance and no auxotrophy), suggesting that the possibility mentioned above can be excluded.

The author also found that ThiI formed an ortholog cluster. The amino acid sequence

of ThiI from *A. oryzae* exhibited 79.3% and 85.8% identity to *A. nidulans* XP_001400106.2 and *A. niger* XP_868888.1, respectively. Although the function of these proteins has not yet been elucidated, amino acid sequence identities suggest that they function as thiamine transporters. Furthermore, phylogenetic analysis indicated no additional closely related proteins in these genomes, suggesting that these orthologous genes are also the only thiamine transporters in their respective genomes. Whether *thiI* homologous genes in other *Aspergilli* also have applications as PT resistance markers requires further investigation.

It is noteworthy that PT resistance conferred by *thiI* mutations is recessive because ThiI is supposed to function as a thiamine transporter. This is in contrast to the PT resistance conferred by mutations within the 5' UTR of *thiA*, which are dominant because ThiA functions as a thiamine synthetase. The different resistance mechanisms may explain why the author could acquire only a single *thiI* mutant from 10 PT resistant mutants after selection from UV-irradiated spores. In this regard, increasing the proportion of uninucleate protoplasts may improve the efficiency of genome editing with *thiI*. For example, increasing the proportion of uninucleate conidia using filter separation or medium modification (38) is expected to further increase the genome editing efficiency using *thiI* as a marker.

In this study, the author employed *sreA* as a target gene for the estimation of co-editing efficiency. Although colony coloration was reported in *sreA* loss-of-function mutants, this is the first report to show that *sreA* is a useful gene to study transformation efficiency just by looking at the colony appearance, similar to the phenotype of *wA*. Further study for *sreA* mutants is also expected because the siderophore produced by *A. oryzae* has application as a food additive and repression by iron is a problem for siderophore production as mentioned in Chapter II.

In this study, the author investigated genome co-editing by direct introduction of Cas9/sgRNA ribonucleoprotein. The direct introduction method shows several advantages compared to transformation using a plasmid that stably expresses Cas9. First, constant expression of Cas9 may be toxic and can decrease the rate of mutant survival (22). Secondly, although isogenicity is a prerequisite for industrial applications of genome editing species, unintended integration of plasmid DNA into the genome frequently occurs, resulting into loss of isogenicity. Genome co-editing using *thiI* as performed in the present study will be a good choice for the transformation of *A. oryzae*.

Summary

In this study, a novel PT resistance marker was investigated considering its potential applications in genome editing. A mutant resistant to PT was selected from UV-mutagenized *A. oryzae* RIB40. Whole genome analysis was conducted on the mutants, and a novel candidate gene for PT resistance was identified. This candidate gene exhibited similarity to the thiamine transporter gene *thi9* of *Schizosaccharomyces pombe* and was designated as *thiI*. A *thiI* loss-of-function mutant was generated using the CRISPR/Cas9 genome editing system to investigate its effect on PT resistance. This mutant showed PT resistance and exhibited no growth defect or auxotrophy. The *thiI* gene was further investigated for its use as a selection marker in genome co-editing. Ribonucleoprotein complex comprising recombinant Cas9 nuclease and sgRNA targeting *thiI* or another target gene (*wA* or *sreA*) was prepared and simultaneously introduced into *A. oryzae* RIB40. *thiI* and target gene double loss-of-function mutants were efficiently selected on PT-containing medium. *thiI* was shown to be a useful marker gene in *A. oryzae* for use in genome editing. This study is expected to provide insights, which will promote basic research and industrial applications of *A. oryzae*.

Section 2

Development of high-efficiency targeted knock-in method using CRISPR/Cas9 in *Aspergillus oryzae*

As mentioned in Section I, genome editing technologies have enabled the acquisition of targeted knock-out mutants without the laborious host strain preparation. On the other hand, acquiring targeted knock-in mutants is still laborious since it is based on HR, wherein long length homology (usually > 500 bp) of the template is essential (1,8). Recently, two alternative DNA DSB repair pathways, namely MMEJ and SSA, have been employed as targeted knock-in methods in combination with genome editing technologies in mammalian cells (9). Compared with HR, MMEJ/SSA requires a shorter homology length of the template, thereby making template preparation easier. However, the application of MMEJ/SSA in *A. oryzae* has not been sufficiently studied.

In the present study, the author examined the efficiency of targeted knock-in mediated by CRISPR/Cas9 and MMEJ/SSA in *A. oryzae*. This approach enabled the efficient development of targeted knock-in transformants without host preparation using only a short homology template.

Materials and methods

Strains and medium

Escherichia coli strain DH5 α (Takara Bio, Shiga, Japan) was used for plasmid propagation. It was cultured according to a standard protocol (39). The *A. oryzae* strains RIB40 and RIB40 Δ *ligD* (1) were used as host strains for the transformation assay to determine knock-in efficiency. Medium compositions are described in Section 1.

Preparation of vectors and transformation

The fragments were amplified by PCR using the genome of RIB40 as the template. KOD-FX Neo (Toyobo Co., Ltd., Osaka, Japan) was used for PCR according to the manufacturer's protocol. To evaluate the CRISPR/Cas9-mediated knock-in efficiency, the PT resistance marker *ptrA* (27) and *sodM* promoter (*PsodM*)(40) were conjugated and inserted into the 5' UTR region of the glucoamylase gene *glaB*, neutral protease gene *nptB*, and aspartic protease gene *pepA* (*PglaB*, *PnptB*, and *PpepA*, respectively). For vector preparation, the pPTRI-*PsodM* plasmid was prepared as follows. The original pPTRI plasmid (Takara Bio, Shiga, Japan) harboring the *ptrA* sequence was linearized using inverse PCR. *PsodM* amplified from the RIB40 genome was then inserted into the linearized vector using an In-Fusion cloning kit (Takara Bio, Shiga, Japan). Subsequently, the *ptrA;PsodM* fragment flanked by 0, 15, 30, or 50 bp homology arms (HAs) homologous to *PglaB* was prepared by PCR using pPTRI-*PsodM* as the template. The HA sequences are indicated in Fig. 2-1. Similarly, the *ptrA;PsodM* fragment flanked by 0, 15, or 50 bp HAs homologous to *PpepA* and *PnptB* sequence were prepared. The HA sequences are indicated in Fig. 2-2. For genome editing, Cas9 nuclease (EnGen Cas9 NLS; New England Biolabs Inc., MA, USA) and the sgRNA synthesis kit (EnGen sgRNA Synthesis Kit, *S. pyogenes*; New England Biolabs Inc., MA, USA) were used according to the manufacturer's instructions. The CRISPR/Cas9 target sequences specific to each target region were designed and prepared as mentioned in Section 1. The ribonucleoprotein complex was prepared using 20 μM (3.22 $\mu\text{g}/\mu\text{L}$) Cas9 and 20 μM sgRNA (0.65 $\mu\text{g}/\mu\text{L}$) dissolved in a buffer supplied by the supplier to a final volume of 5 μL (5 μg as Cas9 protein). Cas9/sgRNA ribonucleoprotein complexes were prepared immediately prior to transformation. Transformation procedure was mentioned in Section 1.

enzyme. Total RNA was extracted from the mycelia using ISOGEN (Nippon Gene, Tokyo, Japan) with DNase I treatment. *glab* expression was estimated using the One Step TB Green™ PrimeScript™ RT–PCR Kit (Takara Bio, Shiga, Japan). Thermal Cycler Dice (Takara Bio, Shiga, Japan) was used for real-time PCR. The expression levels were normalized to the internal standard (histone H2B gene) and shown as relative to the control strain using the $2^{-\Delta\Delta C_t}$ method (41). The primer sequences used for real-time PCR are listed in Table 2-1.

Bioinformatics analysis

For bioinformatics analysis, genomic DNA was extracted from the mycelia using ISO Plant II (Nippon Gene, Tokyo, Japan) with RNase treatment. DNA sequencing was performed using a commercial service (Fasmac Co., Ltd., Kanagawa, Japan) with a 3730xl DNA Analyzer (Thermo Fisher Scientific, MA, USA). The primer sequences used for PCR are listed in Table 2-1.

Statistical analysis

The transformation assays and fermentation experiments were performed using three independent procedures. The results are shown as the mean \pm standard deviation of three independent experiments. Statistical significance was determined by one-way analysis of variance (ANOVA) followed by the Tukey–Kramer test to compare more than three groups or by the two-tailed unpaired Student's *t*-test to compare with the control. Excel Statistics 2015 for Windows (Social Survey Research Information Co., Ltd., Tokyo, Japan) was used for the calculations. Statistical significance was set at $p < 0.05$.

Table 2-1. Oligonucleotide sequences used in the present study

Oligonucleotide name	Sequence (5'-3')	Description
pPTRI_for_single_strand_1	GAGCTGATTTAACAAA AATTTAACG	Linearization of the pPTRI
pPTRI_for_single_strand_2	ATTTTTTAACCAATAG ACCGAAATC	Linearization of the pPTRI
pPTRI_sodM_Inf_F	TTGTTAAATCAGCTCA TTCGAGCTCGGTAC	Amplification of the <i>sodM</i> promoter region for cloning into linearized pPTRI
pPTRI_sodM_Inf_R	TATTGGTTAAAAAATT TTGGGTGGTTTGGT	Amplification of the <i>sodM</i> promoter region for cloning into linearized pPTRI
0HA_1	GGCAATTGATTACGGG ATCC	Amplification of <i>ptrA;PsodM</i> fragment without homology arms
0HA_2	TTTGGGTGGTTTGGTT GGTA	Amplification of <i>ptrA;PsodM</i> fragment without homology arms
15HA_PglaB_1	ATGAGGCAGCCAACA GGCAATTGATTACGG	Amplification of <i>ptrA;PsodM</i> fragment with 15 bp homology arms targeting <i>PglaB</i>
15HA_PglaB_2	ATGACTGTAGCTGTTT TTGGGTGGTTTGGT	Amplification of <i>ptrA;PsodM</i> fragment with 15 bp homology arms targeting <i>PglaB</i>
30HA_PglaB_1	AAATTCTCACTGCGAA TGAGGCAGCCAACAG GCAATTGATTACGG	Amplification of <i>ptrA;PsodM</i> fragment with 30 bp homology arms targeting <i>PglaB</i>
30HA_PglaB_2	TCCAAGAAACAAGAA ATGACTGTAGCTGTTT TTGGGTGGTTTGGT	Amplification of <i>ptrA;PsodM</i> fragment with 30 bp homology arms targeting <i>PglaB</i>
50HA_PglaB_1	TCGCGCTATAAAGAGA CCTGAAATTCTCACTG CGAATGAGGCAGCCA ACAGGCAATTGATTAC GG	Amplification of <i>ptrA;PsodM</i> fragment with 50 bp homology arms targeting <i>PglaB</i>
50HA_PglaB_2	TCCGCATGATGGTGGT GACTTCCAAGAAACAA GAAATGACTGTAGCTG TTTTTGGGTGGTTTGG T	Amplification of <i>ptrA;PsodM</i> fragment with 50 bp homology arms targeting <i>PglaB</i>
RNAsyn_PglaB	TTCTAATACGACTCAC TATAGAAATGACTGTA GCTGTTTGTGTTTTAG AGCTAGA	Synthesis of sgRNA specific to <i>glaB</i> 5'UTR region, target sequence: AAATGACTGTAGCTGTTTGT
<i>glaB</i> _forKnockInC_heck_F	GGTAAATGTCATGCAG CCCCG	Amplification of the <i>glaB</i> 5' UTR region for sequencing
<i>glaB</i> _forKnockInC_heck_R	AGCGGTCTTGAGGGTA GGAT	Amplification of the <i>glaB</i> 5' UTR region for sequencing
15HA_PnptB_1	ACTATAAAGCCCTCGG GCAATTGATTACGG	Amplification of <i>ptrA;PsodM</i> fragment with 15 bp homology arms targeting <i>PnptB</i>
15HA_PnptB_2	AGAGTCGCTGGACAAT TTGGGTGGTTTGGT	Amplification of <i>ptrA;PsodM</i> fragment with 15 bp homology arms targeting <i>PnptB</i>

Table 2-1. Oligonucleotide sequences used in the present study (continued)

Oligonucleotide name	Sequence (5'-3')	Description
50HA_PnptB_1	CTATTTTGAAGGCCAT CAGACCAGAAGGAAT CGAGACTATAAAGCCC TCGGGCAATTGATTAC GG	Amplification of <i>ptrA</i> ; <i>PsodM</i> fragment with 50 bp homology arms targeting <i>PnptB</i>
50HA_PnptB_2	TACTCAACAAGCTGAA TTGTCTTGAATCTAAG TGAAGAGTCGCTGGAC AATTTGGGTGGTTTGG T	Amplification of <i>ptrA</i> ; <i>PsodM</i> fragment with 50 bp homology arms targeting <i>PnptB</i>
RNAsyn_PnptB	TTCTAATACGACTCAC TATAGAAGAGTCGCTG GACAACGAGTTTTAGA GCTAGA	Synthesis of sgRNA specific to <i>nptB</i> 5'UTR region, target sequence: GAAGAGTCGCTGGACAACGA
nptB_forKnockInCheck_F	TGGCGGTTTGGAAAGA AGGG	Amplification of the <i>nptB</i> 5' UTR region for sequencing
nptB_forKnockInCheck_R	TGGCAAGGCCTGAAG AAGTG	Amplification of the <i>nptB</i> 5' UTR region for sequencing
15HA_PpepA_1	AAGAGTCTGAGTTCGG GCAATTGATTACGG	Amplification of <i>ptrA</i> ; <i>PsodM</i> fragment with 15 bp homology arms targeting <i>PpepA</i>
15HA_PpepA_2	AAGACAAGCCTAGAT TTGGGTGGTTTGGT	Amplification of <i>ptrA</i> ; <i>PsodM</i> fragment with 15 bp homology arms targeting <i>PpepA</i>
50HA_PpepA_1	CCTGAGTAGCTCATCA CTCTCCCATCCTCTCC ACAAGAGTCTGAGTT CGGGCAATTGATTACG G	Amplification of <i>ptrA</i> ; <i>PsodM</i> fragment with 50 bp homology arms targeting <i>PpepA</i>
50HA_PpepA_2	AAGACGGAACGAAAG ACTGGATGTGAAAGA ATGACAAGCACAAGC CTAGATTTGGGTGGTT TGTT	Amplification of <i>ptrA</i> ; <i>PsodM</i> fragment with 50 bp homology arms targeting <i>PpepA</i>
pepA_forKnockInCheck_F	GGGTGAGCTTGTAAC GGGC	Amplification of the <i>pepA</i> 5' UTR region for sequencing
pepA_forKnockInCheck_R	GATGGTGAATCCCCGA CGAG	Amplification of the <i>pepA</i> 5' UTR region for sequencing
glaB_realtime_F	CGCATCCGTCCTTCCC TATC	Amplification of <i>glaB</i> for quantitative real-time PCR
glaB_realtime_R	AGGCTACAACGATACC AGCG	Amplification of <i>glaB</i> for quantitative real-time PCR
histonH2B_realtime_F	GGAATCTCCACTCGTG CCAT	Amplification of histone H2B for quantitative real-time PCR
histonH2B_realtime_R	ATAAGCGGCCAGTTTG GAGG	Amplification of histone H2B for quantitative real-time PCR

Results

CRISPR/Cas9-mediated knock-in efficiency in *A. oryzae*

The author investigated whether the efficiency of targeted knock-in transformation can be improved by the use of CRISPR/Cas9 genome editing, wherein a recombinant Cas9 protein/sgRNA ribonucleoprotein complex and a knock-in template were simultaneously introduced. RIB40 and RIB40 Δ *ligD* were used as the hosts for the assay. The *glaB* gene was used as the target, since GlaB protein production can be evaluated easily using an enzymatic assay. The genome editing target site was selected from the *PglaB* sequence, wherein the expected cleavage site was -47 bp from the start codon. A knock-in template harboring the PT resistance marker *ptrA* and *PsodM* flanked by 0-, 15-, or 50-bp sequence homologous to *PglaB* was introduced, as shown in Fig. 2-1. The HAs that were 15 and 50 bp in size corresponded to the required lengths of MMEJ (2–20 bp) and SSA (> 25 bp) reported in mammalian cells, respectively (42). After selection based on PT resistance, the mutants were further analyzed for the sequence around the CRISPR/Cas9 target site to confirm whether the intended knock-in had occurred. As shown in Fig. 2-3A, when the RIB40 wild type was used as the host, precise knock-in transformants could be obtained with the use of Cas9 protein whereas no such transformants were acquired without Cas9 protein. The number of correct transformants was higher with the 50 bp HA template, approximately six transformants per procedure. On the other hand, fewer than two transformants were acquired with 0 or 15 bp HA templates. Furthermore, the author conducted the experiment with the Δ *ligD* host, which lacks an NHEJ repair pathway, to investigate the relationship of NHEJ with this knock-in transformation mechanism (Fig. 2-3B). When HA templates of > 15 bp were used, > 50 transformants were acquired per procedure; in contrast, no transformants were acquired with the 0 bp HA template.

To further investigate the trend in knock-in efficiency, an additional comparison of 30 and 50 bp HA was conducted. As shown in Fig. 2-4, the number of transformants was higher with 50 bp HA when using the RIB40 wild type; however, no significant difference was observed when RIB40 Δ *ligD* was used as the host.

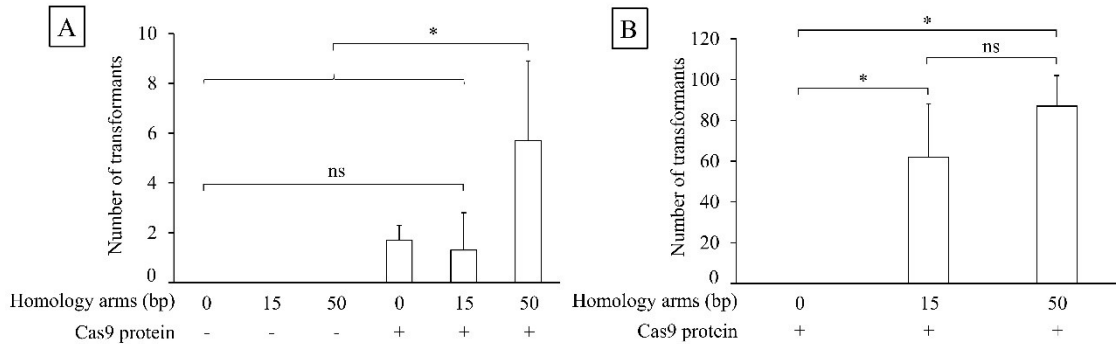


Fig. 2-3. Efficiency of targeted knock-in transformation. The numbers represent the acquired mutants targeting the *glbB* upstream region using RIB40 wild type (A) and RIB40 Δ *ligD* (B). Amount of template DNA and Cas9 protein: 5 μ g each. The numbers are presented as the mean \pm standard deviation of three independent experiments. Asterisks indicate significant differences ($p < 0.05$). ns, not significant.

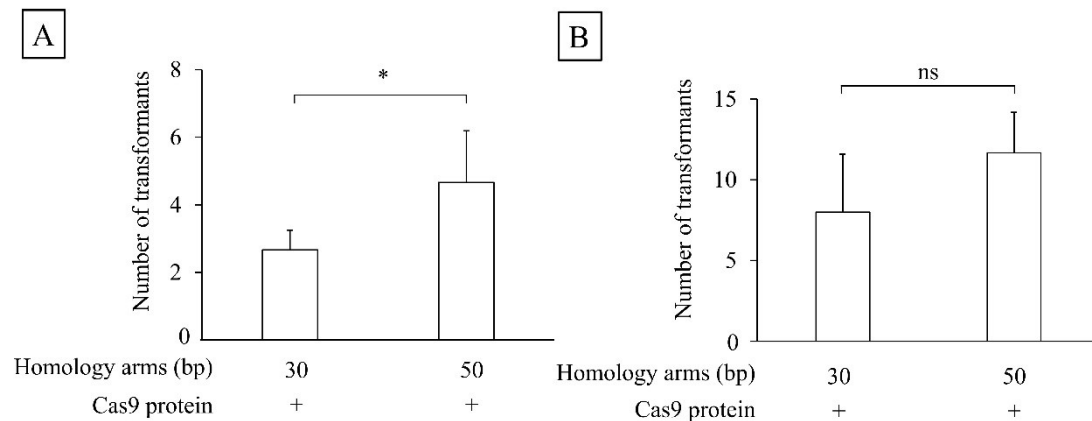


Fig. 2-4. Efficiency of targeted knock-in transformation. The numbers represent the acquired mutants using RIB40 wild type with 5 μ g each of template DNA and Cas9 protein (A), and RIB40 Δ *ligD* with 1 μ g each of template DNA and Cas9 protein (B). The numbers are presented as the mean \pm standard deviation of three independent experiments. Asterisks indicate significant differences ($p < 0.05$). ns, not significant.

Finally, two additional target genes, *nptB* and *pepA*, were tested to assess the versatility of the knock-in system. As shown in Fig. 2-5, 50 bp HAs were the most effective, resulting in approximately 9 to 20 transformants per procedure. Overall, these results show that HA lengths for targeted knock-in can be drastically shortened compared with those needed for the traditional method.

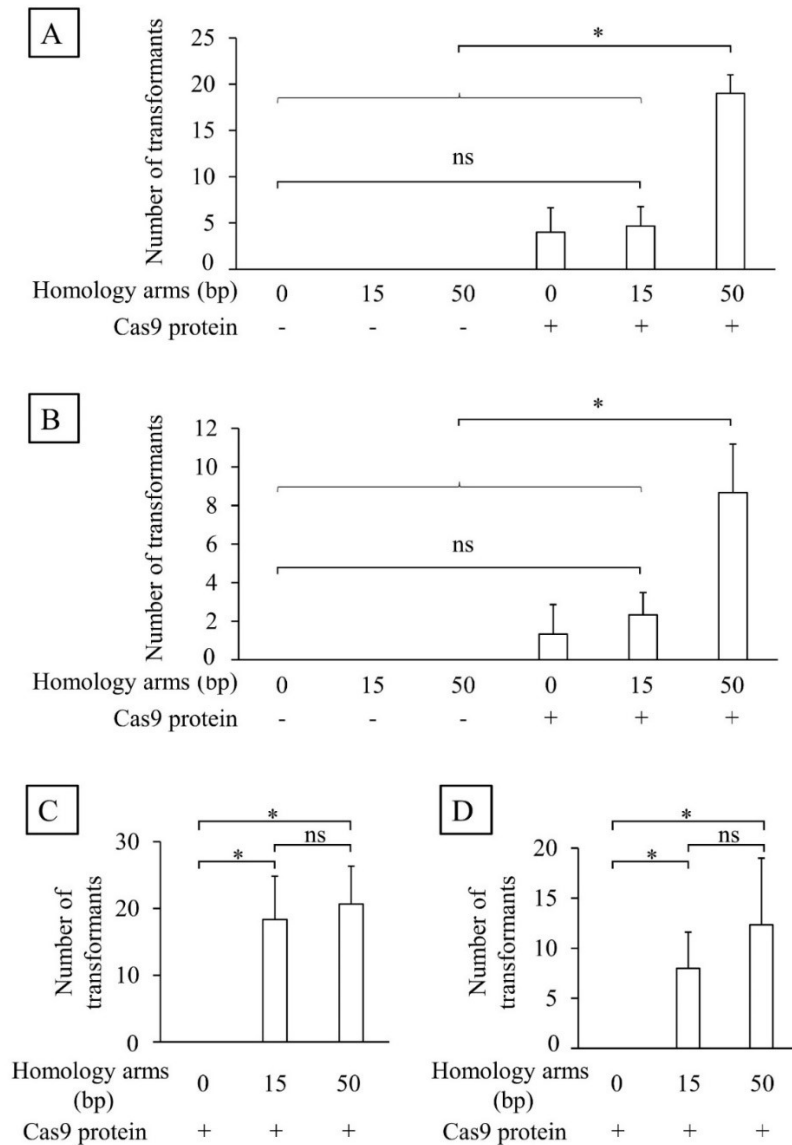


Fig. 2-5. Efficiency of targeted knock-in transformation. The numbers represent the acquired mutants from RIB40 wild type with 5 μ g each of template DNA and Cas9 protein targeting *nptB* (A) and *pepA* (B), and from RIB40Δ*ligD* with 1 μ g each of template DNA and Cas9 protein targeting *nptB* (C) and *pepA* (D). Data represent the mean \pm standard deviation of three independent experiments. Asterisks indicate significant differences ($p < 0.05$). ns, not significant.

Effect of promoter knock-in

Next, to confirm the effect of integrated cassettes, the *glaB* gene expression in the precise knock-in strain was analyzed by real-time quantitative PCR. As shown in Fig. 2-6A, compared with the host strains, precise *PsodM* knock-in transformants (*PsodM:glaB*) expressed higher levels of *glaB*. These differences were assumed to be the result of different regulations. Native *PglaB* is strongly repressed during submerged fermentation (43), whereas *PsodM* shows strong expression under these conditions (40). Furthermore, the increased GlaB production was confirmed using an enzymatic assay of glucoamylase activity. As shown in Fig. 2-6B, the enzymatic assay revealed a significant increase in glucoamylase activity in *PsodM:glaB* when compared with that in the host strain, thereby indicating that GlaB was functionally secreted. Taken together, these results indicate that the CRISPR/Cas9-mediated knock-in of *PsodM* effectively increased target gene expression.

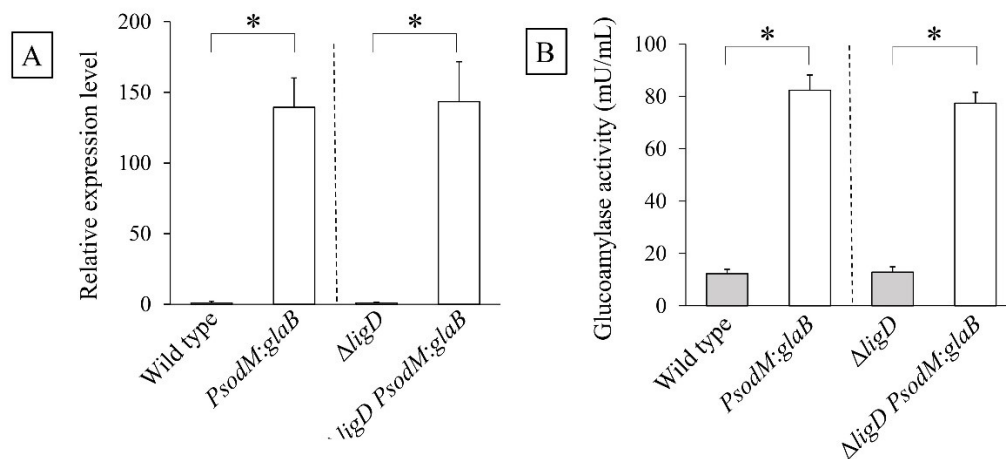


Fig. 2-6. Confirmation of *glaB* gene expression. (A) *glaB* gene expression estimation using quantitative real-time PCR. The expression levels were normalized to that of histone H2B and are shown relative to the control strain. (B) Glucoamylase activity estimation. The values of the transformants were compared with those of the control strain (gray) and are shown as the mean \pm standard deviation of three independent experiments. Asterisks indicate significant differences ($p < 0.05$).

Discussion

Repair pathway choice in *A. oryzae* after CRISPR/Cas9 associated DNA DSB

The present study showed that the targeted knock-in transformation of *A. oryzae* becomes easier by using the CRISPR/Cas9 system. Furthermore, some novel insights were observed. As shown in Fig. 2-3, 50 bp length was sufficient to efficiently obtain precise knock-in transformants when CRISPR/Cas9 was used. It is notable that there were a few correct transformants with the 0 bp HA template when using RIB40 as the host strain, although there were no obvious homologies between the target site and template sequences (Fig. 2-3A). These strains are believed to result from the NHEJ repair pathway, which can join two blunt ends, as they were not observed when using the $\Delta ligD$ strain as the host strain (Fig. 2-3B). The higher knock-in efficiency with 50 bp HA suggests the involvement of the SSA repair pathway. Considering the poor knock-in efficiency in the control procedure (without Cas9), SSA mediated knock-in is not efficient when the genome DNA is intact. Additionally, knock-in transformation was frequent in the $\Delta ligD$ background with 15 to 50 bp HA templates. This indicates that both MMEJ and SSA repair pathways exist independent of *ligD* and are promoted by *ligD* disruption in *A. oryzae*. This is consistent with a previous report on *A. fumigatus* using CRISPR/Cas9 and a template with 39 bp HAs (44). However, the author's result is inconsistent with a previous report on *A. oryzae* using TALENs, wherein decreased MMEJ efficiency was indicated in $\Delta ligD$ (4). Considering that TALENs create DNA DSB with overhangs(45) and CRISPR/Cas9 generates blunt ends (46), the difference in cleavage site may have influenced the activity of the repair pathway. In addition, the amount of the donor DNA differed because this study used temporal DNA fragments, while the former used self-reproducing plasmid as the DNA template (4).

CRISPR/Cas9-mediated knock-in as a novel genetic engineering method

As shown in Fig. 2-3 and Fig. 2-5, CRISPR/Cas9-mediated knock-in was effective in obtaining the targeted knock-in transformant for three different target sites. The number of acquired mutants varied depending on the target sites, likely owing to the impact of target spacer sequences on CRISPR/Cas9 cleavage efficiency (3). Furthermore, the *PsodM* knock-in strain produced significantly more functional proteins when compared with the host strain (Fig. 2-6). As a targeted knock-in system, CRISPR/Cas9-mediated knock-in has some advantages over classical HR-based knock-in. First, it is useful that targeted knock-in can be accomplished without the preparation of the host. To date, most genetic engineering studies on *A. oryzae* have been conducted using a limited number of model strains such as RIB40 because of the laborious process for the preparation of an NHEJ-disruptant host strain, despite the fact that industrially important *A. oryzae* strains have a wide diversity of secretory hydrolases and secondary metabolites (47). The preparation of an NHEJ-disruptant strain has other disadvantages in addition to the laborious process; for example, it may induce undesirable mutations in the host, because developing an NHEJ-disruptant strain requires preparing auxotroph mutants as the first step (1,2), which is usually accomplished by UV irradiation or chemical mutagens. Furthermore, the permanent loss of NHEJ lacks a vital DNA repair pathway and may affect fitness, such as sensitivity to irradiation (48) or ethyl methanesulfonate (1). Considering these disadvantages and the limitation of the host strain, CRISPR/Cas9-mediated knock-in is preferred from the perspective of the host strain.

Second, the laborious steps for preparing the vector can be reduced. In HR-based knock-in, constructs harboring HAs of approximately > 500 bp need to be prepared for each target locus (1). The process is usually completed by several repeated cycles of PCR, plasmid construction, and subcloning into *E. coli*, as shown in Fig. 2-7. In contrast, in

CRISPR/Cas9-mediated knock-in, template preparations are much easier once the basic plasmid harboring a marker and knock-in purpose, such as a promoter, is prepared. For example, using the plasmid prepared in the present study, another targeted knock-in vector can be prepared with only a single PCR. Furthermore, CRISPR/Cas9-mediated knock-in will also be applicable to other systems, such as GFP knock-in. Taken together, CRISPR/Cas9-mediated knock-in is advantageous over classical HR-based methods, although further experiments using other strains are needed to confirm the versatility of this method. However, CRISPR/Cas9-mediated knock-in has a limitation in that the Cas9 target site requires the 5'-NGG-3' PAM (46). Recently, other variations of CRISPR systems with different PAM recognition, such as CRISPR/Cas9-NG (49) and CRISPR/Cpf1 (50), have been successfully applied to yeast (51) and *A. oryzae* (52). The use of these alternative genome editing technologies may aid in overcoming this limitation. Overall, the use of the CRISPR/Cas9-mediated knock-in system will facilitate the acquisition of targeted knock-in transformants, especially from industrially important non-model strains of *A. oryzae*. Furthermore, there are fewer studies on genome editing with SSA/MMEJ in microorganisms compared with mammalian cells. While there are relatively more reports on the model microorganism *Saccharomyces cerevisiae*, *S. cerevisiae* differs from many other fungi in its preferential use of HR repair (53). In other fungi, although the number of reports using genome editing is increasing, studies utilizing SSA/MMEJ are limited to several species (54) such as *A. fumigatus* (44), *Magnaporthe oryzae* (55), and *Rhizopus microspores* (56). Therefore, the results obtained in this study will be beneficial for future research on filamentous fungi.

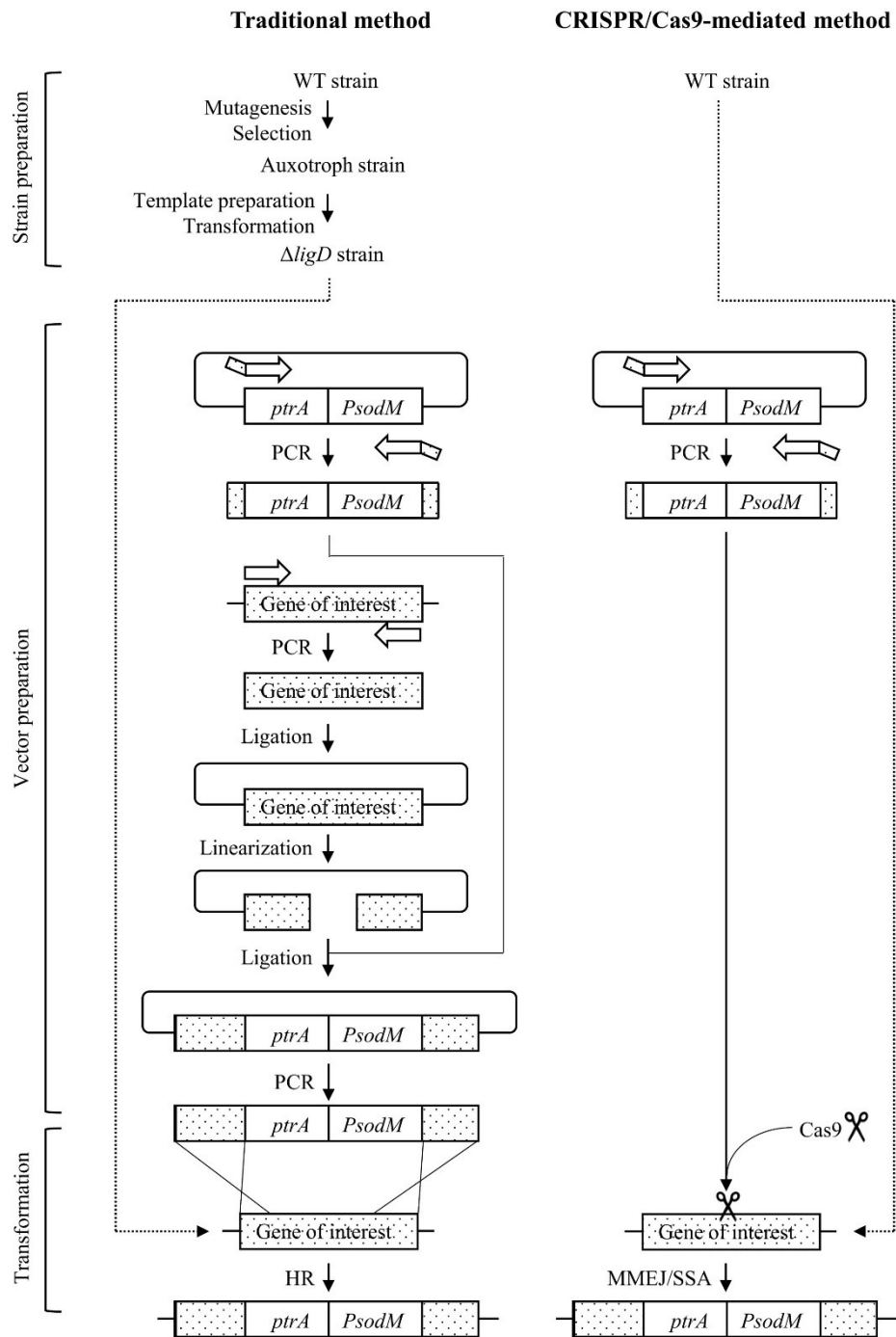


Fig. 2-7. Comparison of experimental flow of targeted knock-in transformation. Flow for the (left) classical method and (right) CRISPR/Cas9-mediated method.

Summary

In the present study, the author examined alternative targeted knock-in mediated by CRISPR/Cas9, in which MMEJ and SSA repair system was employed. This approach enabled the efficient development of targeted knock-in transformants without host preparation using only a short homology template. The author conclude that this new method could be applied to facilitate the transformation of *A. oryzae*, and will make it easier to acquire targeted knock-in transformants, especially from industrially important non-model strains.

Section 3

Identification of the gene responsible for the production of the precursor of the off-flavor compound 4-vinylguaiacol in sake

In this Section, the abovementioned genome editing technology was utilized to elucidate the unknown mechanism of 4-VG production in sake brewing. 4-VG is an important phenolic compound found in various alcoholic beverages, with its unique flavor described as “spicy” or “smoky”. 4-VG is essential for several types of beer, such as Weizenbier beer (57), however, 4-VG is an undesired off-flavor for most other beer styles, wine, and sake (10). In these alcoholic beverages, 4-VG is formed from its precursor ferulic acid (4-hydroxy-3-methoxycinnamic acid) via enzymatic conversion by *Saccharomyces cerevisiae* or other contaminant microorganisms such as *Bacillus* spp. (11) and *Lactobacillus* spp. (12). In *S. cerevisiae*, phenylacrylic acid decarboxylase (*PADI*) and ferulic acid decarboxylase (*FDCI*) are required for 4-VG formation, and loss of function of either of the two proteins diminishes 4-VG production (13). Although *S. cerevisiae* strains used for sake brewing have lost their ability to produce 4-VG because of the loss of function of *FDCI* (14), 4-VG formation due to contamination by wild yeast and bacteria remains a problem, as it reduces sake quality (15).

In sake brewing, ferulic acid, the precursor of 4-VG, is thought to be released from feruloyl polysaccharide by feruloyl esterase produced by *Aspergillus oryzae* or *S. cerevisiae*. A previous study has shown the relationship between the feruloyl esterase activity of *koji* and formation of 4-VG (58). In addition, in beer brewing, the contribution of *S. cerevisiae* to the release of ferulic acid has been indicated (59). However, microorganisms that play a major role in the release of ferulic acid in sake brewing have not yet been identified. Feruloyl esterases are classified into four types (A to D) based on

their substrate specificity (60) and 13 subfamilies (SF1 to SF13) based on their phylogeny (61). Previous studies have identified genes categorized for all four types of feruloyl esterases in *A. oryzae*, namely *AofaeA*, *AofaeB*, *AofaeC*, and *AofaeD* (hereafter simply referred to as *faeA*, *faeB*, *faeC*, and *faeD*, respectively) (12–14).

In this study, the author assessed the role of FaeA in 4-VG formation in sake brewing. For this purpose, the author constructed a *faeA*-deficient strain by genome co-editing using RIB40 as the host. *Koji* and sake were fermented using these strains, and their quality was evaluated. This study elucidated that FaeA is responsible for the release of ferulic acid in sake mash, indicating that future breeding targeting FaeA will help prevent 4-VG formation and improve the quality of sake.

Materials and methods

Strains and media

The *A. oryzae* strain RIB40 was used as the host for genome co-editing. RIB40 Δ *thiI*, prepared as described in Section 1 was used as the control strain for the comparison with the *faeA*-deficient strain obtained by genome co-editing. Medium compositions used for *A. oryzae* transformation are described in Section 1. The *S. cerevisiae* strain G046 in the author's library was screened by preliminary test for sake brewing. This strain showed a high alcohol productivity similar to sake yeast and high 4-VG productivity similar to wild yeasts. The presence of both functional *PADI* and *FDCI* in the G046 genome was further confirmed by whole genome sequence analysis (Data not shown). For sake brewing, *S. cerevisiae* G046 was precultured in YPD medium and used for fermentation as described below.

Selection of the target gene and construction of a mutant strain by genome co-editing

For the selection of the target gene that plays the major role in the release of ferulic acid, the activity of FaeA, FaeB, FaeC, and FaeD at pH 4.0, around which sake is fermented, was investigated on the basis of previous reports as summarized below. FaeA exhibited the optimum activity under acidic conditions, wherein the highest activity was observed at pH 5.0, and approximately 80% of this activity was observed at pH 4.0 (62). Both FaeB and FaeC exhibited the optimum activity at pH 6.0, and only approximately 5% and 15% of this activity, respectively, was retained at pH 4.0 (13). FaeD exhibited the optimum activity at pH 7.0, and only 10% of this activity was observed at pH 4.0 (63). Thus, *faeA* (AO090001000207) was selected as the target for genome editing, as FaeA was expected to show the highest activity in sake mash among the four feruloyl esterases. To test this hypothesis, a *faeA*-deficient strain was constructed by genome co-editing using the CRISPR/Cas9 genome editing system (3). Briefly, genome co-editing is a modified genome editing method, in which two genes are simultaneously targeted for disruption. For genome co-editing, Cas9 nuclease (EnGen Cas9 NLS) and sgRNA synthesis kit (EnGen sgRNA Synthesis Kit, *S. pyogenes*) were used according to the manufacturer's instruction (New England Biolabs Inc., MA, USA), as mentioned in the Section 1. To generate a *faeA*-deficient strain using genome editing, the target sequence specific for *faeA* was designed using the web-based program CRISPRdirect (29) with the *faeA* mRNA sequence as template (XM_001818700.1). In genome co-editing, two types of RNA-protein complexes consisting of recombinant Cas9 nuclease and sgRNA targeting either *faeA* or *thiI* (marker gene) were simultaneously introduced into RIB40 cells using the protoplast PEG transformation method as mentioned in Section 1. The target sequence and oligonucleotide template sequence used for sgRNA synthesis are shown in Table 3-1.

Table 3-1. Oligonucleotide sequences used in the study.

Oligonucleotide name	Sequence (5'-3')	Description
RNA _{syn} AO090001 000207	TTCTAATACGACTCACTATAGTT TCCCGCACTGGTGATTGCGTTTT AGAGCTAGA	synthesis of sgRNA specific to AO090001000207 target sequence: TTTCCCGCACTGGTGATT GC
AO090001000207 P 480073	GGGTTTCGATACCTCTGCCC	Primer for amplification and sequencing of AO090001000207
AO090001000207_ M481382	TTCACACAACCAGCACTCCA	Primer for amplification and sequencing of AO090001000207

Bioinformatics analysis

To validate the mutations induced by genome editing, genomic DNA was extracted from the PT-resistant mutants. The *faeA* gene was amplified by PCR using KOD-FX Neo (Toyobo Co., Ltd., Osaka, Japan) according to the manufacturer's instructions. Sequencing was performed using 3730xl DNA Analyzer (Thermo Fisher Scientific, MA, USA). The primer sequences used for PCR are listed in Table 3-1. The deduced amino acid sequence of the mutant *faeA* gene was compared with native amino acid sequences of FaeA from *Aspergillus niger* CBS 513.88 (XP_001393337) and *A. oryzae* RIB40 (XP_001818752.1).

Preparation of *koji* and sake

For *koji* preparation, rice (Nipponbare) was polished to a weight of 72%. The polished rice was then soaked in water at 4°C for 16 h, steamed for 30 min, and cooled to 35°C. Next, the spores of *A. oryzae* (50 mg/kg) were inoculated onto the steamed rice, which was then incubated at 35°C and 90% humidity in a humidity chamber (LHL-114; ESPEC Corp., Osaka, Japan) for 44 h.

Small-scale sake fermentation was performed as follows. First, *S. cerevisiae* strain G046 was precultured in YPD medium at 30°C for 24 h. Next, the precultured *S. cerevisiae* (2.3×10^9 cells) were inoculated to a mixture of 120 mL of water, 95 g of steamed rice, 12 g of *koji*, and 20 μ L of lactic acid. The mixed mash was fermented at 15°C for 14 days. Fermentation was monitored by examining CO₂ emission, as indicated by the weight loss of the sake mash. The sake mash was then centrifuged at $8000 \times g$ for 10 min at 4°C. The supernatant was heated at 65°C for 10 min, cooled to 25°C, and immediately used for further analysis, or stored at 4°C until its use for sensory evaluation.

Enzyme activity assay

To analyze the enzymatic activity of *koji*, 5 g of *koji* was mixed with 25 mL of extraction buffer (0.01 M sodium acetate–acetic acid buffer at pH 5.0, containing 5 g/L NaCl) in a 50-mL conical tube, followed by incubation at 20°C for 3 h at 60 rpm reciprocal shaking. The mixture was then centrifuged at $8,000 \times g$ for 20 min, and the supernatant was used as the crude enzyme. Saccharification and α -amylase activities were measured using a commercial assay kit (Kikkoman Biochemifa Company, Tokyo, Japan). The enzyme activities are shown by enzyme units as defined by the official method of the National Tax Agency of Japan (64). Feruloyl esterase activity was measured as previously reported (65) using methyl ferulate (MFA) as a substrate with sodium acetate–acetic acid buffer (pH 4.0). Enzyme activity was expressed as unit/g *koji*, where 1 unit is defined as the release of 1 μ mol ferulic acid per min at 37°C.

Analysis of sake

To measure ethanol concentration, the sake was distilled and analyzed using a density/specific gravity meter DA-650 (Kyoto Electronics Manufacturing Co. Ltd., Kyoto, Japan). Acidity and amino acid levels were measured using an automatic potentiometric titrator AT-710 (Kyoto Electronics Manufacturing Co. Ltd., Kyoto, Japan) according to the method of the National Tax Agency of Japan. Ferulic acid content in sake was determined by high performance liquid chromatography (HPLC)-photo diode array using an LC-20A series system (Shimadzu Corporation, Kyoto, Japan), according to the previously reported method (65). 4-VG content was measured by headspace gas chromatography-mass spectrometry (HS-GC-MS) using a GCMS-QP2020 NX and HS-20 Trap system (Shimadzu Corporation, Kyoto, Japan). For sensory evaluation, an equal volume of sake fermented in three independent experiments (stored from 3 to 18 days) were mixed and used. Quantitative descriptive analysis was performed by nine panels of experts. The panels were chosen from the sake manufacturing company and trained for detection of off-flavors in sake using standard addition method, in which 4-VG concentration was set at 530 $\mu\text{g/L}$ as 90% detection threshold (66). The experts evaluated the sake according to the basic procedure of sake tasting (67) at room temperature (20°C) in a blinded manner. 4-VG level in each sample was evaluated using a 5-point scale ranging from 1 (weak) to 5 (strong). The experts also indicated whether they could detect 4-VG in the samples. In sensory evaluation, the experiment was conducted in agreement with the Declaration of Helsinki and was approved by the Ethical Committee of Gekkeikkan Research Institute. Panelists aged 20 years or older voluntarily participated in the experiments, and they were informed as well as they agreed that the samples contained alcohol and were produced using a genetically modified organism.

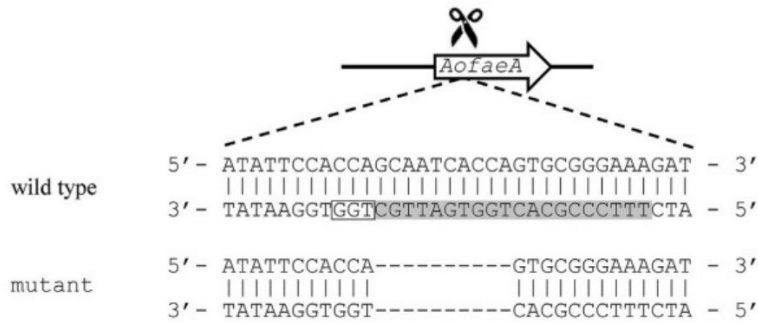
Statistical analysis

Koji and sake fermentation was performed as a series of experiments that were repeated three times independently. The results are shown as mean \pm standard deviation. Differences were evaluated using the two-tailed unpaired Student's *t*-test for parametric data (quantitative analysis) and Wilcoxon signed-rank test for non-parametric data (sensory analysis). A *p*-value of <0.05 was considered statistically significant.

Results

Construction of a *faeA*-deficient strain

To generate a *faeA*-deficient strain, genome co-editing was conducted using the *thiI* gene marker. Following selection by PT resistance, which indicates the loss of *thiI* gene function, the author obtained approximately 30 candidate colonies. Eight randomly chosen PT-resistant mutants were further investigated by sequence analysis of the *faeA* gene. One mutant harboring a 10-bp deletion in *faeA* was obtained. This frame shift mutation caused the loss of the native function of the gene of this mutant strain (hereafter referred to as $\Delta faeA$) (Fig. 3-1). Under standard culture conditions on Czapek-dox agar plates or YPD agar plates, there were no obvious morphological changes or growth defects in the $\Delta faeA$ strain compared with the control $\Delta thiI$ strain (Fig. 3-2A and B).

A**B**

AnFaeA	<u>MKQFS</u> AKYALILLATAGQALAASTQGIS	EDLYNRLVEMATISQAAYADLCNIPSTIIKGE
AoFaeA	MKNFFSMHAILLACSAGAGLAAITQGIS	EGTYSRIVEMATISQAAYANLCNIPPAITSAG
AoFaeA (mutant)	MKNFFSMHAILLACSAGAGLAAITQGIS	EGTYSRIVEMATISQAAYANLCNIPPVRRERST
AnfaeA	KIYNAQTDINGWILRDDTSKEIITVFRGT	GSDTNLQLDNTYTLTPFDTLPCNDCEVHGG
AoFaeA	KIYNAETDINGWVLRDDSRQEIITVFRGT	GSDTNLQLDNTYTPAFDTLPCSCGCAVHGG
AoFaeA (mutant)	MQRRI	STGGFFETIAVKK-----
AnfaeA	YYIGWISVQDQVESLVKQQASQYPDYALT	VTGHS [*] LGASMAALTAQLSATYDNVRLYTFG
AoFaeA	YYVGWVSVKDQVEGLIHQQASQYPDYS	LVVTGHS [*] LGASMAAITAAQLSATYNNITVYTFG
AoFaeA (mutant)	-----	-----
AnfaeA	EPRSGNQAFASYMNDAFQVSSPETTQYFR	VTHSNDGI [*] PNLPPAEQGYAHGGVEYWSVDPY
AoFaeA	EPRTGNQAYASYVDETFQATNPDATKFYR	VTHTNDGI [*] PNLPPTSQGYVHHGTEYWSVEPH
AoFaeA (mutant)	-----	-----
AnfaeA	SAQNTFVCTGDEVQCCEAQGGQGVNDAHT	TYFGMTSGACTW [*]
AoFaeA	GPQNMYLCLGDEVQCCEAQGGQGVNDAHV	TYFGMASGACTW
AoFaeA (mutant)	-----	-----

Fig. 3-1. Sequence analysis of *faeA* mutant obtained by genome editing. (A) Structure and comparison of nucleotide sequence of native *faeA* of *A. oryzae* RIB40 (AO090001000207, *AofaeA*) with its mutant strain. The sgRNA spacer sequence was designed to target the antisense strand of *faeA* as shown in shaded. PAM sequence is shown in box. (B) Comparison of amino acid sequences of the deduced amino acid sequence of the mutant *faeA* gene, *Aspergillus niger* CBS 513.88 XP_001393337 (AnFaeA), and *A. oryzae* RIB40 XP_001818752.1 (AoFaeA). N-terminal residues of AnFaeA shown in box are signal peptides removed in the secreted protein. Asterisks show the previously reported catalytic triad essential for enzyme function.

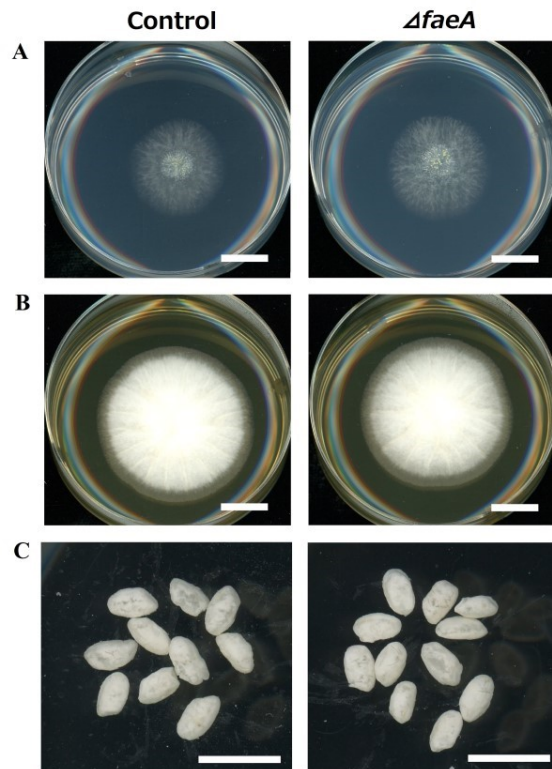


Fig. 3-2. Comparison of the growth of $\Delta faeA$ with control. (A) Growth on Czapek-dox agar plate at 30°C for 3 days. (B) Growth on YPD agar plate at 30°C for 3 days. (C) Growth on steamed rice at 35°C for 44 h (*koji*). Scale bar = 10 mm.

Estimation of enzyme activity of *faeA*-deficient strain

The author next produced *koji* by fermenting rice with the $\Delta faeA$ strain and the control $\Delta thiI$ strain. *Koji* was produced according to a traditional procedure using 72% polished rice. No morphological differences or growth defects were observed in the *koji* fermented with $\Delta faeA$ strain compared with that of the control strain (Fig. 3-2C). Enzyme activity in sake fermentation was analyzed using enzymes extracted from *koji* (Table 3-2). There were slight differences in saccharification and α -amylase activities ($p = 0.21$ and 0.07 , respectively) between the control and $\Delta faeA$ strains, but the differences were not significant. Next, the author analyzed feruloyl esterase activity using MFA as a substrate. The feruloyl esterase activity of the *faeA*-deficient strain was reduced to approximately 40% of that of the control ($p < 0.01$).

Table 3-2. Analysis of the enzyme activity of *koji*.

	Control	$\Delta faeA$
Saccharification activity (U/g)	269±12	282±10
α -amylase activity (U/g)	1462±65	1596±66
Feruloyl esterase activity (U/g)	39.6±2.5	17.3±0.6*

Mean \pm standard deviation, * $p < 0.05$.

Sake fermentation and 4-VG analysis using *faeA*-deficient strain

Next, sake was fermented using *koji* and *S. cerevisiae* strain G046, which exhibits functional *PADI* and *FDC1*. The sake fermented using $\Delta faeA$ *koji* showed a similar fermentation profile to the control sake, as shown by CO₂ emission (Fig. 3-3). The general profile of the sake (alcohol content, acidity, amino acid content, and glucose content) was determined (Table 3-3). The values were not significantly different between the control and $\Delta faeA$, although alcohol concentration was slightly higher in $\Delta faeA$ *koji* ($p = 0.10$). However, there was a significant difference in the ferulic acid concentration. Ferulic acid was reduced to 13% of that in the control sake. Furthermore, 4-VG content was measured by HS-GC-MS. Sake fermented using $\Delta faeA$ *koji* showed a significantly lower 4-VG level, which was reduced to 10% of that of the control sake. The effect of this 4-VG reduction was also evaluated by sensory analysis using nine expert panels. Sensory evaluation also showed a significant difference in acceptance. 4-VG intensity was significantly lower in $\Delta faeA$ *koji* sake, with only 2 of 9 expert panels noticing 4-VG in the sake, whereas 9 of 9 panels noticed 4-VG in the control sake.

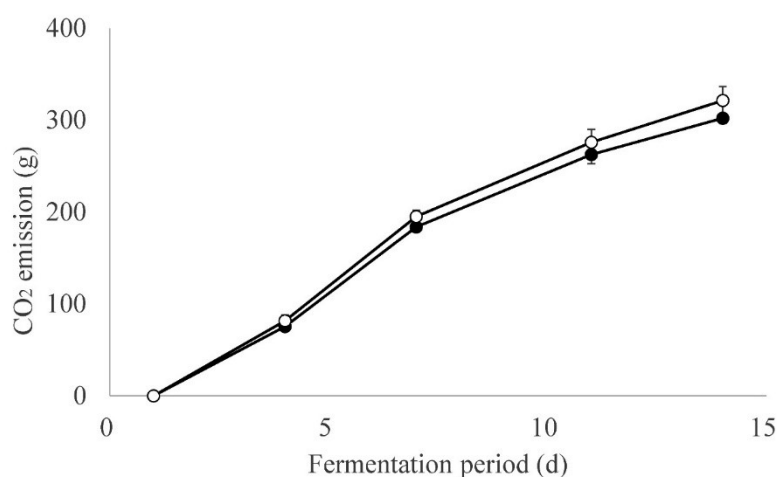


Fig. 3-3. Sake fermentation profiles. Sake fermentation profile was determined by monitoring CO₂ emissions, as estimated by the loss of weight. Data are shown as the mean \pm standard deviation of three independent studies. The sake mash was prepared on day 1. Closed circles, control; opened circles, $\Delta faeA$.

Table 3-3. Analysis of sake.

	Control	$\Delta faeA$
Analytical value		
Alcohol (% v/v)	15.6 \pm 0.2	15.9 \pm 0.2
Acidity (ml)	3.3 \pm 0.2	3.3 \pm 0.1
Amino acid content (ml)	1.3 \pm 0	1.3 \pm 0
Glucose (g/dL)	0.3 \pm 0	0.2 \pm 0
Weight loss (g/kg rice used)	302 \pm 5	321 \pm 15
Ferulic acid (mg/L)	24.1 \pm 1	3.2 \pm 0.2*
4-VG (μ g/L)	1479 \pm 150	157 \pm 33*
Sensory evaluation		
Evaluation score	3.7 \pm 1.1	1.2 \pm 0.6*
4-VG detectability	9 of 9	2 of 9

Mean \pm standard deviation, * $p < 0.05$

Discussion

Construction of a *faeA*-deficient strain by genome co-editing

In this study, the author produced a *faeA*-deficient strain via genome co-editing using the CRISPR/Cas9 system and *thiI* gene marker. Obtaining the mutant strain was easier using this system than using the classical genetic strategy because the laborious process to construct a vector was bypassed, and host strain (*ligD* or *ku70* deficient) preparation for improved HR efficiency (1,2) was not necessary. In this study, the author obtained a strain harboring a mutation in the *faeA* gene that caused a frame shift at alanine 55 and a stop codon mutation at residue 79 (Fig. 3-1 B). In the closely related *A. niger* FaeA homolog, whose function has been well studied, loss of the conserved serine 133 residue (the sequence excludes the 21 amino acid N-terminal signal sequence), which is essential to the catalytic machinery, led to complete loss of its activity (68). In the mutant the author constructed, the deduced amino acid sequence is truncated to 78 amino acids (including the 21 amino acid hypothetical N-terminal signal sequence) and the active site serine corresponding to that of *A. niger* is lost; this mutation is thought to cause the complete loss of its native feruloyl esterase activity.

Enzyme activity of Δ *faeA* *koji*

The author prepared *koji* using the Δ *faeA* strain. Saccharification activity and α -amylase activity were not significantly different between the Δ *faeA* and control strain. It appeared that the loss of the *faeA* gene had little effect on the productivity of these enzymes. Feruloyl esterase activity assay using MFA showed a reduced activity in Δ *faeA* *koji*, which was estimated to be 40% of that of the control *koji*. The remaining feruloyl esterase activity in Δ *faeA* *koji* is supposed to be derived from any of other feruloyl esterases (FaeB, FaeC, and FaeD), which still exist in the strain. It is noteworthy that the

results of feruloyl esterase activity assay using MFA were not in accordance with the results observed for ferulic acid concentration in sake. Ferulic acid content in the $\Delta faeA$ sake was only 13% of that in the control sake. This is most likely explained by the difference in enzyme specificity toward the substances. In rice, ferulic acid is present as a component of feruloyl polysaccharide (26), and various feruloyl esterases are known to act on various substances (70). FaeA of *A. oryzae* may show higher activity toward feruloyl polysaccharide from rice, and the effect of its loss was more obvious in sake brewing conditions than in the model conditions using MFA.

Reduction in ferulic acid release and 4-VG content in sake using $\Delta faeA$ koji

Although a previous study has reported the feruloyl esterase activity in *A. oryzae*, the effect of *koji* on ferulic acid release in sake mash and the gene responsible for this effect in *A. oryzae* are unknown (71). This is the first study to clearly demonstrate the role of *A. oryzae* in ferulic acid release and to identify the gene *faeA* responsible for this role, as the author showed that ferulic acid and 4-VG productions were obviously reduced using $\Delta faeA$ koji. Sensory evaluation also revealed a significant change in 4-VG detection. Several studies have investigated the 4-VG threshold, ranging from approximately 30 to 440 ppb (9,29,30). In general, thresholds are estimated to be lower when evaluated in model conditions such as water or synthesized model liquid, and to be higher when evaluated in real fermented products. Sunao et al. reported that the 4-VG threshold of sake seems to be higher than 140 ppb in their study using a model liquid (73). The data obtained in this study support this, as only 2 of 9 expert panels noticed 150 ppb 4-VG in sake.

The results validated the hypothesis that *A. oryzae* FaeA is the major enzyme that causes the release of ferulic acid in sake mash, and that the loss of FaeA function results

in the reduction of ferulic acid and 4-VG content in sake. Although Coghe et al. have previously indicated the existence of feruloyl esterase activity in *S. cerevisiae* beer strain under beer fermentation conditions (59), in the author's results it is unlikely that feruloyl esterase from *S. cerevisiae* plays a significant role in sake mash. This is in accordance with the result reported by Mo et al. that *S. cerevisiae* showed no feruloyl esterase activity under Chinese rice wine brewing conditions (74). Dilokpimol et al. investigated putative feruloyl esterase genes among 247 fungal genomes and found that cellulose-degrading species such as *Aspergillus* spp., *Fusarium* spp., and *Aureobasidium* spp. have multiple putative feruloyl esterase genes; however, no putative feruloyl esterase genes were found in *Pichia* spp., *Saccharomyces* spp., and *Shizosaccharomyces* spp. (61). Considering that the function of feruloyl esterases is to enhance hemicellulose hydrolysis by removing ferulic acid crosslink (75), it is reasonable to assume that *S. cerevisiae* does not exhibit feruloyl esterase genes and activity. The lack of putative feruloyl esterase genes in *S. cerevisiae* is in contrast with the fact that *PAD1* and *FDC1* are generally retained in this species except industrial yeasts (2). This difference may be explained by the function of Pad1 and Fdc1, which are involved in the detoxification of phenylacrylic acids found in plant cell walls (5).

Future applications of *A. oryzae* *faeA*-deficient strain

Although *S. cerevisiae* strains used for sake brewing have usually lost their ability to produce 4-VG, it is difficult to completely avoid contamination by other microorganisms. In particular, high-class sakes such as Daiginjo-shu, which are often products of handiwork, are more susceptible to contamination by microorganisms that can convert ferulic acid to 4-VG (15). Therefore, a strategy to reduce the risk of sake spoilage by

reducing the precursor of 4-VG seems reasonable. As shown in this study, the use of *A. oryzae faeA*-deficient strains will be the best choice.

Because of consumer demand for more variety in sake, sake brewed using *S. cerevisiae* other than the traditional sake yeast is gaining increasing attention. One of the limitations in the screening of wild yeasts is their 4-VG productivity, considering that wild yeasts tend to possess active Pad1 and Fdc1 (10). Thus, only few wild yeasts screened from the natural environment can be suitable for sake brewing (76). Therefore, exploring another strategy to avoid 4-VG production independent of yeast strain, as shown in this study, will be helpful for the future use of wild yeast for sake brewing.

In this study, the author produced a *faeA*-deficient strain by genome editing. The use of gene-deletion mutants acquired by genome editing in the food industry is permitted in countries such as Japan and the United States after a precise administrative procedure (77). Nevertheless, understanding of its safety by consumers seems to need more time. From this perspective, further studies are needed to establish a screening method for *faeA*-deficient strains among naturally occurring mutants so that the advantages shown in this study (prevention of 4-VG formation caused by contamination and the use of more variable wild yeast strains) will be more helpful.

Summary

In this study, the author investigated the effect of FaeA on 4-VG formation in sake. The FaeA loss-of-function strain was produced by genome co-editing. The feruloyl esterase activity of the *faeA*-deficient strain was drastically reduced. Sake was fermented using *koji* with *S. cerevisiae* strain G046, which can convert ferulic acid to 4-VG. Fermented sake was analyzed by measuring the 4-VG content and sensory evaluation. 4-VG content was reduced to approximately 10% of that of sake fermented with control

koji. Sensory evaluation revealed that 4-VG was almost undetectable. The author's findings showed that disruption of *faeA* in *A. oryzae* is a promising strategy to reduce 4-VG off-flavors in sake.

Chapter II

Development of production technology for the iron chelator deferriferrichrysin from *Aspergillus oryzae* and evaluation of its functional properties in food applications

Section 1

Production of deferriferrichrysin and evaluation as a novel food-grade antioxidant

Lipid oxidation in foods is a serious problem that causes a loss of nutritional quality and increases the risk of diseases such as atherosclerosis (78), and cancer. (79,80) Metal chelators such as ethylenediaminetetraacetic acid (EDTA) are used to prevent lipid oxidation in foods because metals, especially iron, are the main catalyst of lipid oxidation (16). Recently, increasing demand for natural products has led to the exploration of natural alternatives of EDTA such as gallic acid (81), phytic acid (16), lactoferrin (16), and citric acid (82). These compounds, however, have not shown satisfactory results, likely because of their lower binding constant to iron and lower stability compared to EDTA (16).

Siderophores are small iron-chelating compounds produced by microorganisms that bind ferric ion with high affinity and specificity; the typical binding constant to Fe^{3+} reaches 1.0×10^{30} (83), whereas that of EDTA is approximately 1.3×10^{25} (84). Siderophores could potentially be used for therapeutic applications such as treating or preventing iron overload (85), Alzheimer's disease (86), anemia caused by iron deficiency (87), atherosclerosis (88), and cancer (89,90). Despite these beneficial effects, commercialized food-grade siderophore products are not available. An obvious obstacle that prevents the further application of siderophores is their low production by host organisms, as siderophore production is easily repressed by only a small amount of iron (91).

Dfcy is a cyclic hexapeptide siderophore produced by *A. oryzae* and related species. Dfcy binds ferric ion with high affinity and specificity to become its iron-chelated form ferrichrysin (Fcy). Fcy is known as an unwanted by-product of sake because it is responsible for unfavorable red coloration in sake (92), although no other sensory changes occur. Therefore, studies of Dfcy have focused mainly on the reduction or removal of Fcy in sake brewing. For example, through the attempt to remove Fcy from sake, a novel fucose-specific lectin was discovered (93,94). However, Dfcy is a desirable candidate for a food-grade iron-chelator because of its safety for consumption, as it has long been ingested along with sake, which contains 4–14 mg/kg Dfcy and/or 0–7 mg/kg Fcy (92).

In this study, the author produced Dfcy by submerged culture of *A. oryzae* and also evaluated it as a food-grade antioxidant. First, the author optimized the medium composition in shake flasks and investigated the effects of agitation and aeration conditions on Dfcy production using stirred tanks. Second, the author evaluated the safety of the fermentation products and measured the stability of Dfcy and Fcy at various temperatures and pH. Finally, the author evaluated its antioxidant activity in an O/W emulsion.

Materials and methods

Strains

A. oryzae strain F0 was selected from the author's library of strains reserved for sake brewing after screening for high Dfcy production. To further increase Dfcy production, strain F70-9 was obtained by UV mutagenesis of strain F0 and selection according to its higher productivity of Dfcy. Loss of aflatoxin productivity in F0 and F70-9 was confirmed by sequencing of the aflatoxin synthesis gene cluster (95). Further investigation of mycotoxin productivity is described below.

Flask experiments

The basal medium was prepared based on Czapek-Dox minimal medium (28) modified with the following compounds per liter of distilled water: 1 g of K₂HPO₄, 0.5 g of

MgSO₄·7H₂O, 0.5 g of KCl, 30 g of sucrose, 5 g of NaNO₃, and 3 g of sodium carboxymethylcellulose (CMC). The initial pH was adjusted to 5.0 using 0.1N HCl. To identify the optimal nitrogen source, NaNO₃ as the sole nitrogen source in the basal medium was replaced with the following alternative nitrogen sources: (NH₄)₂SO₄, yeast extract (YE), or hydrolysate of sake lees (SLH). All media with different nitrogen sources contained equal amounts of nitrogen. To identify the optimal carbon source, sucrose was replaced with the following alternative carbon sources: glycerol, glucose, fructose, maltose, or potato starch. All carbon sources were added to the medium at a concentration of 30 g/L. To investigate the inhibitory effect of iron on Dfcy production, the basal medium was supplemented with 20–200 µg/L iron as FeSO₄. The total iron concentration of the medium was determined by colorimetric assay using FerroZine[®](96). For flask experiments, 40 mL of medium in a 100-mL Erlenmeyer flask was inoculated with 4.0 × 10⁷ spores of *A. oryzae* strain F0 scraped from PDA and incubated on a rotary shaker at 120 rpm at 30°C for 64 h. Flask experiments were performed in triplicate.

Preparation of hydrolysate of sake lees

The production scheme of sake and sake lees used in this study is shown in Fig. 4-1. Sake lees are a by-product of sake brewing. The sake lees were crushed and suspended in water, and the slurry was hydrolyzed with protease from *A. oryzae* (Sumizyme LP; Shin Nihon Chemical Co., Ltd., Aichi, Japan) at 50°C for 16 h. The hydrolysate was then heated at 80°C for 10 min to inactivate the enzyme. The absence of Dfcy in SLH was confirmed by analyzing a 2.0% suspension of SLH by HPLC as described in the analytical methods section below.

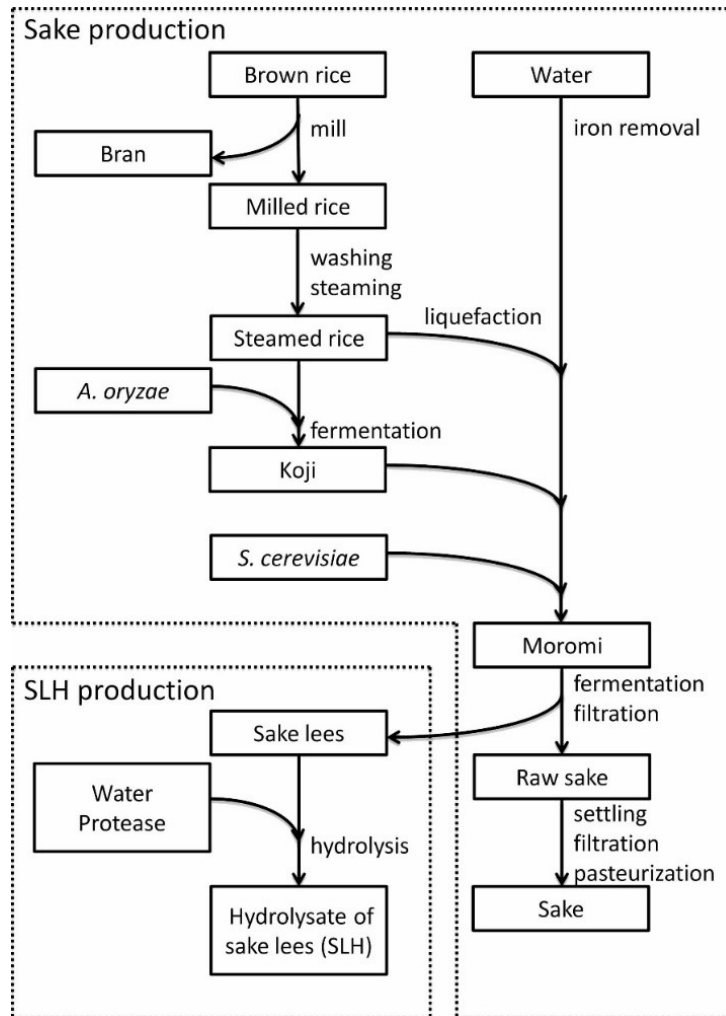


Fig. 4-1. Production scheme for sake and sake lees hydrolysate. For sake production, brown rice is milled and washed to remove the outer layer, which is rich in minerals containing iron. Milled rice is then steamed and inoculated with spores of *Aspergillus oryzae* and fermented to form Koji. Iron is removed from the water, and the water is mixed with Koji, steamed rice, and cultured *Saccharomyces cerevisiae* and fermented to generate *Moromi*. *Moromi* is then filtered to separate raw sake and sake lees. For SLH preparation, sake lees were then hydrolyzed by protease.

Stirred tank experiments

For stirred tank experiments, *A. oryzae* F70-9 was pre-cultured in 300-mL Erlenmeyer flasks under the same fermentation conditions used for the flask experiments described above, with 100 mL of medium containing 1 g of K_2HPO_4 , 0.5 g of $MgSO_4 \cdot 7H_2O$, 0.5 g of KCl, 30 g of glycerol, 17 g of SLH, 2 g of $(NH_4)_2SO_4$, and 3 g of CMC per liter of distilled water. A 4-day seed culture (300 mL) was transferred to a 5-L stirred tank (KMJ-

5C; Mitsuwa Frontech Corp., Osaka, Japan) equipped with two Rushton turbine impellers (six-bladed, 70-mm diameter) with a 3-L working volume. The medium used had the same composition as the seed culture medium, except that CMC was omitted and an antifoaming agent (Adekanol LG-109; ADEKA Corp., Ltd., Tokyo, Japan) was added at a concentration of 0.25 g/L. Food-grade ingredients were used to prepare the medium for stirred-tank experiments. Fermentation was performed at 30°C with an agitation rate of 300 rpm and an aeration rate of 0.67 vvm (2.0 L/min) unless indicated otherwise. The pH was maintained at 4.0 using 0.1N NaOH and 0.1N H₂SO₄, and 80 mL of 500 g/L glycerol was fed at 64 and 96 h. Stirred tank experiments were performed in duplicate.

Analytical methods

For Dfcy quantification, the culture broth was centrifuged at 13,000 × g for 3 min and the supernatant was filtered through a 0.45-µm polyvinylidene fluoride filter (Millex[®]; Merck Millipore Corp., Billerica, MA, USA). Then, 100 µL of fluid flow-through was mixed with 20 µL of ferric solution containing 3 g/L ferric citrate such that Dfcy was converted to Fcy. The Fcy concentration of the mixture was then analyzed by HPLC according to the method of Konetschny-Rapp *et al* (97). To measure fungal growth, 5 mL of culture broth containing fungal biomass was filtered with pre-weighed filter paper (No. 101; Toyo Roshi Kaisha, Ltd., Tokyo, Japan), washed, dried in an oven at 105°C for 3 h, and weighed.

Determination of the chemical composition

For determination of the chemical composition of the crude extract of fermented *A. oryzae* culture, a crude extract of the culture broth from the stirred tank was prepared by centrifugation and filtration as described above except that the culture broth was sterilized beforehand in the tank at 121°C for 20 min. Moisture, ash, crude protein, and lipid content was determined according to AOAC standard methods (98). The conversion factor of the crude protein was 6.25.

Confirmation of safety for food application

For confirmation of the safety of the fermentation products, samples were prepared by freeze-drying the crude extract mentioned above and assayed. The genotoxic potential was evaluated by the Ames assay according to the method of Ames et al. (99), using *Salmonella typhimurium* strains TA98, TA100, TA1535, and TA1537 and *Escherichia coli* strain WP2uvrA. The concentration of Dfcy in the samples was 1.22, 4.88, 19.5, 78.1, 313, 1250, and 5000 µg per plate, with or without metabolic activation with S9 mixture. After preincubation at 120 rpm at 37°C for 20 min, top agar was added and plated. Revertants were counted after incubation at 37°C for 48 h. Acute oral toxicity and repeated dose studies in rats were conducted in accordance with Japanese law *Act on Welfare and Management of Animals*. For acute oral toxicity, female Slc:Wistar rats were administered the samples at a Dfcy dose of 2000 mg/kg. The rats were observed for 7 days, weighed at days 0 and 7, and sacrificed for pathological examination at day 7. For repeated-dose studies, CrI:CD(SD) rats of both sexes were administered the samples at a Dfcy dose of 300 and 1000 mg/kg/day. The rats were observed for 28 days, weighed at days 1, 8, 15, 22, and 28, and sacrificed for hematological and pathological examination at day 28. The Ames test and animal experiments were conducted by Japan Food Research Laboratories.

Stability analysis of Dfcy and Fcy

For the analysis of the stability of Dfcy and Fcy, a crude extract prepared as described above was diluted with distilled water to give a solution containing approximately 300 mg/L Dfcy. The pH of the solution was adjusted from 3 to 11 with KOH or H₂SO₄. For storage stability investigation, samples were incubated at 4°C or 25°C for 4 weeks. For thermostability investigation, samples were pasteurized in a heat block at 63°C for 30 min, or sterilized in an autoclave at 120°C for 4 min. Dfcy and Fcy concentrations were analyzed as described above in duplicate, and the results are shown as the rate compared with untreated sample.

Preparation of O/W emulsion

To evaluate the antioxidant effect of Dfcy in an O/W emulsion, linseed oil (Nacalai Tesque, Inc., Kyoto, Japan) was suspended in a buffer solution (0.05 M Tris-HCl, 0.15 M KCl, 10 g/L Tween 20, pH 7.0) at a concentration of 50 g/L. An antioxidant solution was prepared that contained Dfcy, α -tocopherol, or EDTA·2Na in the same buffer solution. A pro-oxidant solution was prepared with FeSO₄·7H₂O in the same buffer solution. The solutions were mixed to contain 50 g/L linseed oil; 0.02, 0.2, or 2.0 mM antioxidant; and 0.09 mM iron. The pure Dfcy used for the evaluation was prepared as described previously (93). A control was prepared without the antioxidant solution.

Oxidation and evaluation of antioxidant activity

Each mixture was stirred in a 100 mL glass beaker on a stirrer in the dark at 50°C for 48 h. Antioxidant activity was evaluated by measuring peroxide value (PV) and TBARS. PV was measured by the acetate-isooctane method according to the methods of the AOCS (100). TBARS was measured according to the method of Huber *et al* (101). Each measurement was performed in triplicate. The inhibition rate was calculated using the following equation: % inhibition = $(1 - B/A) \times 100$, where A and B are the PV/TBARS values of the control and experimental samples, respectively.

Statistical analysis

Statistical significance was determined by one-way ANOVA followed by Tukey's HSD test ($p < 0.05$) for multiple comparisons or Dunnett's test ($p < 0.05$) for comparison with the control, using Excel Statistics 2012 for Windows (Social Survey Research Information Co., Ltd., Tokyo, Japan).

Results

Optimization of medium composition for Dfcy production

Four nitrogen sources and 6 carbon sources were evaluated to determine the optimal submerged culture medium for Dfcy production by *A. oryzae*. The culture medium was prepared based on Czapek-Dox minimal medium containing NaNO₃ and sucrose as sole nitrogen and carbon sources, respectively, without FeSO₄.

To optimize the nitrogen source, NaNO₃ was replaced with (NH₄)₂SO₄, YE, SLH, SLH+NaNO₃ (mixtures of equal parts SLH and NaNO₃), or SLH+(NH₄)₂SO₄. The effects of the various nitrogen sources on fungal biomass and Dfcy production are shown in Table 4-1. Dfcy production was enhanced when NaNO₃ was replaced with (NH₄)₂SO₄, SLH, SLH+NaNO₃, or SLH+(NH₄)₂SO₄, and SLH+(NH₄)₂SO₄ gave the highest Dfcy yield. In contrast, replacement with YE had a deleterious effect on Dfcy production, which indicated that Dfcy production was inhibited by the relatively high iron contamination in YE in comparison with the other nitrogen sources, as reported previously for other *Aspergillus* spp (102,103).

To further confirm this inhibitory effect of iron, an additional flask experiment with iron concentrations ranging from approximately 20 to 230 µg/L was conducted. As depicted in Table 4-2, Dfcy production was reduced proportionally with increasing iron concentration beyond 70 µg/L iron, and totally abolished by 230 µg/L iron.

Table 4-1. Effects of different nitrogen sources on growth and Dfcy production

Nitrogen source	NaNO ₃	(NH ₄) ₂ SO ₄	YE	SLH	SLH + NaNO ₃
Biomass (dry cell weight, g/L)	5.6±0.4d	6.7±0.7cd	7.7±0.2bc	8.8±0.5b	7.4±0.0c
Dfcy production (mg/L)	22.5±0.3d	60.1±0.9c	ND	56.4±3.7c	73.7±4.1b
Iron concentration (µg/L)	17	57	454	52	43

Aspergillus oryzae strain F0 was cultured in 100-mL Erlenmeyer flasks with various nitrogen sources for 64 h. Results are expressed as the mean ± SD for triplicate cultures. Means with the same letter in a row are not significantly different ($p < 0.05$, Tukey's HSD test). SLH, hydrolysate of sake lees; YE, yeast extract.

Table 4-2. Effects of iron concentration on growth and Dfcy production.

Iron concentration ($\mu\text{g/L}$)	supplemental	0	20	50	100	200
	total	17	42	70	124	230
Biomass (dry cell weight, g/L)		4.5 \pm 0.5	5.0 \pm 0.2	5.1 \pm 0.5	5.1 \pm 0.1	5.1 \pm 0.4
Dfcy production (mg/L)		22.4 \pm 0.9a	27.7 \pm 0.5a	26.7 \pm 0.4a	12.1 \pm 4.0b	ND

Aspergillus oryzae strain F0 was cultured in 100-mL Erlenmeyer flasks with various concentrations of supplemental iron as FeSO_4 for 64 h. Results are expressed as the mean \pm SD for triplicate cultures. Means with the same letter in a row are not significantly different ($p < 0.05$, Tukey's HSD test).

Table 4-3. Effects of different carbon sources on growth and Dfcy production.

Carbon source	glucose	fructose	sucrose	maltose	starch	glycerol
Biomass (dry cell weight, g/L)	10.9 \pm 0.3a	10.1 \pm 1.0ab	9.2 \pm 0.9bc	9.1 \pm 0.5bc	8.1 \pm 0.1cd	6.9 \pm 0.2d
Dfcy production (mg/L)	83.1 \pm 1.4b	112.0 \pm 5.9a	87.0 \pm 1.7b	91.7 \pm 4.1b	67.9 \pm 3.4c	119.8 \pm 4.3a

Aspergillus oryzae strain F0 was cultured in 100-mL Erlenmeyer flasks with various carbon sources for 64 h. Results are expressed as the mean \pm SD for triplicate cultures. Means with the same letter in a row are not significantly different ($p < 0.05$, Tukey's HSD test).

Table 4-3 depicts the effects of various carbon sources on fungal growth and Dfcy production. Among the 6 carbon sources tested, glycerol was associated with the lowest biomass production but the highest Dfcy yield, which is 1.4-fold higher than the original carbon source sucrose.

Overall, this analysis revealed 5-fold higher production of Dfcy in medium containing $\text{SLH}+(\text{NH}_4)_2\text{SO}_4$ and glycerol when compared with basic Czapek-Dox medium containing NaNO_3 and sucrose as the sole sources of nitrogen and carbon, respectively.

Optimization of fermentation conditions in stirred tanks

The optimal stirred tank conditions for Dfcy production were also examined in the present study by altering agitation and aeration rates. F70-9, an enhanced Dfcy-producing mutant of F0, was used as a production strain. F70-9 had slightly weaker repression, but it was regulated by excess iron as shown in Table 4-4. There were no obvious differences between F0 and F70-9 except for Dfcy productivity.

To investigate the effect of agitation rate on Dfcy production, the agitation rate was increased from 300 rpm to 500 or 700 rpm after 17 h incubation with a constant aeration rate of 0.67 vvm (2.0 L/min). Increases in the rate of agitation tended to increase the dissolved oxygen concentration (DO) (Fig. 4-2B). In contrast, Dfcy production did not increase proportionally (Fig. 4-2A). Dfcy production at 700 rpm was higher than that at 300 rpm but was almost the same as that at 500 rpm. These results suggest that fungal damage was caused by agitation at 700 rpm. As shown in Fig. 4-2C, damage to mycelia was confirmed by microscopy. The same pulp-like morphology, consisting of entangled hyphae, was observed at agitation rates from 300 to 700 rpm, but fragmentation of mycelia was found only in the culture agitated at 700 rpm.

The effect of different aeration conditions on Dfcy production was also examined. A pure oxygen supply was used to provide sufficient oxygen under the restricted range of agitation rates investigated in this study. At a constant agitation rate of 450 rpm, at which no mycelial damage was observed, aeration conditions were changed from 0.67 vvm air to 0.17 or 0.50 vvm (0.5 or 1.5 L/min) pure oxygen after 18 h cultivation. As shown in Fig. 4-3, cultures supplied with 0.50 vvm oxygen produced more Dfcy. No morphological differences were observed between the oxygen- and air-supplied conditions. The Dfcy concentration reached 2800 mg/L after 118 h of cultivation in the presence of 0.50 vvm oxygen along with glycerol feeding.

Table 4-4. Effects of iron concentration on growth and Dfcy production using F70-9.

Iron concentration ($\mu\text{g/L}$)	supplemental	0	20	50	100	200
	total	20	41	71	122	224
Biomass (dry cell weight, g/L)		4.7 ± 0.5	5.3 ± 0.2	5.3 ± 0.3	5.4 ± 0.2	5.4 ± 0.3
Dfcy production (mg/L)		$62.8 \pm 4.2a$	$67.2 \pm 2.0a$	$68.0 \pm 1.7a$	$37.8 \pm 2.1b$	$7.4 \pm 2.6b$

Aspergillus oryzae strain F70-9 was cultured in 100-mL Erlenmeyer flasks with various concentrations of supplemental iron as FeSO_4 for 64 h. Results are expressed as the mean \pm SD for triplicate cultures. Means with the same letter in a row are not significantly different ($p < 0.05$, Tukey's HSD test).

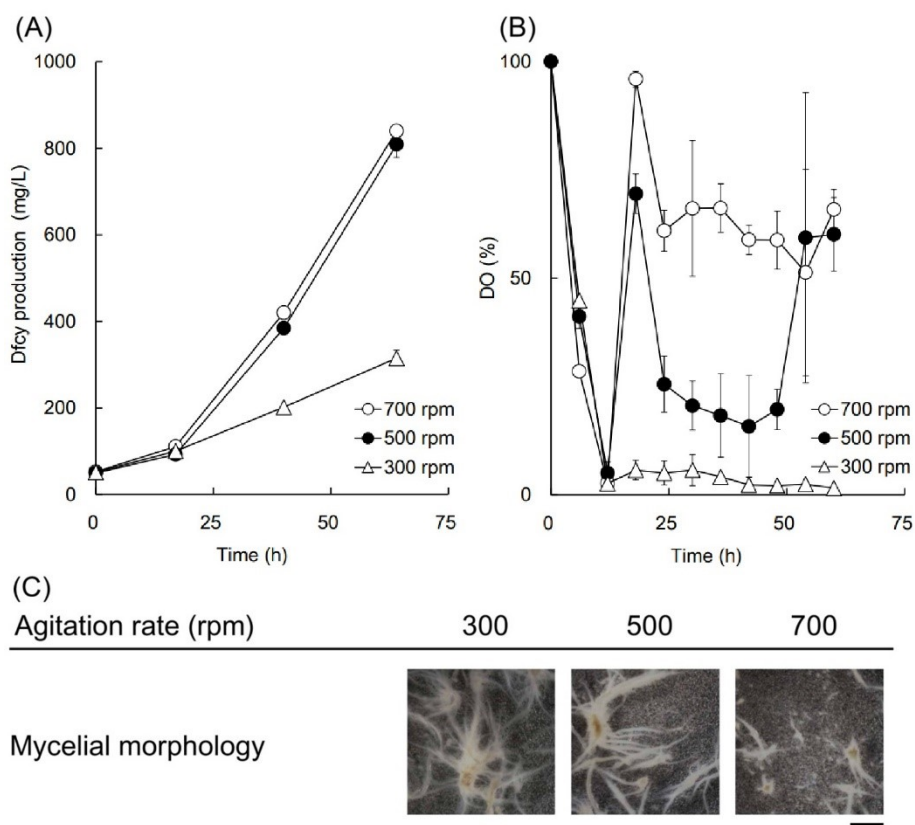


Fig. 4-2. Effects of agitation rate in stirred tanks. *Aspergillus oryzae* strain F70-9 was cultured in a 5-L stirred tank agitated at 300 rpm with 0.67 vvm aeration at 30°C. After 17 h of cultivation, the agitation rate was changed to 700 rpm (open circles) or 500 rpm (closed circles) or kept constant at 300 rpm (open triangles). The graphs show Dfcy production (A), DO (B), and the mycelial morphology after 64 h of fermentation (C). Error bars represent the SD for duplicate experiments. Scale bar: 1 mm.

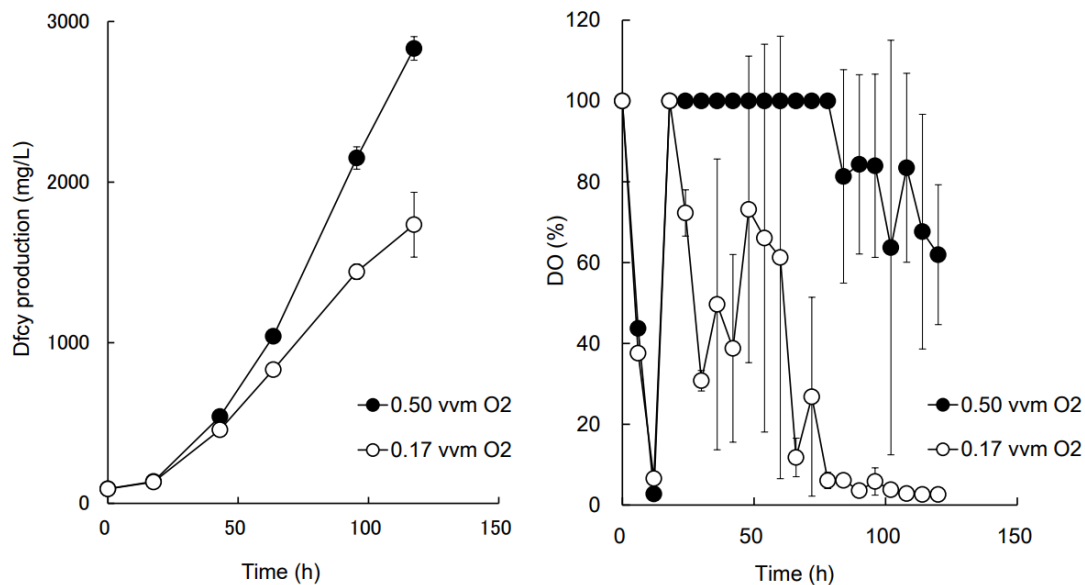


Fig. 4-3. Effect of oxygen supply on Dfcy production. *Aspergillus oryzae* strain F70-9 was cultured in a 5-L stirred tank agitated at 450 rpm with 0.67 vvm aeration at 30°C. After 18 h of cultivation, the aeration conditions were changed to 0.17 vvm oxygen (open circles) or 0.50 vvm oxygen (closed circles). The graphs show Dfcy production (A) and DO (B). Error bars represent the SD for duplicate experiments.

Evaluation of the safety of the fermentation products and the stability of Dfcy

To investigate the potential of Dfcy as an antioxidant food additive, the safety of the crude extract of fermentation broth was investigated. Although *A. oryzae* is generally regarded as safe because of the loss of mycotoxin productivity under general food production processes, induced mutation and different fermentation conditions might have influenced the silent gene clusters of secondary metabolites.

First, sequence analyses were performed for the F0 aflatoxin biosynthesis gene homolog cluster. F0 had the group 1 cluster pattern, which is the same as that of the *A. oryzae* model strain RIB40, whose lack of aflatoxin production has been confirmed (95). In RIB40, *aflJ*, which is essential for aflatoxin biosynthesis (104), is dysfunctional (105). F0 and F70-9 had the same *aflJ* gene sequences as RIB40.

Next, animal tests were performed for comprehensive evaluation of the safety of the fermentation products. In the Ames test, there was no significant increase in the number

of spontaneous revertants by fermentation products; thus, no mutagenic effect was found. Next, an acute systemic toxicity test and a repeated dose toxicity test were conducted in rats. There was no significant abnormality on general observation, in body weight, or on pathological examination in both experiments. Hematological examination was also conducted in repeated dose toxicity test because of the concern of anemia and related disorders, as Dfcy has high iron-chelating activity, but there was no significant abnormality. The dose for acute oral toxicity (LD₅₀) and NOAEL was found to be greater than 2000 mg/kg and 1000 mg/kg/day, respectively, measured as the concentration of Dfcy.

Next, the stability of Dfcy was investigated. Stability is an essential factor for commercial application because food products generally undergo sterilization and/or pasteurization, in addition to storage. The stability assay was conducted at 120°C for 4 min, 63°C for 30 min, 4°C for 4 weeks or 25°C for 4 weeks at pH 3-11, based on the common food processes mentioned above. The stability assay for Dfcy was performed using the crude extract of the cultured broth from a stirred tank. The chemical composition of the crude extract is shown in Table 4-5. The concentration of Dfcy was 2.36 g/kg, and the concentration of Dfcy in dry matter was 139 g/kg. The results of the stability assay of Dfcy and Fcy are shown in Table 4-6. The SD values were lower than 0.03. Dfcy was fairly stable, and over 80% of Dfcy remained except when sterilization was performed under alkaline conditions over pH 9. The stability of Fcy was also measured because once Dfcy chelates iron, it remains in foods as Fcy. The stability of Fcy was similar to that of Dfcy or even higher, as 66% remained even after sterilization at pH 11 and 120°C for 4 min.

Table 4-5. Chemical composition of the crude fermentation extract of *A. oryzae*

Component	g/kg
Moisture	983 ± 4
Ash	0.92 ± 0.15
Protein	5.89 ± 0.08
Dfcy	2.36 ± 0.02
Fat	0.031 ± 0.007

Results are expressed as the mean ± SD for triplicate analyses.

Table 4-6. Stability of Dfcy and Fcy

Dfcy/Fcy temperature and time	pH								
	3	4	5	6	7	8	9	10	11
Dfcy									
4°C									
1 week	0.99	1.00	1.00	0.99	0.99	1.00	1.00	0.99	0.98
2 weeks	0.97*	1.00	1.00	1.00	1.00	1.00	1.00	0.99	0.96*
4 weeks	0.95*	0.99	1.00	1.00	1.00	1.00	1.00	0.99	0.95*
25°C									
1 week	0.90*	0.99	1.00	1.01	1.01	1.00	0.99	0.96*	0.89*
2 weeks	0.82*	0.98*	0.97*	0.97*	0.97*	0.96*	0.96*	0.93*	0.86*
4 weeks	0.68*	0.96*	0.96*	0.97*	0.96*	0.95*	0.94*	0.89*	0.81*
63°C									
30 min	0.95*	0.95*	0.96	0.96*	0.96	0.95*	0.95*	0.94*	0.92*
120°C									
4 min	0.84*	0.90*	0.91*	0.90*	0.87*	0.81*	0.60*	0.25*	0.18*
Fcy									
4°C									
1 week	1.00	1.00	1.00	1.00	0.99	1.00	1.00	0.99	0.99
2 weeks	0.96*	0.98	0.99	0.98	0.98	1.00	1.00	0.99	1.00
4 weeks	0.96*	0.98*	0.98*	0.98*	0.98*	1.00	1.00	0.98*	0.99
25°C									
1 week	1.00	1.00	1.01	1.00	1.00	0.99	1.00	1.00	1.00
2 weeks	1.00	1.00	1.00	1.00	0.99	0.95*	0.96*	0.96*	0.97*
4 weeks	1.00	1.00	1.00	0.99	0.99	0.95*	0.96*	0.96*	0.96*
63°C									
30 min	0.95*	0.96*	0.95*	0.95*	0.95*	0.95*	0.95*	0.94*	0.92*
120°C									
4 min	0.77*	0.81*	0.86*	0.89*	0.93*	0.93*	0.92*	0.88*	0.66*

Dfcy was stored (4°C or 25°C for 4 weeks), pasteurized (63°C for 30 min), or sterilized (120°C for 4 min) under various pH values. The results are presented as the mean amount remaining in triplicate analyses. Statistical significance is indicated by * compared to untreated control ($p < 0.05$, Dunnett's test).

Evaluation of antioxidant activity of Dfcy

To evaluate the antioxidant activity of Dfcy and estimate its commercial value, its activity was compared with that of α -tocopherol and EDTA in O/W emulsion. α -tocopherol and EDTA are among the most popular antioxidants and act through chain-breaking and metal-chelating effects, respectively. Lipid oxidation was measured by PV and TBARS to estimate both primary and secondary oxidation products, respectively. Fig. 4-4 depicts the activity of each antioxidant. The maximum rate of primary oxidation inhibition for Dfcy, EDTA, and α -tocopherol at 48 h was 83%, 75%, and 9.9%, respectively. The corresponding maximum inhibition rate for secondary oxidation was 75%, 72%, and 39%, respectively. The antioxidant activity of Dfcy was equal to or higher than that of EDTA and α -tocopherol in the O/W emulsion model at each equimolar concentration. The antioxidant activity of Dfcy increased in a concentration-dependent manner, whereas the PV of EDTA at a high concentration indicated a pro-oxidative effect as previously reported (106).

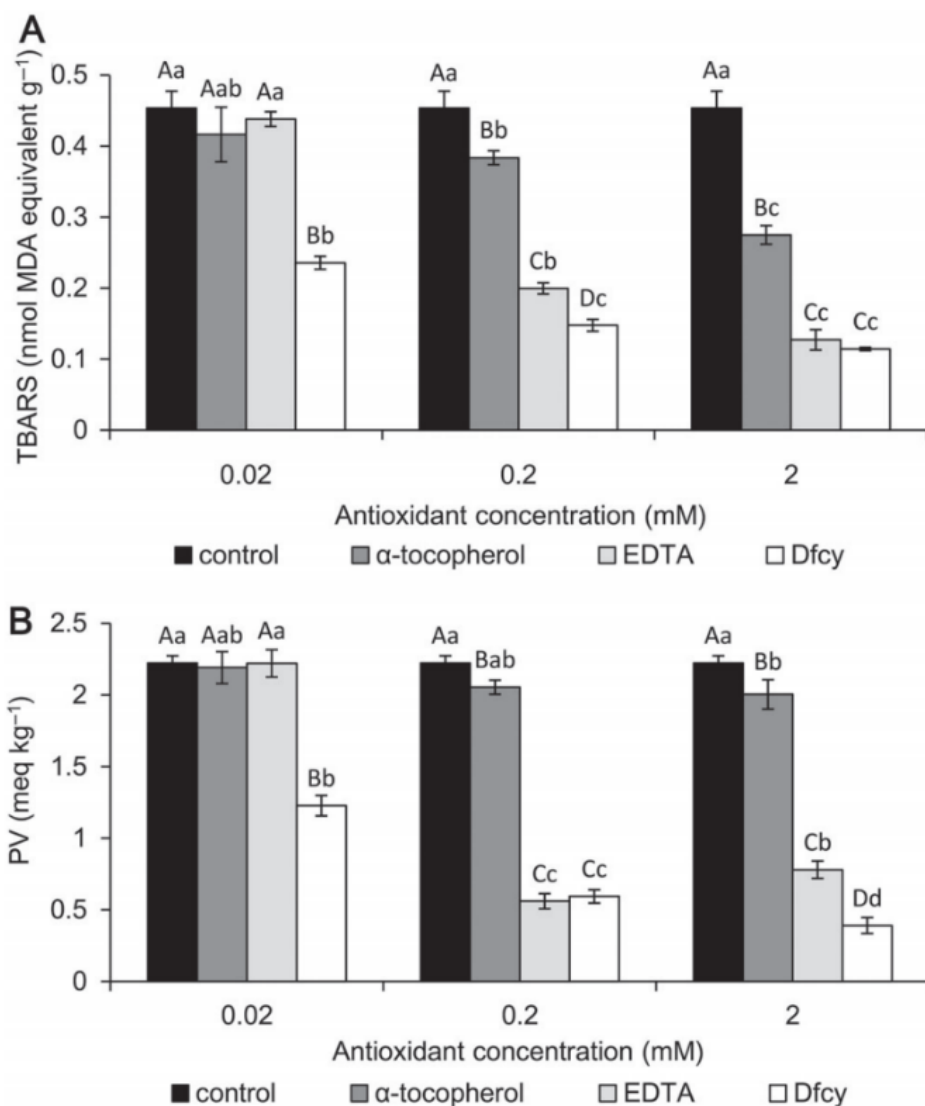


Fig. 4-4. Antioxidant activity of Dfcy in O/W emulsion Notes: Samples were incubated at 50°C for 48 h. Each sample contained 0.02, 0.2, or 2 mM of α -tocopherol (gray), EDTA (light gray), Dfcy (white), or no antioxidant (blank; black). Graphs show the PV values (A) and TBARS values (B). Error bars represent the SD for triplicate analyses. The different capital letters above the bars indicate significant differences within the same concentration ($p < 0.05$, Tukey's HSD test). The different small letters above the bars indicate significant differences within the same antioxidant ($p < 0.05$, Tukey's HSD test).

Discussion

To establish a production method for Dfcy, which is a potential candidate for a novel food-grade antioxidant, the author optimized the production conditions because Dfcy production is typically very low. SLH was found to be an efficient nitrogen source for Dfcy production, likely because of its low iron concentration (Table 4-1). Sake lees contained only a low level of iron because the raw material is milled rice, which has already lost the majority of its iron with bran (Fig. 4-1). However, use of sake lees also has an ecological advantage in that it utilizes a by-product of sake production. Rice wine including sake is one of the most traditional and popular alcoholic beverages produced in almost all Asian countries where rice is the major crop. Lees produced by the separation process are a major by-product common in rice wine production, and their utilization has been investigated extensively (107–110).

The inhibitory effect of iron on Dfcy production by *A. oryzae* F0 was shown (Table 4-). In *Aspergillus* spp., two conserved transcription factors, SreA and HapX, are known to regulate siderophore biosynthesis in response to iron availability (102,103). These transcription factors are targets in future productivity analyses and strain breeding to maximize Dfcy production because F70-9, an enhanced Dfcy-producing mutant of F0, was still under regulation of excess iron (Table 4-2).

In stirred tank experiments, when the agitation rate was increased to 700 rpm, mycelial fragmentation was observed and there was no further increase in Dfcy production (Fig. 4-2). This finding that higher agitation results in reduced productivity is in line with previous studies on the fermentation by filamentous fungi in stirred tanks for production of penicillin by *Penicillium chrysogenum*, tannase by *Aspergillus niger*, and lovastatin by *Aspergillus terreus* (111–114). Thus, the author's findings suggest that agitation intensity must be controlled within an appropriate range to prevent a decline in productivity.

The limited range of suitable agitation rates led to the investigation of methods to increase oxygen availability without inducing mycelial damage. Oxygen supplementation increased Dfcy production without affecting mycelial morphology, and a final Dfcy concentration of 2800 mg /L was obtained (Fig. 4-3). This is the highest concentration

of fungal siderophore production ever reported. The results obtained from the investigations of agitation rate and oxygen supply clearly demonstrate the importance of sufficient oxygen for Dfcy production.

Dfcy showed high potential as an antioxidant food additive. First, safety of the fermentation products was confirmed by both genetic background and comprehensive evaluation. The *aflJ* gene sequences of F0 and F70-9 strongly suggest that these strains still lack aflatoxin production because their AflJ is thought to be as dysfunctional as that of RIB40. Further, the results of the Ames test, acute oral toxicity test, and repeated dose toxicity test suggest that the fermentation products do not present obvious risks for intake and can be regarded as safe as other foods fermented by *A. oryzae*. Thus, the mutation induced in the strain and the modification of the fermentation conditions does not seem to result in production of toxic secondary metabolites.

Second, Dfcy was stable at various pH values; its stability at pH 3-9 will cover almost all foods, considering that the pH of foods usually does not exceed 9 (115). Furthermore, the higher stability of Fcy than Dfcy indicates that once Dfcy chelates iron, its chelation activity is sustained. This high stability is noteworthy considering that coprogen, which is a member of the same trihydroxamate class of fungal siderophore as Dfcy, has been reported to be less stable and difficult for food application (116). The cyclic hexapeptide structure of Dfcy may be responsible for its higher stability compared to coprogen, which has a linear structure containing an ester bond.

Finally, the antioxidant activity of Dfcy was more efficient than that of EDTA or α -tocopherol in the O/W emulsion model. In this study, the antioxidant activity of α -tocopherol was limited, indicating that a chain-breaking antioxidant alone is insufficient to prevent lipid oxidation. It is also noteworthy that the antioxidant activity of Dfcy was concentration-dependent in this range, whereas EDTA exhibited a slightly pro-oxidative effect at higher concentrations. The reason why Dfcy functioned equally to or more efficiently than EDTA may involve its high binding constant toward Fe^{3+} , which reached 1.0×10^{30} ; in contrast, the binding constant of EDTA was 1.3×10^{25} . Metals including iron are an important driving force for lipid oxidation, and antioxidant activity depends

on the binding constant toward iron and stability in the solution (16). From this perspective, Dfcy may be the most efficient metal-chelating antioxidant because it is the strongest iron chelator found in foods except only for desferrioxamine E, a bacterial siderophore (84). The binding constant of Dfcy toward Fe^{3+} is much higher than those of other natural iron-chelating ingredients investigated previously such as citric acid (82) and lactoferrin (16), whose binding constants are approximately 1.0×10^{12} and 1.0×10^{20} , respectively (84,117).

This is the first report demonstrating the production of Dfcy in an applicable concentration with evaluation of its antioxidant potential. The use of siderophores and hydroxamates to prevent lipid oxidation has been studied previously. For example, Chen *et al.* studied the effect of siderophore as iron chelator in bulk oils containing reverse micelles using deferoxamine (118). Tian *et al.* developed a packaging material grafting polyhydroxamate to chelate iron (119). These studies clearly exhibited the high potential of siderophores and their structure for inhibiting lipid oxidation. Despite the potential of siderophores as antioxidants, however, studies focusing on their production have been very limited. Emri *et al.* reported the production of coprogen by *Penicillium nalgiovense* for application in high-siderophore-content foods, but they concluded that the use of coprogen may be limited because of its instability in the media and because of β -lactam production by the fungus (116). The same group also reported medium optimization for the production of triacetylfulvarinin C and ferricrocin by *A. fumigatus*, although their focus was on its applications for medicinal studies (120). In addition, *A. fumigatus* is a pathogen and appears to be unsuitable for food production (121). Compared to the compounds of those recent studies, Dfcy produced by *A. oryzae* has advantages such as confirmed safety of the production host and high stability, as demonstrated in this study. Furthermore, the antioxidant potential of Dfcy clearly indicates that it could be the first natural alternative to the synthesized iron chelator antioxidant EDTA. Although the use of EDTA for foods is conditionally permitted in countries such as EU, USA, and Japan, consumers are increasingly demanding foods containing fewer synthesized components. To apply the present Dfcy production method for commercial use, further scale-up studies are needed.

To further investigate the potential of Dfcy as a food-grade antioxidant, studies on combined application with other antioxidants as well as prolonged stability tests in food models will also be important.

Summary

In this study, the author produced Dfcy by submerged culture of *A. oryzae* and also evaluated it as a food-grade antioxidant. The author optimized culture conditions to improve Dfcy production to 2800 mg/L from 22.5 mg/L under typical conditions. Then, the author evaluated the potential of Dfcy as a food additive by measuring its safety, stability, and antioxidant activity. Dfcy was sufficiently stable that over 90% remained after pasteurization at 63°C for 30 min at pH 3-11, or after sterilization at 120°C for 4 min at pH 4-6. Dfcy showed high antioxidant activity in an O/W model, where inhibition of lipid oxidation was measured by PV and TBARS assays. Dfcy decreased PV and TBARS by 69% and 86%, respectively. Dfcy was more efficient than the synthetic chelator EDTA at an equimolar concentration. This study provides the first practical method for production of Dfcy. The stability and antioxidant activity of Dfcy suggest that it can be a novel food-grade antioxidant and the first natural alternative to the synthesized iron chelator EDTA.

Section 2

Inhibition of lipid oxidation and hexanal production in cooked meats by deferriferrichrysin

Meat has been a major nutritional source for humans since ancient times, and it remains an indispensable element of food cultures around the world. Lipids are responsible for many desirable characteristics of meats, including flavor and aroma, tenderness, and juiciness. However, lipid oxidation is responsible for the quality deterioration of meat by producing primary and secondary oxidation products, thereby reducing the nutritional quality of meat (17). It also imparts an unpleasant off-odor to the heat-processed meat, thus affecting consumers' acceptability of meat. Additionally, lipid oxidation products such as malondialdehyde (MDA) and 4-hydroxy-nonenal pose health hazards to humans (18). To prevent lipid oxidation, the plant-derived antioxidants have garnered intensive interest (17), however, they sometimes impart a strong flavor and/or taste, which limits their applicability in the food industry (122,123). Therefore, it is necessary to identify alternative sources of natural antioxidants. Although the potential of Dfcy to inhibit lipid oxidation in an O/W model was discovered as mentioned in Section 1, its antioxidant efficiency in real food products has not yet been elucidated.

In this study, the author investigated the inhibitory effect of Dfcy on lipid oxidation and off-odor production in heated meat products. Dfcy showed inhibition of hexanal production with over 90% reduction at 50 to 100 mg/kg in chicken, pork, and beef meat. Dfcy was shown to be an efficient inhibitor of lipid oxidation and off-odor production for heated meat products.

Materials and methods

Collection of commercially available sake

To determine the Dfcy concentration of commercially available sake, the author used eight commercially available sake. They were purchased from local supermarket and stored at 4°C until analysis. Dfcy concentration of sake samples was analyzed as described below.

Fermentation of *koji* for Dfcy-enhanced sake

Dfcy-enhanced sake was fermented to achieve a higher Dfcy concentration than commercially available sake. Fermentation of sake is, in summary, driven by *S. cerevisiae* with its ingredients, water, steamed rice, and *koji*, in descending order. *Koji*, polished rice fermented by *A. oryzae*, was first prepared as follows. Rice was polished to a 72% weight after removing the bran, then soaked in water at 4 °C for 16 h, steamed for 30 min, and cooled to 35 °C. An aliquot of the steamed rice was inoculated with spores of *A. oryzae* (10 mg/kg) and incubated at 35 °C with 95% humidity in a humidity chamber (LHL-114, ESPEC Corp., Osaka, Japan) for 50–98 h. Three different *A. oryzae* strains, namely, RIB40, RIB69, and F16, were used for *koji* production because Dfcy productivity differs with strains. RIB40 and RIB69 are commercially available *A. oryzae* model strains with comparatively high Dfcy production (124). Both RIB40 and RIB69 were obtained from the National Research Institute of Brewing (NRIB), Japan. F16 is a mutant generated by UV-mutagenesis that showed increased efficiency of Dfcy production screened as mentioned in Chapter II section 1.

Fermentation of sake

Sake was prepared as described below. First, yeast culture was prepared using *S.*

cerevisiae strain K7 (obtained from the Brewing Society of Japan) by pre-culturing in YE peptone dextrose (YPD) medium (10 g/L YE, 20 g/L polypeptone, 20 g/L glucose) using a reciprocal shaking incubator at 120 rpm at 30 °C for 2 days, followed by centrifugation at $8,000 \times g$ for 10 min. The sake mash was prepared by mixing water, steamed rice, and *koji* in a 6: 3: 1 (w/w/w) ratio, followed by the inoculation with the yeast culture (*S. cerevisiae* culture) at a concentration of 1×10^7 cells/mL. The mixed mash was then fermented at 15 °C for 14 days, where saccharification and alcohol fermentation proceeded simultaneously. After fermentation, sake mash was centrifuged at $8,000 \times g$ for 10 min, and the supernatant was stored at 4 °C until further experiments.

Preparation of purified Dfcy

To evaluate efficiency to inhibit lipid oxidation and sensory evaluation, purified Dfcy was prepared according to the previously reported procedure. In brief, *A. oryzae* F16 was cultured in a synthetic liquid medium as mentioned in Chapter II section 1, and the culture supernatant was purified by HPLC (93).

Analysis of Dfcy concentration

For the analysis of Dfcy in *koji*, Dfcy was extracted from *koji* by soaking *koji* in 10 volumes of water and incubating in a rotary shaker with reciprocal shaking (60 rpm) at 4 °C for 3 h. The mixture was then filtered using a PVDF 0.45 μm filter (Whatman Mini-UniPrep, Cytiva, Japan) to collect the aqueous solution containing Dfcy. The filtrate was then used to measure Dfcy concentration by HPLC, as reported previously (93). For the analysis of Dfcy in sake, sake was filtered using the same PVDF filter and subjected to HPLC analysis.

Sensory evaluation of Dfcy

To test the applicability of Dfcy as a food ingredient, its sensory acceptance was investigated based on a triangle test, where panelists test randomly set three samples (containing one or two test samples and the rest is control sample) in blind coded and select the odd sample. The experiment was designed to investigate the existence of a sensory difference between 100 mg/L Dfcy sample and blank water. The test conditions were set as below, α (false positive rate) = 0.1, β (false negative rate) = 0.1, Pd (proportion of distinguishers) = 0.3. The test was performed by 12 expert panels in quadruplicate (N = 48). Panels were recruited among workers engaged in food manufacturing who routinely participate in sensory evaluation of food products. The level of statistical significance and sample size were designed according to the previously reported standard (125).

Preparation and analysis of meat samples

Freshly prepared minced meats— chicken (breast), pork (rib), and beef (thigh) —were purchased from a local market in Kyoto, Japan. Each kind of meat was separately blended to homogenize and divided into three parts, whose iron and lipid content was measured before being heated. Total iron content was measured according to the method of Min et al. (126). Total lipid was extracted and quantified by the method of Bligh and Dyer (127). For the preparation of cooked meats, each meat sample (50 g) was treated either with 0.5 ml of purified Dfcy solution (0, 1000, 2000, or 5000 mg Dfcy /L, dissolved in water) or with 0.5 ml or 2.5 ml of Dfcy-enhanced sake and completely homogenized. Then, 30 g of mixed meat was then packed into polyethylene bags and heated at 70 °C for 70 min,

as previously described (128). Cooked meat packed in polyethylene bag was then cooled and stored at 4 °C for 10 days in the dark. Then the samples were analyzed for the estimation of lipid oxidation.

Analysis of lipid oxidation

The thiobarbituric acid reactive substances (TBARS) assay was conducted following the method of (129), and the values were shown as mg MDA equivalent/kg sample. To measure the hexanal contents, 2.0 g of cooked meat was placed in a glass vial followed by helium flushing. Then the hexanal content of samples was analyzed by dynamic HS-GC-MS using a GCMS-QP2020 NX and HS-20 Trap system (Shimadzu Corporation, Kyoto, Japan) filled with Tenax TA according to a previously reported method (130). The inhibition percentage was calculated using the following equation: % inhibition = $(1 - B / A) \times 100$, where A and B are the control and experimental samples' values, respectively. The control for both purified Dfcy-treated samples, and Dfcy-enhanced sake-treated samples is a Dfcy-untreated sample, shown in the first column of the tables.

Statistical analyses

For statistical analysis of lipid oxidation, each packet of meat was used as the experimental unit, where different kinds of meats (chicken, pork, and beef) were analyzed independently. For the treatments—Dfcy-untreated control or samples treated with different concentrations of Dfcy—experiments were carried out in triplicate. The statistical significance of differences among treatments were analyzed by one-way ANOVA followed by Tukey's HSD test. The *p*-values < 0.05 were considered significantly different. For statistical analysis, BellCurve for Excel (Social Survey

Research Information Co., Ltd., Tokyo, Japan) was used.

Results

Analysis of Dfcy in commercially available sake

The antioxidant activity and inhibition of lipid oxidation by Dfcy in an O/W emulsion was shown in Section 1. The author hypothesized that these properties of Dfcy could be exploited to prevent lipid oxidation and inhibit hexanal production in cooked meat. First, the Dfcy concentration of eight commercially available sakes was determined to investigate whether the Dfcy amount is sufficient as an antioxidant. As shown in Table 5-1, the maximum Dfcy concentration was only 24 mg/L. This concentration seems insufficient, because when Dfcy was mixed to meat in a 5% ratio, the Dfcy content in meats (approximately 1.2 mg/L) would be lower than iron content in meats such as 3–6 mg/kg in chicken, and 11–25 mg/kg in beef thighs (131). These results warranted the investigation of an alternative sake with increased Dfcy.

Table 5-1. Dfcy concentration in commercially available sake products.

Sakes	Dfcy concentration (mg/L)
Sake A	11
Sake B	4.4
Sake C	3.5
Sake D	2.1
Sake E	13
Sake F	22
Sake G	24
Sake H	19

Improvement of Dfcy concentration in *koji*

Considering the insufficiency of Dfcy concentrations in commercially available sake as explained above, the author speculated that the increased Dfcy concentration in *koji* could increase the Dfcy concentration in sake. To test this, the author first investigated the effect of the *A. oryzae* strain and fermentation time on the Dfcy concentration in *koji* using three different strains, namely F16, RIB40, and RIB69. Of the three strains, F16 produced a higher amount of Dfcy at both 50 h (1.45 mg/g) and 98 h (5.07 mg/g) as compared to the RIB40 and RIB69 strains (Fig. 5-1).

Fermentation of Dfcy-enhanced sake

Next, the author fermented the sake using *koji* with the highest Dfcy concentration (F16, 98 h), water, steamed rice, and yeast. After fermentation, the concentration of Dfcy in the Dfcy-enhanced sake increased to 512 mg/L, which is about 20 times higher than that of commercially available sake. These results validated the author's speculations that enhancement of Dfcy content in *koji* can effectively increase Dfcy concentration in sake.

Sensory evaluation of Dfcy

Before the investigation of Dfcy as an antioxidant for meat products, the sensory aspect of Dfcy was investigated to estimate its effect on food products. The test was conducted using 100 mg/L Dfcy in a triangle test by 12 expert panels ($n = 4$). The number of the correct response was 14, which was smaller than the minimum number 20 to show the existence of a statistically significant difference (Table 5-2).

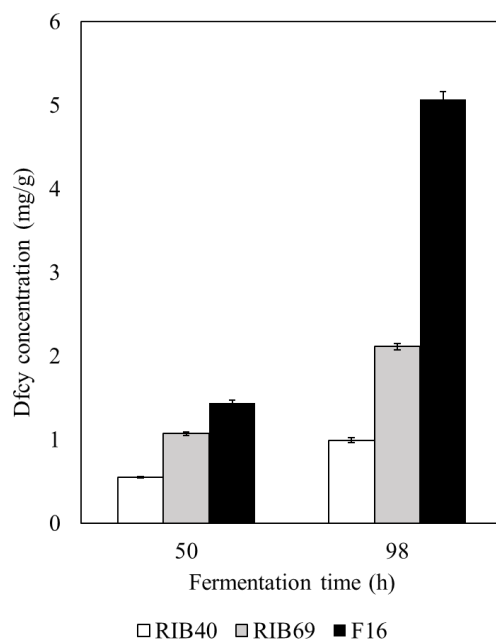


Fig. 5-1. Dfcy concentration of *koji* fermented with different strain and fermentation time. Data shows mean values (n = 3) ± standard error (S.E.) of three replications.

Table 5-2. Result of sensory triangle test of Dfcy

Number of responses (total 48)		
Correct	Incorrect	Critical value
14	34	20

Dfcy (100 mg/L) was compared with blank control (water) by triangle test.

Critical value is the minimum number of the correct responses to determine the existence of significant difference. Statistical parameters were as follows, α (false positive rate) = 0.1, β (false negative rate) = 0.1, and Pd (proportion of distinguishers) = 0.3.

Use of Dfcy as an antioxidant for meat products for inhibition of TBARS values and hexanal

To identify the ability of Dfcy to inhibit lipid oxidation, chicken, pork, and beef meat mince were prepared. Their total iron and lipid contents were analyzed (Fig. 5-2). Each type of meat was mixed with purified Dfcy or Dfcy-enhanced sake, followed by heating and storage. Cooked meats were analyzed for TBARS assay and hexanal concentration. As shown in Table 5-3, the addition of Dfcy progressively reduced TBARS values. The maximum reduction of TBARS values was observed with the addition of 100 mg/kg Dfcy, in which inhibition percentages were 75%, 85%, and 61% for chicken, pork, and beef, respectively. The effect of Dfcy was more outstanding in the reduction of hexanal content. More than 90% reduction was observed with purified Dfcy over 50 mg/kg in chicken and pork, wherein it was achieved by 100 mg/kg Dfcy in beef meat (Table 5-4). Using Dfcy-

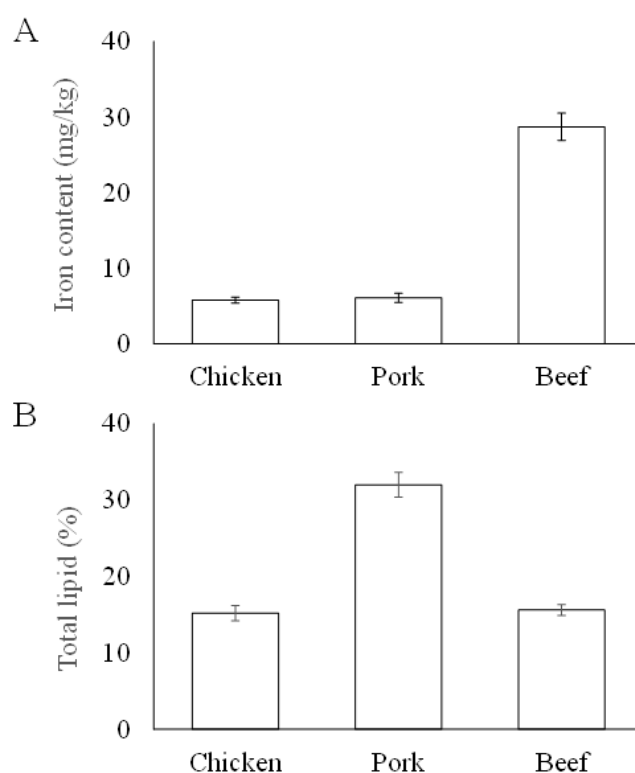


Fig. 5-2. Iron content and total lipid content of meat used in this study. Data shows mean values ($n = 3$) \pm standard error (S.E.) of three replications.

enhanced sake as the Dfcy source, hexanal production and TBARS values of heated meats were also reduced. The values of samples treated with Dfcy-enhanced sake at 24 mg/kg were similar to those of samples treated with purified Dfcy 20–50 mg/kg, indicating that the efficiency of Dfcy is not reduced when Dfcy was added to meat as sake.

Discussion

Development of Dfcy-enhanced sake

The author first hypothesized that Dfcy could be exploited to prevent lipid oxidation and inhibit hexanal production in cooked meat. The use of iron chelators as antioxidants is reasonable, considering that iron is a major initiator of radical formation and the facilitator of lipid oxidation in meat (132). Once radicals initiate lipid oxidation, it causes a chain reaction where the lipid oxidation products themselves further fuel radical production. At this point, antioxidants that scavenge radicals tend to lose their activity by scavenging radicals, whereas iron chelators can efficiently stop the first-step radical formation by inactivating the initiator iron (132). However, eight commercially available sakes contained insufficient Dfcy, whose maximum value was only 24 mg/L. In general, Dfcy is regarded as an unfavorable byproduct that causes coloration when chelating iron.

Table 5-3. TBARS values of heated meats supplemented with different concentrations of Dfcy.

Dfcy source	Purified Dfcy					Dfcy-enhanced sake		
	0	10	20	50	100	5.1	24	
Meat	Chicken	11.5 ± 1.7a	6.6 ± 1.7b	5.3 ± 0.2bc	0.1 ± 0.0d	0.0 ± 0.0d	7.8 ± 0.5b	3.0 ± 0.4c
		21.7 ± 2.9a	12.4 ± 1.2b	10.5 ± 1.0b	0.0 ± 0.0c	0.1 ± 0.0c	18.1 ± 2.4a	1.1 ± 0.3c
	Pork	7.5 ± 0.6a	6.4 ± 0.8a	6.9 ± 0.9a	1.6 ± 0.2b	0.2 ± 0.0b	4.9 ± 0.3c	4.8 ± 0.2c
	Beef							

Data shows mean values (n = 3) ± standard error (S.E.) of three replications. Dfcy concentration is the calculated final concentration of Dfcy in meat products. The different letters in rows indicate significant differences among treatments ($p < 0.05$). TBARS values are shown as μM MDA equivalent / kg

Table 5-4. Hexanal content (mg/kg) in heated meats supplemented with different concentrations of Dfcy.

Dfcy source	Purified Dfcy					Dfcy-enhanced sake		
	Dfcy concentration (mg/kg)	0	10	20	50	100	5.1	24
Meat	Chicken	24.1 ± 3.0a	13.5 ± 2.8b	12.7 ± 0.2b	5.2 ± 0.7c	6.0 ± 1.0c	16.6 ± 0.7b	14.5 ± 1.2b
	Pork	39.4 ± 4.4a	46.4 ± 3.7b	21.4 ± 1.5c	7.3 ± 0.4d	6.4 ± 0.4d	19.7 ± 2.2c	12.6 ± 1.5d
	Beef	35.6 ± 2.2a	30.1 ± 3.2b	25.1 ± 2.9bc	15.7 ± 1.5de	13.5 ± 1.4e	23.2 ± 1.4c	20.5 ± 0.9cd

Data shows mean values (n = 3) ± standard error (S.E.) of three replications. Dfcy concentration is the calculated final concentration of Dfcy in meat products. The different letters in rows indicate significant differences among treatments ($p < 0.05$).

From this perspective, *A. oryzae* strain losing Dfcy production was developed and used for sake fermentation (133,134). Meanwhile, from the viewpoint of using sake as the iron chelator for meat products, higher Dfcy content in sake was favorable. The author investigated the effect of *A. oryzae* strain and fermentation time to improve Dfcy concentration in koji. As a result, F16 produced a higher amount of Dfcy and prolonged fermentation time further increased the concentration. The Dfcy concentration of 5.07 mg/g in koji and 512 mg/L in sake are the highest value ever reported. Furthermore, this is the first report of food containing siderophores at a concentration over 500 mg/kg.

Dfcy as an inhibitor of lipid oxidation

Sensory evaluation of Dfcy showed that the addition of 100 mg/L Dfcy in water cannot be distinguished, which would be an advantage of Dfcy if Dfcy does not affect the taste of foods, whereas other natural antioxidants derived from herbs may alter the flavor and taste of the original food (122,123). In addition, Dfcy showed high effect in the reduction of TBARS values and hexanal content. The strong iron-chelating ability of Dfcy could explain the high efficiency of inhibition. Dfcy shows an incredibly high binding constant

toward ferric iron, $K = 1.0 \times 10^{30.0}$, where $K = [\text{chelated iron}] / [\text{free iron}][\text{chelator}]$, which is higher than that of the synthesized iron chelator EDTA ($K = 1.0 \times 10^{25.1}$) (92). In addition, it has been shown that Dfcy is stable even after thermal treatment at 121 °C for 20 min at pH 3–8 (Section 1 Table 4-6), contributing to its chemical stability against pH and heat, consequently increasing its efficiency against radical formation during meat heating. Therefore, it can be inferred that Dfcy can maintain its antioxidant activity even after the heating process, whereas other natural-based substances might lose their activity under acidic conditions or heating (135,136).

It is noteworthy that the effect of Dfcy differed with the type of meat, which could be due to the difference in iron content in each type of meat. Beef meat contained more iron than chicken and pork and might have released more free iron that worked as a pro-oxidant.

Other than sake, other kinds of rice wines are also very popular in almost all Asian countries where rice is a major crop. In these rice wines, the fungi *Trichoderma* spp. and *Rhizopus oryzae* are used for saccharification (137). The current strategy demonstrated in this study can be used for the preparation of iron chelator-enriched rice wines because these fungi also excrete iron chelators (138).

Summary

In this study, the efficacy of Dfcy against lipid oxidation of meat was investigated. Purified Dfcy and Dfcy-enhanced sake were prepared and added to three kinds of meat (chicken, pork, and beef) and heated at 70 °C for 70 min, followed by storage at 4 °C for 10 days and analysis of the efficacy to inhibit lipid oxidation. Dfcy reduced TBARS values of meat products by over 50% with the addition of 100 mg/kg of Dfcy. Hexanal production was more efficiently reduced, i.e., over 90% reduction with the addition of 50

to 100 mg/kg of Dfcy. The findings suggest Dfcy and Dfcy-containing sake as promising novel natural antioxidants to inhibit lipid oxidation in meat products.

CONCLUSIONS

In this study, the author conducted the development of molecular breeding methods of *A. oryzae* and applied them for elucidation of *A. oryzae* gene function in sake fermentation. Furthermore, the author also developed the production technology of iron chelator Dfcy from *A. oryzae* and demonstrated that Dfcy efficiently inhibits lipid oxidation in both model systems and real meat samples.

In Chapter I, the author first identified a novel PT resistance marker gene *thiI*, and showed its application in genome co-editing. In *A. oryzae*, formerly known marker genes all had disadvantages such as causing auxotrophy or being difficult to apply in genome editing. On the other hand, the use of *thiI* had a distinct advantage. Loss of *thiI* function does not cause auxotrophy, and PT definitely functions as low as 0.1 mg/L. Overall, the identification and characterization of *thiI* as a novel selectable marker expands the genome editing toolbox for the industrially important fungus *A. oryzae*.

Next, the author examined a novel targeted knock-in method that utilizes genome editing and MMEJ/SSA. This was because, while efficient knock-out techniques have been established in *A. oryzae*, knock-in remained laborious as it still relied on the HR pathway. The alternative approach enabled efficient generation of targeted knock-in transformants without the need for host strain preparation, using only a short homology template. The author concludes that this novel knock-in method can be applied to facilitate transformation of *A. oryzae*, making it easier to obtain targeted knock-in transformants, especially from industrially important non-model strains.

The novel method utilizing *thiI* marker was further applied to unravel the unidentified ferulic acid liberation process in sake fermentation, as ferulic acid is the precursor of an important off-flavor 4-VG. The candidate gene *faeA* was successfully disrupted more

conveniently than the classical genetic approach. The generated *faeA*-deficient strain exhibited significantly lower feruloyl esterase activity and the resulting sake contained almost undetectable amount of 4-VG. These results indicate that the lowering FaeA activity is a promising strategy to mitigate the risk of off-flavor generation or to employ diverse yeast strains for sake brewing.

In Chapter II, the author considered that utilizing *A. oryzae* might enable the development of solutions for challenges of the food industry. To produce the potential food antioxidant Dfcy, which is typically produced at very low levels, the production conditions were optimized. Dfcy production was increased over 5-fold by medium optimization. In addition, importance of oxygen availability and appropriate agitation rate on Dfcy production were confirmed. Dfcy exhibited high stability across a wide pH range of 3-9, and its antioxidant activity in an oil/water emulsion was more effective than EDTA or α -tocopherol. Dfcy produced by the safe host *A. oryzae* has advantages of high stability, suitability for food use, and strong antioxidant potential.

The author further examined the effect of Dfcy as an antioxidant against lipid oxidation in heated meats. Dfcy showed inhibition of hexanal production with over 90% reduction at 50 to 100 mg/kg in chicken, pork, and beef meat. In conclusion, Dfcy was shown to be a promising material that can help resolve challenges faced by the food industry, such as shelf life and food loss, by inhibiting lipid oxidation and unpleasant odors during meat processing.

In conclusion, the genetic engineering techniques established in this study will contribute to the development of fundamental and applied research on industrially important *A. oryzae*. Furthermore, the finding that Dfcy can effectively inhibit lipid oxidation in foods suggests that this new functional material holds promise for resolving issues of food loss.

REFERENCES

1. **Mizutani O., Kudo Y., Saito A., Matsuura T., Inoue H., Abe K., Gomi K.:** A defect of LigD (human Lig4 homolog) for nonhomologous end joining significantly improves efficiency of gene-targeting in *Aspergillus oryzae*, *Fungal Genet Biol*, **45**, 878–89, (2008).
2. **Takahashi T., Masuda T., Koyama Y.:** Enhanced gene targeting frequency in *ku70* and *ku80* disruption mutants of *Aspergillus sojae* and *Aspergillus oryzae*, *Mol Genet Genomics*, **275**, 460–70, (2006).
3. **Sander J.D., Joung J.K.:** CRISPR-Cas systems for editing, regulating and targeting genomes, *Nat Biotechnol*, **33**, 347–55, (2014).
4. **Mizutani O., Arazoe T., Toshida K., Hayashi R., Ohsato S., Sakuma T., Yamamoto T., Kuwata S., Yamada O.:** Detailed analysis of targeted gene mutations caused by the Platinum-Fungal TALENs in *Aspergillus oryzae* RIB40 strain and a *ligD* disruptant, *J Biosci Bioeng*, **123**, 287–93, (2017).
5. **Katayama T., Tanaka Y., Okabe T., Nakamura H., Fujii W., Kitamoto K., Maruyama J.:** Development of a genome editing technique using the CRISPR/Cas9 system in the industrial filamentous fungus *Aspergillus oryzae*, *Biotechnol Lett*, **38**, 637–42, (2016).
6. **Suzuki S., Tada S., Fukuoka M., Taketani H., Tsukakoshi Y., Matsushita M., Oda K., Kusumoto K.I., Kashiwagi Y., Sugiyama M.:** A novel transformation system using a bleomycin resistance marker with chemosensitizers for *Aspergillus oryzae*, *Biochem Biophys Res Commun*, **383**, 42–7, (2009).

7. **Kubodera T., Watanabe M., Yoshiuchi K., Yamashita N., Nishimura A., Nakai S., Gomi K., Hanamoto H.:** Thiamine-regulated gene expression of *Aspergillus oryzae thiA* requires splicing of the intron containing a riboswitch-like domain in the 5'-UTR, *FEBS Lett*, **555**, 516–20 (2003).
8. **Katayama T., Nakamura H., Zhang Y., Pascal A., Fujii W., Maruyama J.:** Forced recycling of an AMA1-based genome-editing plasmid allows for efficient multiple gene deletion/integration in the industrial filamentous fungus *Aspergillus oryzae*, *Appl Environ Microbiol*, **85**, 1–16 (2019).
9. **Banan M.:** Recent advances in CRISPR/Cas9-mediated knock-ins in mammalian cells, *J Biotechnol*, **308**, 1–9 (2020).
10. **Gallone B., Steensels J., Prah T., Soriaga L., Saels V., Herrera-Malaver B., et al.:** Domestication and divergence of *Saccharomyces cerevisiae* beer yeasts, *Cell*, **166**, 1397–410 (2016).
11. **Dartois R., Divie C., Inra L.D.M.U.A.:** Gene cloning, transcriptional analysis, purification, and characterization of phenolic acid decarboxylase from *Bacillus subtilis*, *Appl Environ Microbiol* **64**, 1466–71 (1998).
12. **Barthelmebs L., Guzzo J., Beumen J. Van, Samyn B., Divie C.:** Purification and characterization of an inducible *p*-coumaric acid decarboxylase from *Lactobacillus plantarum*, *FEMS Microbiol Lett*, **147**, 291–5 (1997).
13. **Mukai N., Masaki K., Fujii T., Kawamukai M., Iefuji H.:** *PADI* and *FDCI* are essential for the decarboxylation of phenylacrylic acids in *Saccharomyces cerevisiae*, *J Biosci Bioeng*, **109**, 564–9 (2010).
14. **Mukai N., Masaki K., Fujii T., Iefuji H.:** Single nucleotide polymorphisms of *PADI* and *FDCI* show a positive relationship with ferulic acid decarboxylation

- ability among industrial yeasts used in alcoholic beverage production, *J Biosci Bioeng*, **118**, 50–5 (2014).
15. **Kaneoke M.:** 4-Vinylguaiacol formation in sake, *J Brew Soc Japan*, **109**, 320–6 (2014).
 16. **Nielsen N.S., Petersen A., Meyer A.S., Timm-Heinrich M., Jacobsen C.:** Effects of lactoferrin, phytic acid, and EDTA on oxidation in two food emulsions enriched with long-chain polyunsaturated fatty acids, *J Agric Food Chem*, **52**, 7690–9 (2004).
 17. **Jiang J., Xiong Y.L.:** Natural antioxidants as food and feed additives to promote health benefits and quality of meat products: A review, *Meat Sci*, **120**, 107–17 (2016).
 18. **Van Hecke T., Van Camp J., De Smet S.:** Oxidation during digestion of meat: interactions with the diet and *Helicobacter pylori* gastritis, and implications on human health, *Compr Rev Food Sci Food Saf*, **16**, 214–33 (2017).
 19. **Liu R., Chen L., Jiang Y., Zhou Z., Zou G.:** Efficient genome editing in filamentous fungus *Trichoderma reesei* using the CRISPR/Cas9 system, *Cell Discov*, **1**, 15007 (2015).
 20. **Jacobs J.Z., Ciccaglione K.M., Tournier V., Zaratiegui M.:** Implementation of the CRISPR-Cas9 system in fission yeast, *Nat Commun*, **5**, 1–5 (2014).
 21. **Wang Q., Cobine P.A., Coleman J.J.:** Efficient genome editing in *Fusarium oxysporum* based on CRISPR/Cas9 ribonucleoprotein complexes, *Fungal Genet Biol*, **117**, 21–9 (2018).
 22. **Foster A.J., Martin-Urdiroz M., Yan X., Wright H.S., Soanes D.M., Talbot N.J.:** CRISPR-Cas9 ribonucleoprotein-mediated co-editing and counterselection in the rice blast fungus, *Sci Rep*, **8**, 1–12 (2018).

23. **Iwashita, K.:** Genomics and genome editing of *Aspergillus oryzae* in Moromics study, Abstracts of 17th Conference on Fungal Genetics and Molecular Biology, pp. 25–27. Fungal Molecular Biology Society of Japan, Japan (2017).
24. **Yamada O., Lee B., Gomi K.:** Transformation system for *Aspergillus oryzae* with double auxotrophic mutations, *niaD* and *sC*, Biosci Biotechnol Biochem, **61**, 1367–9 (1997).
25. **Unkles S.E., Campbell E.I., de Ruiter-Jacobs Y.M.J.T., Broekhuijsen M., Macro J. a, Carrez D., Contreras R., van den Hondel C.A.M.J.J., Kinghorn J.R.:** The development of a homologous transformation system for *Aspergillus oryzae* based on the nitrate assimilation pathway: A convenient and general selection system for filamentous fungal transformation, MGG Mol Gen Genet, **218**, 99–104 (1989).
26. **de Ruiter-Jacobs Y.M.J.T., Broekhuijsen M., Unkles S.E., Campbell E.I., Kinghorn J.R., Contreras R., Pouwels P.H., van den Hondell C.A.M.J.J.:** A gene transfer system based on the homologous *pyrG* gene and efficient expression of bacterial genes in *Aspergillus oryzae*, Curr Genet, **16**, 159–63 (1989).
27. **Kubodera T., Yamashita N., Nishimura A.:** Pyrithiamine resistance gene (*ptrA*) of *Aspergillus oryzae*: Cloning, characterization and application as a dominant selectable marker for transformation, Biosci Biotechnol Biochem, **64**, 1416–21 (2000).
28. **Thom, C. and Raper, K. B.:** A manual of the *Aspergilli*. Williams and Wilkins Company, Baltimore (1945).

29. **Naito Y., Hino K., Bono H., Ui-Tei K.:** CRISPRdirect: Software for designing CRISPR/Cas guide RNA with reduced off-target sites, *Bioinformatics*, **31**, 1120–3, (2015).
30. **Labun K., Montague T.G., Gagnon J.A., Thyme S.B., Valen E.:** CHOPCHOP v2: a web tool for the next generation of CRISPR genome engineering, *Nucleic Acids Res*, **44**, W272–6 (2016).
31. **Gomi K., Iimura Y., Hara S.:** Integrative transformation of *Aspergillus oryzae* with a plasmid containing the *Aspergillus nidulans argB* gene., *Agric Biol Chem*, **51**, 2549–55 (2011).
32. **Saitou, N. and Nei, M.:** The neighbor-joining method: a new method for reconstructing phylogenetic trees, *Mol Biol Evol*, **4**, 406–425 (1987).
33. **Sievers F., Wilm A., Dineen D., Gibson T.J., Karplus K., Li W., Lopez R., McWilliam H., Remmert M., Söding J., Thompson J.D., Higgins D.G.:** Fast, scalable generation of high-quality protein multiple sequence alignments using Clustal Omega, *Mol Syst Biol*, **7**, 1–6 (2011).
34. **Vogl C., Klein C.M., Batke A.F., Schweingruber M.E., Stolz J.:** Characterization of Thi9, a novel thiamine (vitamin B1) transporter from *Schizosaccharomyces pombe*, *J Biol Chem*, **283**, 7379–89 (2008).
35. **Watanabe A., Ono Y., Fujii I., Sankawa U., Mayorga M.E., Timberlake W.E., Ebizuka Y.:** Product identification of polyketide synthase coded by *Aspergillus nidulans wA* gene, *Tetrahedron Lett*, **39**, 7733–6 (1998).
36. **Oberegger H., Schoeser M., Zadra I., Abt B., Haas H.:** SREA is involved in regulation of siderophore biosynthesis, utilization and uptake in *Aspergillus nidulans*, *Mol Microbiol*, **41**, 1077–89 (2001).

37. **Watanabe, H., Sato, T., Yamada, O., Akao, T., Akita, O., and Enei, H.:** Functional analysis of SreAo, a siderophore regulator of *Aspergillus oryzae*, Abst Annu Meet Jap Soc Biosci Biotech Agrochem, 3-6Ba07 (2001).
38. **Hara, S., Tsuji, R. F., Hatamoto, O., and Masuda, T.:** A simple method for enrichment of uninucleate conidia of *Aspergillus oryzae*, Biosci Biotechnol Biochem, **66**, 693–696 (2002).
39. **Malke H, Sambrock J, Fritsch EF, Maniatis T.:** Molecular Cloning, A Laboratory Manual (Second Edition), Volumes 1, 2 and 3. Cold Spring Harbor Laboratory Press. (1990)
40. **Ishida H., Hata Y., Kawato A., Abe Y., Kashiwagi Y.:** Isolation of a novel promoter for efficient protein production in *Aspergillus oryzae*, Biosci Biotechnol Biochem, **68**, 1849–57 (2004).
41. **Livak K.J., Schmittgen T.D.:** Analysis of relative gene expression data using real-time quantitative PCR and the $2^{-\Delta\Delta CT}$ method, **25**, 402–8 (2001).
42. **Sallmyr A., Tomkinson A.E.:** Repair of DNA double-strand breaks by mammalian alternative end-joining pathways, J Biol Chem, **293**, 10536–49 (2018).
43. **Hata Y., Ishida H., Ichikawa E., Kawato A., Suginami K., Imayasu S.:** Nucleotide sequence of an alternative glucoamylase-encoding gene (*glaB*) expressed in solid-state culture of *Aspergillus oryzae*, Gene, **207**, 127–34 (1998).
44. **Zhang C., Meng X., Wei X., Lu L.:** Highly efficient CRISPR mutagenesis by microhomology-mediated end joining in *Aspergillus fumigatus*, Fungal Genet Biol, **86**, 47–57 (2016).
45. **Kim Y., Kweon J., Kim J.S.:** TALENs and ZFNs are associated with different mutation signatures, Nat Methods, **10**, 185 (2013).

46. **Kim H., Kim J.S.:** A guide to genome engineering with programmable nucleases, *Nat Rev Genet*, **15**, 321–34 (2014).
47. **Umemura M., Koike H., Yamane N., Koyama Y., Satou Y., Kikuzato I., et al.:** Comparative genome analysis between *Aspergillus oryzae* strains reveals close relationship between sites of mutation localization and regions of highly divergent genes among *Aspergillus species*, *DNA Res*, **19**, 375–82 (2012).
48. **Meyer V., Arentshorst M., El-Ghezal A., Drews A.C., Kooistra R., van den Hondel C.A.M.J.J., Ram A.F.J.:** Highly efficient gene targeting in the *Aspergillus niger kusA* mutant, *J Biotechnol*, **128**, 770–5 (2007).
49. **Nishimasu H., Shi X., Ishiguro S., Gao L., Hirano S., Okazaki S., et al.:** Engineered CRISPR-Cas9 nuclease with expanded targeting space, *Science*, **361**, 1259–62 (2018).
50. **Zetsche B., Gootenberg J.S., Abudayyeh O.O., Slaymaker I.M., Makarova K.S., Essletzbichler P., Volz S.E., Joung J., Van Der Oost J., Regev A., Koonin E. V., Zhang F.:** Cpf1 Is a Single RNA-Guided Endonuclease of a Class 2 CRISPR-Cas System, *Cell*, **163**, 759–71 (2015).
51. **Gong G., Zhang Y., Wang Z., Liu L., Shi S., Siewers V., Yuan Q., Nielsen J., Zhang X., Liu Z.:** GTR 2.0: gRNA-tRNA array and Cas9-NG based benome disruption and single-nucleotide conversion in *Saccharomyces cerevisiae*, *ACS Synth Biol*, **10**, 1328–37 (2021).
52. **Katayama T., Maruyama J.:** CRISPR/Cpf1-mediated mutagenesis and gene deletion in industrial filamentous fungi *Aspergillus oryzae* and *Aspergillus sojae*, *J Biosci Bioeng*, **133**, 353–61 (2022).

53. **Bai W., Huang M., Li C., Li J.:** The biological principles and advanced applications of DSB repair in CRISPR-mediated yeast genome editing, *Synth Syst Biotechnol*, **8**, 584–96 (2023).
54. **Huang J., Cook D.E.:** The contribution of DNA repair pathways to genome editing and evolution in filamentous pathogens, *FEMS Microbiol Rev*, **46**, 1–21 (2022).
55. **Leisen T., Bietz F., Werner J., Wegner A., Schaffrath U., Scheuring D., Willmund F., Mosbach A., Scalliet G., Hahn M.:** CRISPR/Cas with ribonucleoprotein complexes and transiently selected telomere vectors allows highly efficient marker-free and multiple genome editing in *Botrytis cinerea*, *PLoS Pathog*, **16**, 1–32 (2020).
56. **Lax C., Navarro-Mendoza M.I., Pérez-Arques C., Navarro E., Nicolás F.E., Garre V.:** Stable and reproducible homologous recombination enables CRISPR-based engineering in the fungus *Rhizopus microsporus*, *Cell Reports Methods*, **1**, (2021).
57. **McMurrough I., Madigan D., Donnelly D., Hurley J., Doyle A.M., Hennigan G., McNulty N., Smyth M.R.:** Control of ferulic acid and 4-vinyl guaiacol in brewing, *J Inst Brew*, **102**, 327–32 (1996).
58. **Hashizume K., Ito T., Shirato K., Amano N., Tokiwano T., Ohno T., Shindo S., Watanabe S., Okuda M.:** Factors affecting levels of ferulic acid, ethyl ferulate and taste-active pyroglutamyl peptides in sake, *J Biosci Bioeng*, **129**, 322–6 (2020).
59. **Coghe S., Benoot K., Delvaux F., Vanderhaegen B., Delvaux F.R.:** Ferulic acid release and 4-vinylguaiacol formation during brewing and fermentation:

- indications for feruloyl esterase activity in *Saccharomyces cerevisiae*, *J Agric Food Chem*, **52**, 602–8 (2004).
60. **V. F. Crepin, C. B. Faulds , I. F. Connerton:** Functional classification of the microbial feruloyl esterases, *Appl Microbiol Biotechnol*, **63**, 647–52 (2004).
 61. **Dilokpimol A., Mäkelä M.R., Aguilar-Pontes M.V., Benoit-Gelber I., Hildén K.S., De Vries R.P.:** Diversity of fungal feruloyl esterases: updated phylogenetic classification, properties, and industrial applications, *Biotechnol Biofuels*, **9**, 1–18 (2016).
 62. **Zeng Y., Yin X., Wu M.C., Yu T., Feng F., Zhu T. Di, Pang Q.F.:** Expression of a novel feruloyl esterase from *Aspergillus oryzae* in *Pichia pastoris* with esterification activity, *J Mol Catal B Enzym*, **110**, 140–6 (2014).
 63. **Koseki T., Handa H., Watanabe Y. ya, Ohtsuka M., Shiono Y.:** An unusual feruloyl esterase from *Aspergillus oryzae*: two tryptophan residues play a crucial role for the activity, *J Mol Catal B Enzym*, **133**, S560–8 (2016).
 64. **The Editorial Committee for the commentary for Brewing Standard Analysis Methods (Ed.):** Commentary for National Research Institute of Brewing Standard Analysis Methods. Brewing Society of Japan, Tokyo (2017).
 65. **Xin, Y. G. and Zhang, Y. H.:** Cloning, expression of a feruloyl esterase from *Aspergillus usamii* E001 and its applicability in generating ferulic acid from wheat bran, *J Ind Microbiol Biotechnol*, **40**, 1433–1441 (2013).
 66. **Utsunomiya H.:** Flavor terminology and reference standards for sensory analysis of sake, *J Brew Soc Japan*, **101**, 730–9 (2006).
 67. **Furukawa, S.:** Sake: quality characteristics, flavour chemistry and sensory analysis, alcoholic beverages, pp. 180–195. Woodhead Publishing Limited, Cambridge, UK (2012).

68. **Hermoso J.A., Sanz-Aparicio J., Molina R., Juge N., González R., Faulds C.B.:** The crystal structure of feruloyl esterase A from *Aspergillus niger* suggests evolutive functional convergence in feruloyl esterase family, *J Mol Biol*, **338**, 495–506 (2004).
69. **Mathew S., Abraham T.E.:** Ferulic acid: An antioxidant found naturally in plant cell walls and feruloyl esterases involved in its release and their applications, *Crit Rev Biotechnol*, **24**, 59–83 (2004).
70. **de Vries, R. P., van Kuyk, P. A., Kester, H. C., & Visser J.:** The *Aspergillus niger faeB* gene encodes a second feruloyl esterase involved in pectin and xylan degradation and is specifically induced in the presence of aromatic compounds., *Biochem J*, **386**, 377–86 (2002).
71. **Uno T., Itoh A., Miyamoto T., Kubo M., Kanamaru K., Yamagata H., Yasufuku Y., Imaishi H.:** Ferulic acid production in the brewing of rice wine (sake), *J Inst Brew*, **115**, 116–21 (2009).
72. **Chatonnet P., Dubourdieu D., Boidron J. -n, Lavigne V.:** Synthesis of volatile phenols by *Saccharomyces cerevisiae* in wines, *J Sci Food Agric*, **62**, 191–202 (1993).
73. **Sunao M., Ito T., Hiroshima K., Sato M., Uehara T., Ohno T., Watanabe S., Takahashi H., Hashizume K.:** Analysis of volatile phenolic compounds responsible for 4-vinylguaiacol-like odor characteristics of sake, *Food Sci Technol Res*, **22**, 111–6 (2016).
74. **Mo X., Xu Y.:** Ferulic acid release and 4-vinylguaiacol formation during Chinese rice wine brewing and fermentation, *J Inst Brew*, **116**, 304–11 (2010).
75. **Wong D.W.S.:** Feruloyl esterase: A key enzyme in biomass degradation, *Appl Biochem Biotechnol*, **133**, 87–112 (2006).

76. **Nakagawa T., Uchida M., Hirai N., Okumura M., Yoshimura A., Sawai Y., et al.:** Identification and sake-brewing characteristics of yeast strains isolated from natural environments in Gifu, *J Brew Soc Japan*, **114**, 43–52 (2019).
77. **Menz J., Modrzejewski D., Hartung F., Wilhelm R., Sprink T.:** Genome edited crops touch the market: a view on the global development and regulatory environment, *Front Plant Sci*, **11**, 1–17 (2020).
78. **Kubow S.:** Lipid oxidation products in food and atherogenesis, *Nutr Rev*, **51**, 33–40 (1993).
79. **Kasai H., Maekawa M., Kawai K., Hachisuka K., Takahashi Y., Nakamura H., Sawa R., Matsui S., Matsuda T.:** 4-Oxo-2-hexenal, a mutagen formed by omega-3 fat peroxidation, causes DNA adduct formation in mouse organs, *Ind Health*, **43**, 699–701 (2005).
80. **Niedernhofer L.J., Daniels J.S., Rouzer C. a., Greene R.E., Marnett L.J.:** Malondialdehyde, a product of lipid peroxidation, is mutagenic in human cells, *J Biol Chem*, **278**, 31426–33 (2003).
81. **Jacobsen C., Hartvigsen K., Thomsen M.K., Hansen L.F., Lund P., Skibsted L.H., Hølmer G., Adler-Nissen J., Meyer A.S.:** Lipid oxidation in fish oil enriched mayonnaise: Calcium disodium ethylenediaminetetraacetate, but not gallic acid, strongly inhibited oxidative deterioration, *J Agric Food Chem*, **49**, 1009–19 (2001).
82. **Olsen E., Veberg A., Vogt G., Tomic O., Kirkhus B., Ekeberg D., Nilsson A.:** Analysis of early lipid oxidation in salmon pâté with cod liver oil and antioxidants, *J Food Sci*, **71**, S284–92 (2006).
83. **Neilands J.B.:** Siderophores: structure and function of microbial iron transport compounds, *J Biol Chem*, **270**, 26723–6 (1995).

84. **Furia T.E.:** CRC handbook of food additives, CRC press, UK (1973).
85. **Propper R.D., Cooper B., Rufo R.R., Nienhuis a W., Anderson W.F., Bunn H.F., Rosenthal a, Nathan D.G.:** Continuous subcutaneous administration of deferoxamine in patients with iron overload, *N Engl J Med*, **297**, 418–23 (1977).
86. **Zecca L., Youdim M.B.H., Riederer P., Connor J.R., Crichton R.R.:** Iron, brain ageing and neurodegenerative disorders, *Nat Rev Neurosci*, **5**, 863–73 (2004).
87. **Suzuki S., Fukuda K., Irie M., Hata Y.:** Iron chelated cyclic peptide, ferrichrysin, for oral treatment of iron deficiency: solution properties and efficacy in anemic rats, *Int J Vitam Nutr Res*, **77**, 13–21 (2007).
88. **Pócsi I., Jeney V., Kertai P., Pócsi I., Emri T., Gyémánt G., Fésüs L., Balla J., Balla G.:** Fungal siderophores function as protective agents of LDL oxidation and are promising anti-atherosclerotic metabolites in functional food, *Mol Nutr Food Res*, **52**, 1434–47 (2008).
89. **Richardson D.R., Kalinowski D.S., Lau S., Jansson P.J., Lovejoy D.B.:** Cancer cell iron metabolism and the development of potent iron chelators as anti-tumour agents, *Biochim. Biophys. Acta*, **1790**, 702–17 (2009).
90. **Yu Y., Wong J., Lovejoy D.B., Kalinowski D.S., Richardson D.R.:** Chelators at the cancer coalface: Desferrioxamine to triapine and beyond, *Clin Cancer Res*, **12**, 6876–83 (2006).
91. **Miethke M., Marahiel M. a:** Siderophore-based iron acquisition and pathogen control, *Microbiol Mol Biol Rev*, **71**, 413–51 (2007).
92. **Tadenuma M., Sato S.:** Studies on the colorants in sake, *Agric Biol Chem*, **31**, 1482–9 (1967).

93. **Ishida H., Moritani T., Hata Y., Kawato A., Suginami K., Abe Y., Imayasu S.:** Molecular cloning and overexpression of *fleA* gene encoding a fucose-specific lectin of *Aspergillus oryzae*, *Biosci Biotechnol Biochem*, **66**, 1002–8 (2002).
94. **Matsumura K., Higashida K., Ishida H., Hata Y., Yamamoto K., Shigeta M., Mizuno-Horikawa Y., Wang X., Miyoshi E., Gu J., Taniguchi N.:** Carbohydrate binding specificity of a fucose-specific lectin from *Aspergillus oryzae*: a novel probe for core fucose, *J Biol Chem*, **282**, 15700–8 (2007).
95. **Tominaga M., Lee Y., Hayashi R., Suzuki Y., Yamada O., Sakamoto K., Gotoh K., Akita O.:** Molecular analysis of an inactive aflatoxin biosynthesis gene cluster in *Aspergillus oryzae* RIB strains, *Appl Environ Microbiol*, **72**, 484–90 (2006).
96. **Stookey L.L.:** Ferrozine---a new spectrophotometric reagent for iron, *Anal Chem*, **42**, 779–81 (1970).
97. **Konetschny-Rapp S., Huschka H.G., Winkelmann G., Jung G.:** High-performance liquid chromatography of siderophores from fungi, *Biol Met*, **1**, 9–17 (1988).
98. **Association of Official Analytical Chemists (AOAC):** Official Methods of Analysis, 15th edition. AOAC, USA (1990).
99. **Maron D.M., Ames B.N.:** Revised methods for the Salmonella mutagenicity test., *Mutat Res*, **113**, 173–215 (1983).
100. **Firestone D.:** Official Methods and Recommended Practices of the AOCS, 6th edition, American Oil Chemists' Society, USA (2009).
101. **Huber G.M., Vasantha Rupasinghe H.P., Shahidi F.:** Inhibition of oxidation of omega-3 polyunsaturated fatty acids and fish oil by quercetin glycosides, *Food Chem*, **117**, 290–5 (2009).

102. **Haas H., Zadra I., Stöffler G., Angermayr K.:** The *Aspergillus nidulans* GATA factor SREA is involved in regulation of siderophore biosynthesis and control of iron uptake, *J Biol Chem*, **41**, 1077–89 (1999).
103. **Hortschansky P., Eisendle M., Al-Abdallah Q., Schmidt A.D., Bergmann S., Thön M., et al.:** Interaction of HapX with the CCAAT-binding complex--a novel mechanism of gene regulation by iron, *EMBO J*, **26**, 3157–68 (2007).
104. **Ehrlich K.C., Mack B.M., Wei Q., Li P., Roze L. V., Dazzo F., Cary J.W., Bhatnagar D., Linz J.E.:** Association with AflR in endosomes reveals new functions for AflJ in aflatoxin biosynthesis, *Toxins (Basel)*, **4**, 1582–600 (2012).
105. **Kiyota T., Hamada R., Sakamoto K., Iwashita K., Yamada O., Mikami S.:** Aflatoxin non-productivity of *Aspergillus oryzae* caused by loss of function in the *aflJ* gene product, *J Biosci Bioeng*, **111**, 512–7 (2011).
106. **German B.:** Oxidative stability of fish and algae oils containing long-chain polyunsaturated fatty acids in bulk and in oil-in water emulsions, *J Agric Food Chem*, **50**, 2094–9 (2002).
107. **Saito Y., Wanezaki K., Kawato A., Imayasu S.:** Structure and activity of angiotensin I converting enzyme inhibitory peptides from sake and sake lees, *Biosci Biotech Biochem*, **58**, 1767–71 (1994).
108. **Vu V.H., Kim K.:** Ethanol production from rice winery waste - Rice wine cake by simultaneous saccharification and fermentation without cooking, *J Microbiol Biotechnol*, **19**, 1161–8 (2009).
109. **Wu J.J., Lin J.C., Wang C.H., Jong T.T., Yang H.L., Hsu S.L., Chang C.M.J.:** Extraction of antioxidative compounds from wine lees using supercritical fluids and associated anti-tyrosinase activity, *J Supercrit Fluids*, **50**, 33–41 (2009).

110. **Choi Y.S., Kim H.W., Hwang K.E., Song D.H., Choi J.H., Lee M.A., Chung H.J., Kim C.J.:** Physicochemical properties and sensory characteristics of reduced-fat frankfurters with pork back fat replaced by dietary fiber extracted from makgeolli lees, *Meat Sci*, **96**, 892–900 (2014).
111. **Smith J.J., Lilly M.D., Fox R.I.:** The effect of agitation on the morphology and penicillin production of *Penicillium chrysogenum*, *Biotech Bioeng*, **35**, 1011–23 (1990).
112. **Mahasiswa I., Indonesia E., Mada U.G.:** Effect of agitation speed on morphological changes in *Aspergillus niger* hyphae during production of tannase, *World J Chem*, **4**, 34–8 (2009).
113. **Casas López J.L., Sánchez Pérez J. a, Fernández Sevilla J.M., Rodríguez Porcel E.M., Chisti Y.:** Pellet morphology, culture rheology and lovastatin production in cultures of *Aspergillus terreus*, *J Biotech*, **116**, 61–77 (2005).
114. **Darah I., Sumathi G., Jain K., Hong L.S.:** Involvement of physical parameters in medium improvement for tannase production by *Aspergillus niger* FETL FT3 in submerged fermentation., *Biotechnol Res Int*, **2011**, 897931 (2011).
115. **US Food and Drug Administration:** Bad Bug Book, Foodborne Pathogenic Microorganisms and Natural Toxins, 2nd edition, Center for Food Safety and Applied Nutrition (CFSAN) of the Food and Drug Administration (FDA), USA (2012).
116. **Emri T., Tóth V., Nagy C.T., Nagy G., Pócsi I., Gyémánt G., Antal K., Balla J., Balla G., Román G., Kovács I., Pócsi I.:** Towards high-siderophore-content foods: optimisation of coprogen production in submerged cultures of *Penicillium nalgiovense*, *J Sci Food Agric*, **93**, 2221–8 (2013).

117. **Baker H.M., Baker E.N.:** Lactoferrin and iron: structural and dynamic aspects of binding and release, *BioMetals*, **17**, 209–16, (2004).
118. **Bingcan C., Atikorn P., D. Julian McClements E.A.D.:** New insights into the role of iron in the promotion of lipid oxidation in bulk oils containing reverse micelles, *J Agric Food Chem*, **60**, pp 3524–32 (2012).
119. **Fang Tian , Eric A. Decker and J.M.G.:** Controlling lipid oxidation via a biomimetic iron chelating active packaging material, *J Agric Food Chem*, **61**, pp 12397–404 (2013).
120. **Szigeti Z.M., Szaniszló S., Fazekas E., Gyémánt G., Szabon J., Antal K., Emri T., Balla J., Balla G., Csernoch L., Pócsi I.:** Optimization of triacetylfusarinine C and ferricrocin productions in *Aspergillus fumigatus*, *Acta Microbiol Immunol Hung*, **61**, 107–19 (2014).
121. **Latge J.P.:** *Aspergillus fumigatus* and *Aspergillosis*, *Clin Microbiol Rev*, **12**, 310–50 (1999).
122. **Drewnowski A., Gomez-carneros C.:** Bitter taste, phytonutrients, and the consumer, *Am J Clin Nutr*, **72**, 1424–35 (2000).
123. **Lourenço S.C., Moldão-Martins M., Alves V.D.:** Antioxidants of natural plant origins: From sources to food industry applications, **24**, 14–6 (2019).
124. **Tadenuma M., Yao T., Shimizu K. Sato S.:** Studies on colorants in sake (VII), *J Brew Soc Japan*, **62**, 1397–401 (1967).
125. **Rogers L.:** *Discrimination Testing in Sensory Science A Practical Handbook*, Woodhead Publishing, UK (2017).
126. **Min B., Nam K.C., Cordray J., Ahn D.U.:** Endogenous factors affecting oxidative stability of beef loin, pork loin, and chicken breast and thigh meats, *J Food Sci*, **73**, C439-46 (2008).

127. **Bligh, E. Graham; Dyer W.J.:** A rapid method of total extraction and purification, *Can J Biochem Physiol*, **37**, 911–7 (1959).
128. **Van Hecke T., Ho P.L., Goethals S., De Smet S.:** The potential of herbs and spices to reduce lipid oxidation during heating and gastrointestinal digestion of a beef product, *Food Res Int*, **102**, 785–92 (2017).
129. **Witte V.C., Krause G.F., Bailey M.E.:** A new extraction method for determining 2-thiobarbituric acid values of pork and beef during storage, *J Food Sci*, **35**, 582–5 (1970).
130. **Jeleń H., Gracka A., Myśków B.:** Static headspace extraction with compounds trapping for the analysis of volatile lipid oxidation products, *Food Anal Methods*, **10**, 2729–34 (2017).
131. **Policy Division, Science and Technology Policy Bureau, Ministry of Education, Culture, Sports S. and T. (MEXT):** Standard Tables of Food Composition in Japan, Japan (2020).
132. **Min B., Ahn D.U.:** Mechanism of lipid peroxidation in meat and meat products - A review, *Food Sci Biotechnol*, **14**, 152–63 (2005).
133. **Hara S., Sugama S., Hongo K., Oba T., Hasegawa Y., Murakami H.:** Isolation of Deferriferrichrome-non-producing mutants of sake-koji molds and their mycological characteristics, *J Ferment Technol*, **52**, 306–13 (1974).
134. **Hara S., Sugama S., Furusawa T., Hongo K.:** Pilot scale brewing of sake using Deferriferrichrome-non-producing mutants of koji molds, *J Ferment Technol*, **52**, 314–20 (1974).
135. **Horváthová J., Suhaj M., Šimko P.:** Effect of thermal treatment and storage on antioxidant activity of some spices, *J Food Nutr Res*, **46**, 20–7 (2007).

136. **Chaaban H., Ioannou I., Chebil L., Slimane M., Gérardin C., Paris C., Charbonnel C., Chekir L., Ghoul M.:** Effect of heat processing on thermal stability and antioxidant activity of six flavonoids, *J Food Process Preserv*, **41**, e13203 (2017).
137. **Nout M.J.R., Aidoo K.E.:** Asian fungal fermented food, *Ind Appl*, 29–58 (2011).
138. **Saha M., Sarkar S., Sarkar B., Sharma B.K., Bhattacharjee S., Tribedi P.:** Microbial siderophores and their potential applications: a review, *Environ Sci Pollut Res*, **23**, 3984–99 (2016).

ACKNOWLEDGEMENTS

The author would like to express his sincere gratitude to Dr. Jun Ogawa, Professor of Kyoto University, for his kind guidance and encouragement.

The author expresses special thanks to Mr. Haruhiko Okura, President of Gekkeikan Sake Co. Ltd., for the support throughout this work. The author is very grateful to Dr. Yoji Hata, Executive Managing Director of Gekkeikan Sake Co. Ltd., for giving him the opportunity to continue the research. The author expresses his superior thanks to Dr. Hiroki Ishida, Research Manager of Gekkeikan Sake Co. Ltd., for his guidance and warm encouragements. The author sincerely appreciates his senior colleagues Dr. Kengo Matsumura, Mr. Katsuharu Fukuda, Dr. Atsushi Kotaka, Dr. Hiroaki Negoro, and all colleagues who have worked together in the past and up to the present.

Finally, the author greatly thanks and acknowledges his family for their support.

LIST OF PUBLICATIONS

- [1] **Todokoro, T.**, Fukuda, K., Matsumura, K., Irie, M., Hata, Y.: Production of the natural iron chelator deferriferrichrysin from *Aspergillus oryzae* and evaluation as a novel food - grade antioxidant, *J Sci Food Agric*, **96**, 2998-3006 (2016).
- [2] **Todokoro, T.**, Bando, H., Kotaka, A., Tsutsumi, H., Hata, Y., Ishida, H.: Identification of a novel pyrithiamine resistance marker gene *thiI* for genome co-editing in *Aspergillus oryzae*, *J Biosci Bioeng*, **130**, 227-232 (2020).
- [3] **Todokoro, T.**, Kashihara, H., Fukuda, K., Tsutsumi, H., Hata, Y., Ishida, H.: Inhibition of lipid oxidation and hexanal production in cooked meats by microbial iron chelator deferriferrichrysin from rice wine, *J Food Process Preserv*, **45**, e15943 (2021).
- [4] **Todokoro, T.**, Negoro, H., Kotaka, A., Hata, Y., Ishida, H.: *Aspergillus oryzae* FaeA is responsible for the release of ferulic acid, a precursor of off-odor 4-vinylguaiacol in sake brewing, *J Biosci Bioeng*, **133**, 140-145 (2022).
- [5] **Todokoro, T.**, Hata, Y., Ishida, H.: CRISPR/Cas9 improves targeted knock-in efficiency in *Aspergillus oryzae*, *Biotechnol Notes*, **5**, 58-63 (2024).